Electronic Supplementary Material (ESI) for Journal of Materials Chemistry C.

Highly selective chromoionophores for ratiometric Na^+ sensing based on an oligoethyleneglycol bridged bithiophene unit

Maximilian Moser,*[a] Karl J. Thorley,[a] Floriana Moruzzi,[a] James F. Ponder Jr.,[a] Iuliana P. Maria,[a] Alexander Giovannitti,[b] Sahika Inal[c] and Iain McCulloch [ad]

a. Department of Chemistry and Centre for Plastic Electronics, Imperial College London, London, SW7 2AZ, UK. E-mail: maximilian.moser13@imperial.ac.uk

b. Department of Physics and Centre for Plastic Electronics, Imperial College London, London, SW7 2AZ, UK.

c. Biological and Environmental Sciences and Engineering Division, King Abdullah University of Science and Technology (KAUST), Thuwal 23955-6900, Kingdom of Saudi Arabia

d. King Abdullah University of Science and Technology (KAUST), Physical Sciences and Engineering Division, KAUST Solar Center (KSC), Thuwal 23955-6900, Saudi Arabia

1. General Procedures

All chemicals employed were purchased from Sigma-Aldrich, FluoroChem and Acros Organics and were used without any further purification unless otherwise stated. Dry solvents for anhydrous reactions were Sure/Seal™ brand and acquired from Sigma-Aldrich. All reactions were carried out in oven dried flasks and under an inert atmosphere of argon.

Thin layer chromatography (TLC) was performed on TLC Silicagel 60 F254 plates obtained from Merck. Column chromatography was carried out on Geduran Silicagel Si 60 (40-63 μm) obtained from Merck or on a Biotage Isolera system with Biotage ZIP Silica cartridges.

^{1}H and ^{13}C NMR spectra were recorded on a Bruker AV-400 UltraShield spectrometer (400 MHz for ^{1}H and 101 MHz for ^{13}C) at 298 K and using chloroform-*d* ($CDCl_3$) as solvent, unless otherwise stated. Chemical shifts (δ) are expressed in parts per million (ppm) downfield from tetramethylsilane (TMS) and are referenced to chloroform (δ_H 7.26 and δ_C 77.16). Coupling constants (*J*) are expressed in Hertz (Hz) and multiplicities are indicated as singlet (s), doublet (d), triplet (t), quartet (q) or multiplet (m).

Electrospray ionisation (EI) and atmospheric pressure chemical ionisation (APCI) mass spectrometry were performed with a Micromass LCT Premier and a ThermoFisher Q Exactive Hybrid Quadrupole-Orbitrap mass spectrometer respectively.

UV-vis absorption spectra were measured in solution under ambient conditions by employing quartz cuvettes (pathlength of 1 cm) on a UV-1800 Shimadzu UV Spectrophotometer, whilst fluorescence spectra were recorded on a PerkinElmer LS 55.

DFT calculations were performed at the ωB97XD/6-31G(d) level of theory using Gaussian 09 Rev D.01.[1]

2. Synthetic Procedures

2.1 3,3'-(tetraethylene glycol)-2,2'-bithiophene (1).

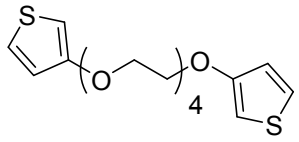

1

1 was prepared as previously described in the literature.[2,3] 5.83 g of a 60% sodium hydride dispersion in mineral oil (145 mmol, 3.00 eq.) and 2.84 g of copper (I) iodide (14.7 mmol, 0.298 eq.) were added to a dried two-neck round bottom flask and purged with argon. 300 mL of anhydrous dimethylformamide were then added followed by dropwise addition of 8.4 mL of tetraethylene glycol (49 mmol, 1.0 eq.). The reaction mixture was stirred until effervescence had ceased. 11.5 mL of 3-bromothiophene (123 mmol, 2.51 eq.) were added subsequently and the resulting reaction mixture was heated at 110 °C overnight. Once complete, the reaction mixture was diluted with approx. 200 mL of distilled water and extracted three times with diethyl ether. The combined organic phase was then washed three times with water, once with brine and was dried over magnesium sulfate. Excess solvent was removed under reduced pressure. The product was purified by column chromatography on silica gel. The final product was obtained as a white solid (7.56 g, 21.1 mmol, 43% yield). ^{1}H NMR (400 MHz, $CDCl_3$, δ): 7.16 (dd, *J* = 5.2 Hz, 3.1 Hz, 2H), 6.77 (dd, *J* = 5.2 Hz, 1.6 Hz, 2H), 6.25 (dd, *J* = 3.1 Hz, 1.6 Hz, 2H), 4.13-4.08 (m, 4H), 3.87-3.81 (m, 4H) and 3.70 (m, 8H).

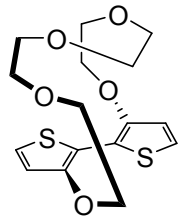

T2-17-crown-5

2.2 3,3'-17-crown-5-2,2'-bithiophene ((17-crown-5)T2).

(17-crown-5)T2 was prepared as previously described in the literature.[2,3] 7.00 g of 3,3'-(tetraethylene glycol)-2,2'-bithiophene (19.5 mmol, 1.00 eq.) were dissolved in 100 mL anhydrous dimethoxyethane and the solution was purged with argon for 15 min. The mixture was then cooled to -30 °C and 20.0 mL of 2.5 M *n*-butyllithium in hexanes (50.0 mmol, 2.56 eq.) was added dropwise. The reaction was stirred for another 30 min at -20 °C before being allowed to warm to 0 °C. The mixture was then transferred dropwise at 0°C to a solution of 5.25 g of copper (II) chloride (39.0 mmol, 2.00 eq.) in 160 mL dimethoxyethane. The reaction mixture was allowed to warm up to room temperature

and was stirred overnight. The solution was diluted with 100 mL of water and extracted three times with diethyl ether. The combined organic extracts were washed three times with water, dried over magnesium sulfate and excess solvent was removed under reduced pressure. The product was purified by flash column chromatography on silica gel to afford the final product as colourless crystals (2.19 g, 6.15 mmol, 32% yield). ^{1}H NMR (400 MHz, $CDCl_3$, δ): 7.15 (d, *J* = 5.6 Hz, 2H), 6.87 (d, *J* = 5.6 Hz, 2H), 4.32-4.26 (m, 4H), 3.83-3.77 (m, 4H) and 3.58-3.46 (m, 8H); ^{13}C NMR (100 MHz, $CDCl_3$, δ): 153.08, 122.86, 117.97, 113.61, 71.55, 71.01, 70.56, 70.50.

2.3 General procedure for the In-catalysed Knoevenagel condensation

The general procedure for the In-catalysed Knoevenagel condensation was based on a previously published method.[4] Bromo-aryl-carboxaldehyde (1.0 eq.) and 28 mg of indium(III)chloride (0.12 mmol, 0.10 eq.) were added to a dry microwave vial and dissolved in 5 mL dry toluene. 0.28 mL of diethyl malonate (1.9 mmol, 1.5 eq.) and 0.12 mL of acetic anhydride (1.2 mmol, 1.0 eq.) were added sequentially and the resulting mixture was heated at 70 °C overnight. The reaction mixture was diluted with water and extracted three times with dichloromethane. The combined organic phases were washed three times with water and once with brine before being dried over magnesium sulfate. Excess solvent was removed under reduced pressure. The product was purified by flash column chromatography using silica gel to afford the final product.

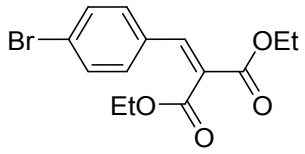

BrPhDEM

2.3.1 Diethyl 2-(4-bromobenzylidene)malonate (BrPhDEM).

BrPhDEM was prepared from 230 mg of 4-bromobenzaldehyde (1.25 mmol, 1.00 eq) and 0.28 mL of diethyl malonate (1.9 mmol, 1.5. eq) according to the general In-catalysed Knoevenagel condensation. The final product was obtained as a pale yellow oil (360 mg, 1.10 mmol, 81% yield). ^{1}H NMR (400 MHz, $CDCl_3$, δ): 7.68 (s, 1H), 7.57- 7.52(m, 2H), 7.37-7.33 (m, 2H), 4.36 (q, *J* = 7.2 Hz, 2H), 4.33 (q, *J* = 7.1 Hz, 2H), 1.36 (t, *J* = 7.2 Hz, 3H), 1.32 (t, *J* = 7.1 Hz, 3H). NMR shifts consistent with those reported in the literature.[5]

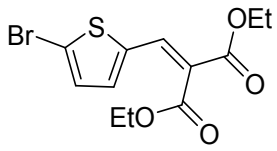

BrThDEM

2.3.2 Diethyl 2-((5-bromothiophen-2-yl)methylene)malonate (BrThDEM).

BrThDEM was prepared from 0.15 mL of 5-bromo-2-thiophenecarboxaldehyde (1.25 mmol, 1.00 eq) and 0.28 mL of diethyl malonate (1.9 mmol, 1.5. eq) according to the general In-catalysed Knoevenagel condensation. The final product was obtained as a pale yellow oil (303 mg, 0.91 mmol, 73% yield). ^{1}H NMR (400 MHz, $CDCl_3$, δ): 7.72 (d, *J* = 0.7 Hz, 1H), 7.13 (dd, *J* = 4.0, 0.6 Hz, 1H), 7.05 (d, *J* = 4.0 Hz, 1H), 4.40 (q, *J* = 7.2 Hz, 2H), 4.29 (q, *J* = 7.1 Hz, 2H), 1.38 (t, *J* = 7.1 Hz, 3H), 1.32 (t, *J* = 7.1 Hz, 3H); ^{13}C NMR (100 MHz, $CDCl_3$, δ): 165.97, 164.31, 137.65, 135.18, 134.68, 130.51, 122.39, 120.19, 61.96, 61.65, 14.14.[6]

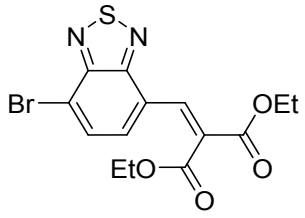

BrBTDEM

2.3.3 Diethyl 2-((7-bromobenzo[c][1,2,5]thiadiazol-4-yl)methylene)malonate (BrBTDEM).

BrBTDEM was prepared from 300 mg of 7-bromo-2,1,3-benzothiadiazole-4-carboxaldehyde (1.25 mmol, 1.00 eq) and 0.28 mL of diethyl malonate (DEM) (1.9 mmol, 1.5. eq) according to the general In-catalysed Knoevenagel condensation. The final product was obtained as a white solid (407 mg, 1.06 mmol, 84% yield). ^{1}H NMR (400 MHz, $CDCl_3$, δ): 8.41 (s, 1H), 7.88 (d, *J* = 7.6 Hz, 1H), 7.69 (dd, *J* = 7.7, 0.9 Hz, 1H), 4.39 (q, *J* = 7.1 Hz, 2H), 4.35 (q, *J* = 7.1 Hz, 2H), 1.40 (t, *J* = 7.1 Hz, 3H), 1.30 (t, *J* = 7.1 Hz, 3H); ^{13}C NMR (100 MHz, $CDCl_3$, δ): 166.62, 165.99, 163.66, 153.25, 135.55, 131.93, 129.26, 129.17, 126.09, 116.76, 62.01, 61.95, 14.14, 13.93; HRMS (EI): 384.9782 Da for $[M+H]^+$ (predicted 383.9779 Da for $C_{14}H_{13}BrN_2O_4S$).

2.4 General procedure for the Pd-catalysed direct C-H arlyation of (17-crown-5)T2

70 mg of **(17-crown-5)T2** (0.20 mmol, 1.0 eq.), aryl bromide coupling partner (2.2 eq.), 20 mg of pivalic acid (0.20 mmol, 1.0 eq.), 191 mg of caesium carbonate (0.588 mmol, 3.00 eq.), 8 mg of tris(dibenzylideneacetone)dipalladium(0) (0.008 mmol, 0.04 eq.) and 6 mg of tris(*o*-methoxyphenyl)phosphine (0.016 mmol, 0.08 eq.) were dissolved in 1 mL anhydrous toluene. The mixture was heated under argon at 110 °C overnight. The reaction was cooled to room temperature

and diluted with distilled water. The aqueous phase was extracted three times with dichloromethane and the combined organic fractions were washed three times with water. Excess solvent was removed under reduced pressure. The product was purified by flash column chromatography using silica gel to afford the final product.

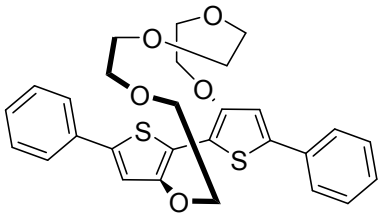

S1

2.4.1 Ph-17-crown-5-bithiophene (S1).

S1 was prepared from 70 mg **(17-crown-5)T2** (0.20 mmol, 1.0 eq.) and 68 mg bromobenzene (0.43 mmol, 2.2 eq) according to the general procedure. The final product was obtained as a yellow solid (95 mg, 0.19 mmol, 95% yield). ^{1}H NMR (400 MHz, $CDCl_3$, δ): 7.66 (d, *J* = 7.7 Hz, 4H), 7.44 (t, *J* = 7.6 Hz, 4H), 7.38 – 7.30 (m, 2H), 7.21 (s, 2H), 4.41 (t, *J* = 4.5 Hz, 4H), 3.86 (t, *J* = 4.5 Hz, 4H), 3.53 (dd, *J* = 5.8, 3.5 Hz, 4H), 3.43 (dd, *J* = 5.8, 3.5 Hz, 4H); ^{13}C NMR (100 MHz, CD_2Cl_2, δ): 153.77, 140.19, 134.76, 133.12, 129.25, 127.86, 125.27, 114.55, 72.36, 71.34, 70.99, 70.71; HRMS (APCI): 509.1451 Da for $[M+H]^+$ (predicted 509.1451 Da for $C_{28}H_{29}O_5S_2$).

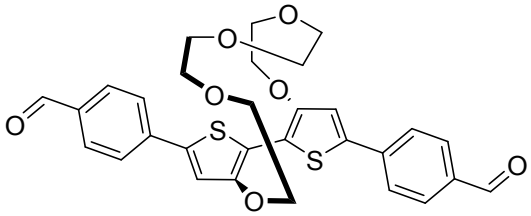

2.4.2 PhCHO-17-crown-5-bithiophene (S2).

S2 was prepared from 70 mg **(17-crown-5)T2** (0.20 mmol, 1.0 eq.) and 80 mg 4-bromobenzaldehyde (0.43 mmol, 2.2 eq) according to the general procedure. The final product was obtained as an orange solid (104 mg, 0.185 mmol, 94% yield). ^{1}H NMR (400 MHz, CD_2Cl_2, δ): 10.02 (s, 2H), 7.95 – 7.90 (m, 4H), 7.86 – 7.80 (m, 4H), 7.37 (s, 2H), 4.51 – 4.43 (m, 4H), 3.88 – 3.82 (m, 4H), 3.50 – 3.44 (m, 4H), 3.37 – 3.30 (m, 4H); ^{13}C NMR (100 MHz, CD_2Cl_2, δ): 191.15, 154.12, 139.89, 137.93, 135.11, 130.28, 124.98, 117.27, 115.83, 72.49, 71.12, 70.78, 70.20; HRMS (APCI): 565.1347 Da for $[M+H]^+$ (predicted 565.1349 Da for $C_{30}H_{29}O_7S_2$).

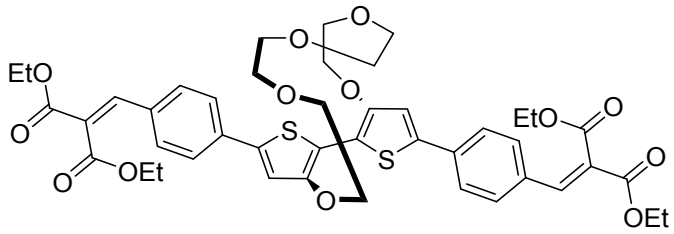

2.4.3 PhDEM-17-crown-5-bithiophene (S3).

S3 was prepared from 70 mg **(17-crown-5)T2** (0.20 mmol, 1.0 eq.) and 140 mg diethyl(4-bromobenzylidene)malonate (0.43 mmol, 2.2 eq) according to the general procedure. The final product was obtained as a red solid (115 mg, 0.136 mmol, 69% yield). ^{1}H NMR (400 MHz, CD_2Cl_2, δ): 7.73 (s, 2H), 7.68 (d, *J* = 8.2 Hz, 4H), 7.52 (d, *J* = 8.3 Hz, 4H), 7.28 (s, 2H), 4.47 – 4.43 (m, 4H), 4.40 (q, *J* = 7.2 Hz, 4H), 4.33 (q, *J* = 7.1 Hz, 4H), 3.84 (dd, *J* = 5.3, 3.3 Hz, 4H), 3.51 – 3.45 (m, 4H), 3.39 – 3.34 (m, 4H), 1.37 (td, *J* = 7.2, 2.1 Hz, 12H); ^{13}C NMR (100 MHz, $CDCl_3$, δ): 166.61, 164.04, 153.87, 140.80, 138.36, 136.41, 131.70, 130.19, 125.84, 124.92, 116.21, 115.02, 72.34, 71.06, 70.72, 70.23, 61.76, 61.60, 13.93, 13.75; HRMS (APCI): 849.2610 Da for $[M+H]^+$ (predicted 849.2609 Da for $C_{44}H_{49}O_{13}S_2$).

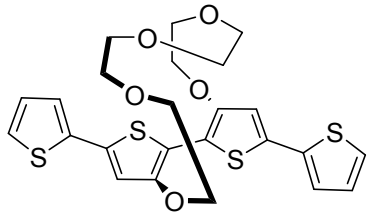

2.4.4 Th-17-crown-5-bithiophene (S4).

S4 was prepared from 70 mg **(17-crown-5)T2** (0.20 mmol, 1.0 eq.) and 70 mg 2-bromothiophene (0.43 mmol, 2.2 eq) according to the general procedure. The final product was obtained as a dark yellow solid (87 mg, 0.17 mmol, 85% yield). ^{1}H NMR (400 MHz, $CDCl_3$, δ): 7.20 (dd, *J* = 5.1, 1.2 Hz, 2H), 7.16 (dd, *J* = 3.6, 1.2 Hz, 2H), 7.01 (dd, *J* = 5.1, 3.6 Hz, 2H), 6.96 (s, 2H), 4.39 – 4.34 (m, 4H), 3.85 – 3.76 (m, 4H), 3.51 (dd, *J* = 5.8, 3.4 Hz, 4H), 3.42 (dd, *J* = 5.7, 3.5 Hz, 4H); ^{13}C NMR (100 MHz, $CDCl_3$, δ): 152.82, 137.91, 133.37, 127.87, 124.23, 122.97, 114.63, 114.03, 72.18, 71.36, 70.90, 70.46. HRMS (APCI): 521.0570 Da for $[M+H]^+$ (predicted 521.0579 Da for $C_{24}H_{25}O_5S_4$).

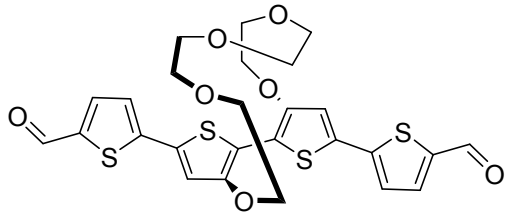

2.4.5 ThCHO-17-crown-5-bithiophene (S5).

S5 was prepared from 70 mg **(17-crown-5)T2** (0.20 mmol, 1.0 eq.) and 83 mg 5-bromo-2-

thiophenecarboxaldehyde (0.43 mmol, 2.2 eq) according to the general procedure. The final product was obtained as an orange solid (99 mg, 0.17 mmol, 87% yield). ^{1}H NMR (400 MHz, acetone-*d*6, δ): 9.93 (s, 2H), 7.93 (d, *J* = 4.0 Hz, 2H), 7.55 (s, 2H), 7.50 (d, *J* = 4.0 Hz, 2H), 4.63 – 4.44 (m, 4H), 3.87 – 3.77 (m, 4H), 3.41 (dd, *J* = 5.7, 4.2 Hz, 4H), 3.26 (dd, *J* = 5.8, 4.1 Hz, 4H); ^{13}C NMR (100 MHz, acetone-*d*6, δ): 182.49, 154.00, 146.66, 141.73, 138.09, 131.54, 123.86, 117.43, 117.09, 72.44, 70.97, 70.57, 69.96.; HRMS (APCI): 577.0478 Da for $[M+H]^+$ (predicted 577.0477 Da for $C_{26}H_{25}O_7S_4$).

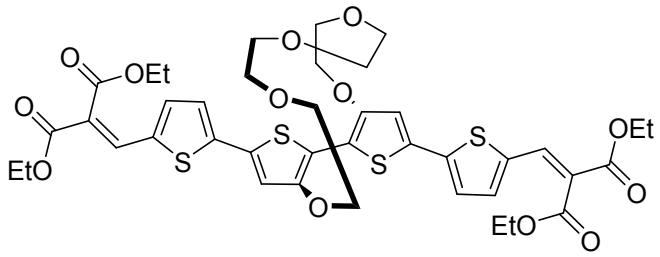

2.4.6 ThDEM-17-crown-5-bithiophene (S6).

S6 was prepared from 70 mg **(17-crown-5)T2** (0.20 mmol, 1.0 eq.) and 144 mg 5-bromo-2-thiophenecarboxaldehyde (0.43 mmol, 2.2 eq) according to the general procedure. The final product was obtained as a red solid (113 mg, 0.132 mmol, 67% yield). ^{1}H NMR (400 MHz, CD_2Cl_2, δ): 7.78 (d, *J* = 0.6 Hz, 2H), 7.32 (dd, *J* = 3.9, 0.6 Hz, 2H), 7.18 (d, *J* = 3.9 Hz, 2H), 7.10 (s, 2H), 4.43 – 4.37 (m, 8H), 4.23 (q, *J* = 7.1 Hz, 4H), 3.78 – 3.75 (m, 4H), 3.38 – 3.35 (m, 4H), 3.25 – 3.20 (m, 4H), 1.36 (t, *J* = 7.2 Hz, 6H), 1.29 (t, *J* = 7.2 Hz, 6H); ^{13}C NMR (100 MHz, CD_2Cl_2, δ): 166.56, 164.67, 154.00, 144.54, 136.74, 134.81, 132.37, 123.51, 121.80, 117.11, 116.03, 73.01, 71.56, 71.17, 70.53, 62.29, 61.86, 14.33, 14.17.; HRMS (APCI): 861.1743 Da for $[M+H]^+$ (predicted 861.1738 Da for $C_{40}H_{45}O_{13}S_4$).

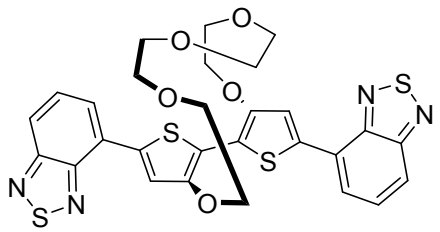

2.4.7 BT-17-crown-5-bithiophene (S7).

S7 was prepared from 70 mg **(17-crown-5)T2** (0.20 mmol, 1.0 eq.) and 92 mg 4-bromo-2,1,3-benzothiadiazole (0.43 mmol, 2.2 eq) according to the general procedure. The final product was obtained as a dark purple solid (87 mg, 0.14 mmol, 71% yield). ^{1}H NMR (400 MHz, $CDCl_3$, δ): 8.13 (s, 2H), 7.93 (dd, *J* = 8.7, 0.9 Hz, 2H), 7.87 (dd, *J* = 7.2, 1.0 Hz, 2H), 7.64 (dd, *J* = 8.7, 7.1 Hz, 2H), 4.58 – 4.52 (m, 4H), 3.96 – 3.92 (m, 4H), 3.57 (dd, *J* = 5.7, 3.6 Hz, 4H), 3.44 (dd, *J* = 5.8, 3.5 Hz, 4H); ^{13}C NMR (100 MHz, $CDCl_3$, δ): 155.68, 153.91, 152.06, 135.32, 129.60, 127.57, 124.13, 119.78, 119.35, 116.64, 72.26, 71.32, 70.94, 70.44; HRMS (APCI): 625.0698 Da for $[M+H]^+$ (predicted 625.0702 Da for $C_{28}H_{25}N_4O_5S_2$).

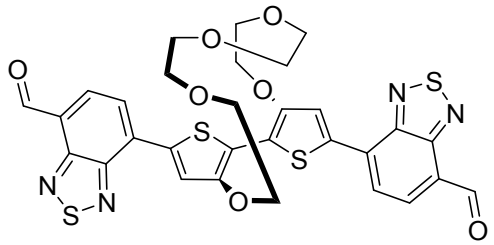

2.4.8 BTCHO-17-crown-5-bithiophene (S8).

S8 was prepared from 70 mg **(17-crown-5)T2** (0.20 mmol, 1.0 eq.) and 104 mg 7-bromo-2,1,3-benzothiadiazole-4-carboxaldehyde (0.43 mmol, 2.2 eq) according to the general procedure. The final product was obtained as a dark blue solid (103 mg, 0.151 mmol, 77% yield). ^{1}H NMR (400 MHz, $CDCl_3$, δ): 10.75 (s, 2H), 8.33 (s, 2H), 8.25 (d, *J* = 7.6 Hz, 2H), 8.02 (d, *J* = 7.5 Hz, 2H), 4.66 – 4.61 (m, 4H), 3.97 – 3.89 (m, 4H), 3.51 (dd, *J* = 5.7, 3.7 Hz, 4H), 3.36 (dd, *J* = 5.6, 3.7 Hz, 4H); ^{13}C NMR (100 MHz, $CDCl_3$, δ): 188.46, 155.30, 153.98, 152.33, 134.80, 132.92, 132.58, 125.25, 122.82, 121.25, 120.65, 72.84, 71.52, 71.12, 70.35; HRMS (APCI): 681.0591 Da for $[M+H]^+$ (predicted 681.0601 Da for $C_{30}H_{25}N_4O_7S_4$).

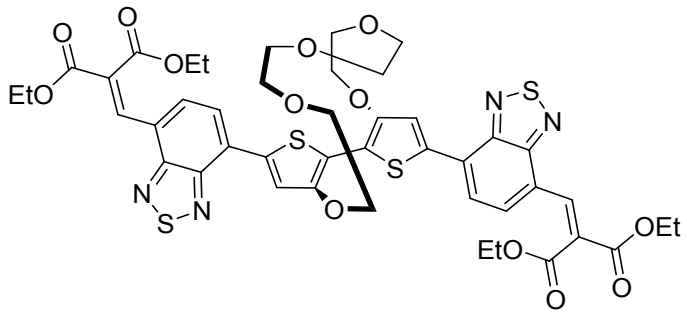

2.4.9 BTDEM-17-crown-5-bithiophene (S9).

S9 was prepared from 70 mg **(17-crown-5)T2** (0.20 mmol, 1.0 eq.) and 167 mg 2-bromothiophene (0.43 mmol, 2.2 eq) according to the general procedure. The final product was obtained as a dark blue solid (184 mg, 0.191 mmol, 97% yield). ^{1}H NMR (400 MHz, $CDCl_3$, δ): 8.53 (s, 2H), 8.20 (s, 2H), 7.86 (d, *J* = 7.7 Hz, 2H), 7.83 (d, *J* = 8.1 Hz, 2H), 4.59 (dd, *J* = 5.5, 3.1 Hz, 4H), 4.46 – 4.35 (m, 8H), 3.96 – 3.90 (m, 4H), 3.51 (dd, *J* = 5.8, 3.6 Hz, 4H), 3.37 (dd, *J* = 5.7, 3.6 Hz, 4H), 1.41 (t, *J* = 7.1 Hz, 6H), 1.35 (t, *J* = 7.1 Hz, 6H); ^{13}C NMR (100 MHz, $CDCl_3$, δ): 166.56, 164.04, 154.68, 154.64, 151.70, 136.10, 134.97, 129.40, 129.27, 127.46, 124.23, 123.58, 120.16, 118.95, 72.62, 71.45, 71.06, 70.36, 61.87, 61.82, 14.22, 14.03. HRMS (APCI): 965.1861 Da for $[M+H]^+$ (predicted 965.1860 Da for $C_{44}H_{45}N_4O_{13}S_4$).

3. ^{1}H and ^{13}C NMR Spectra

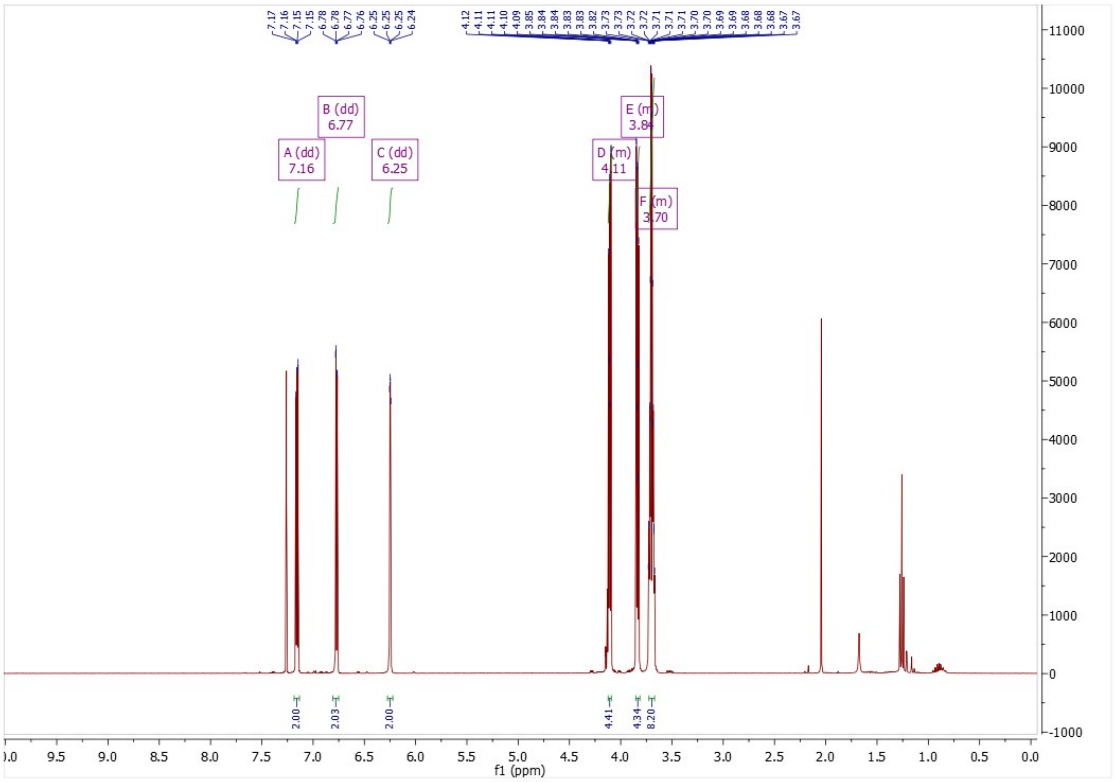

Fig. S1 ^{1}H NMR spectrum of **1**.

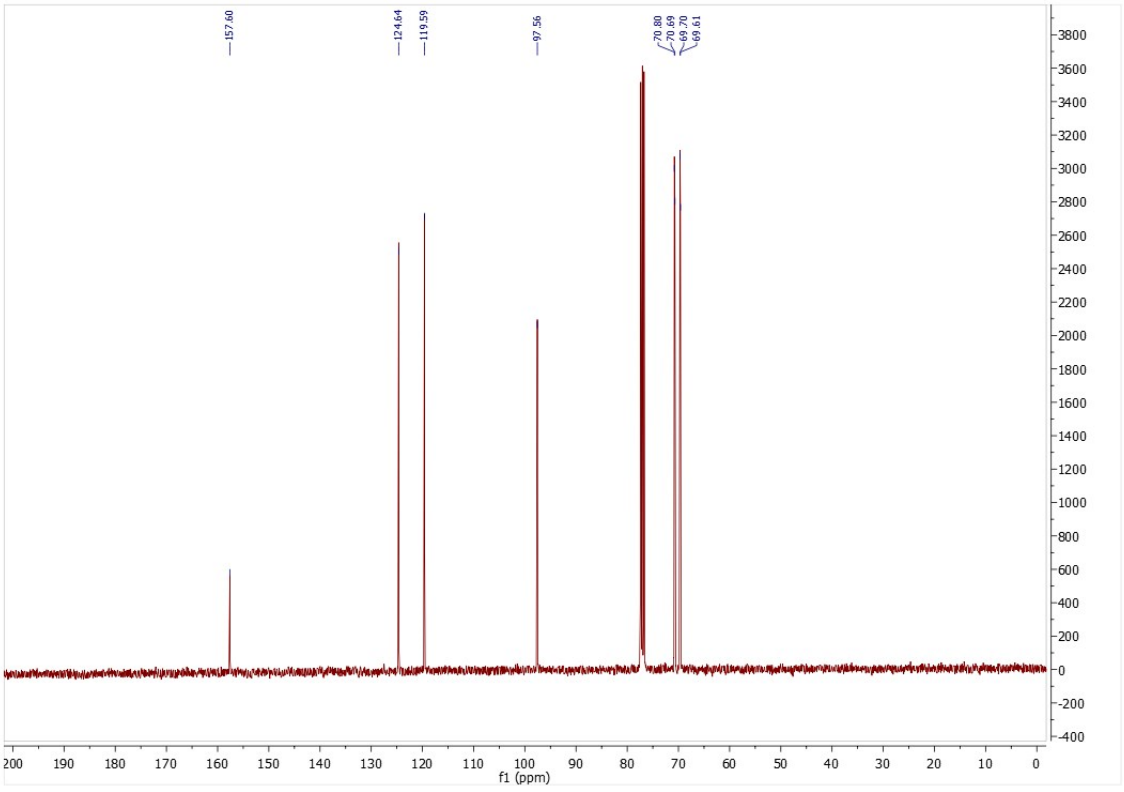

Fig. S2 ^{13}C NMR spectrum of **1**.

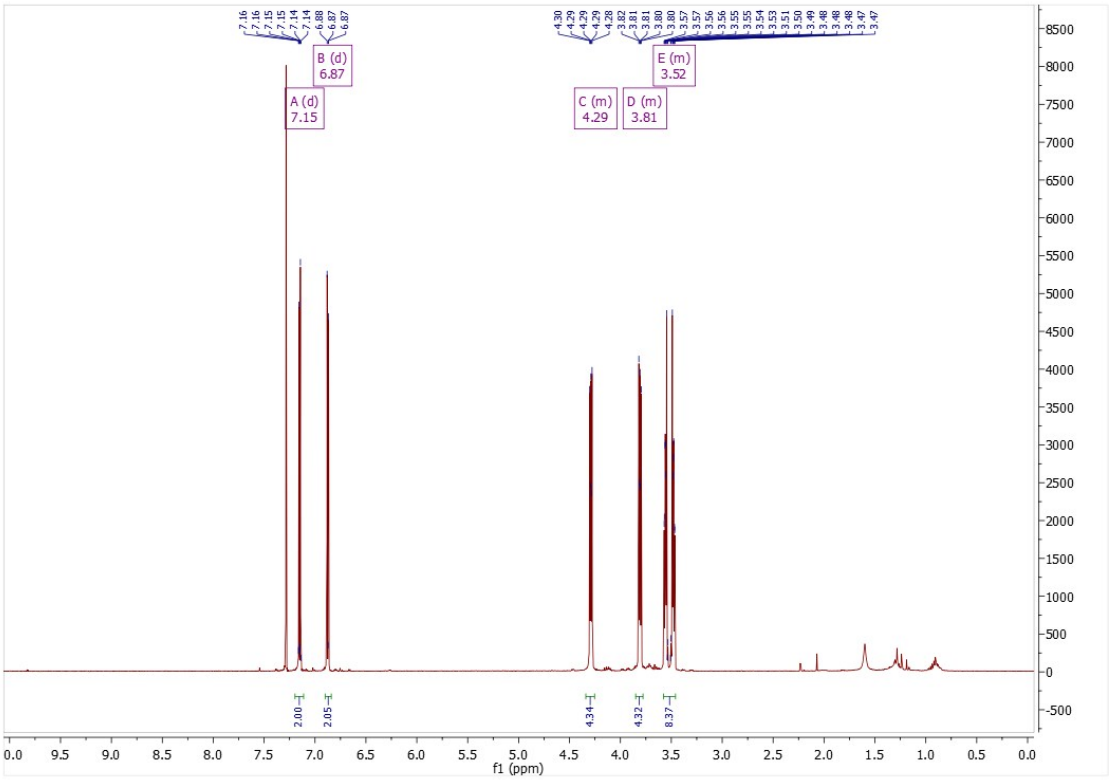

Fig. S3 ^{1}H NMR spectrum of **(17-crown-5)T2**.

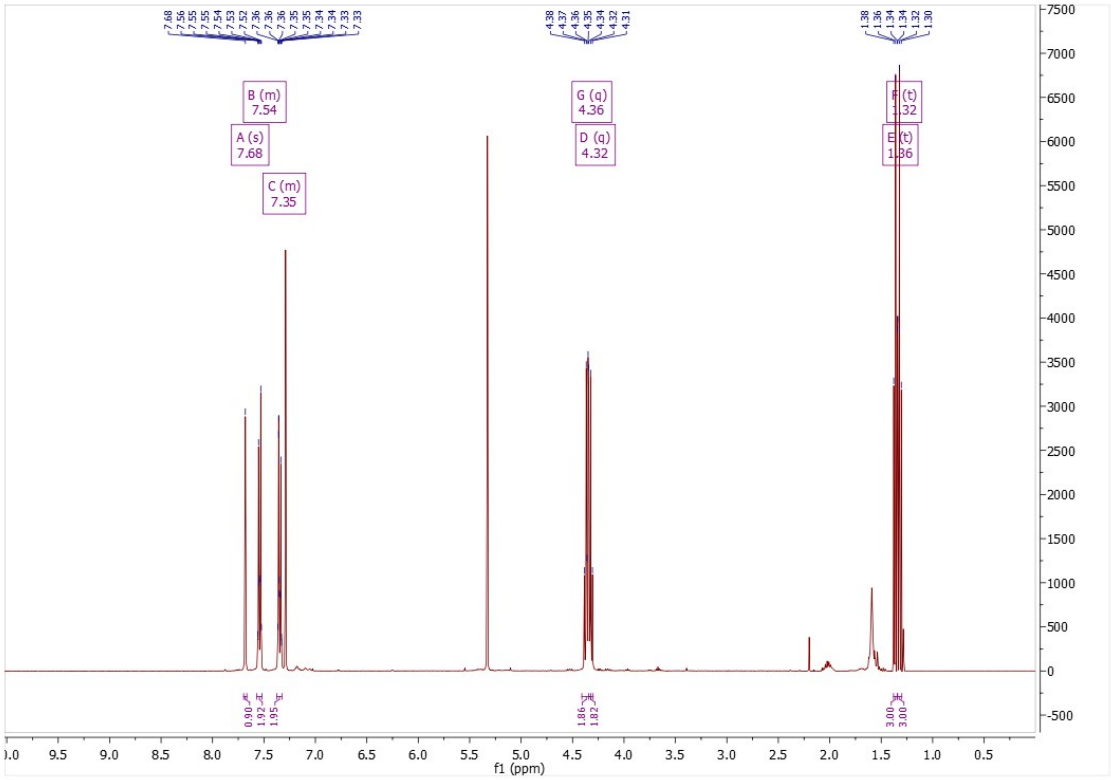

Fig. S4 ^{1}H NMR spectrum of **BrPhDEM**.

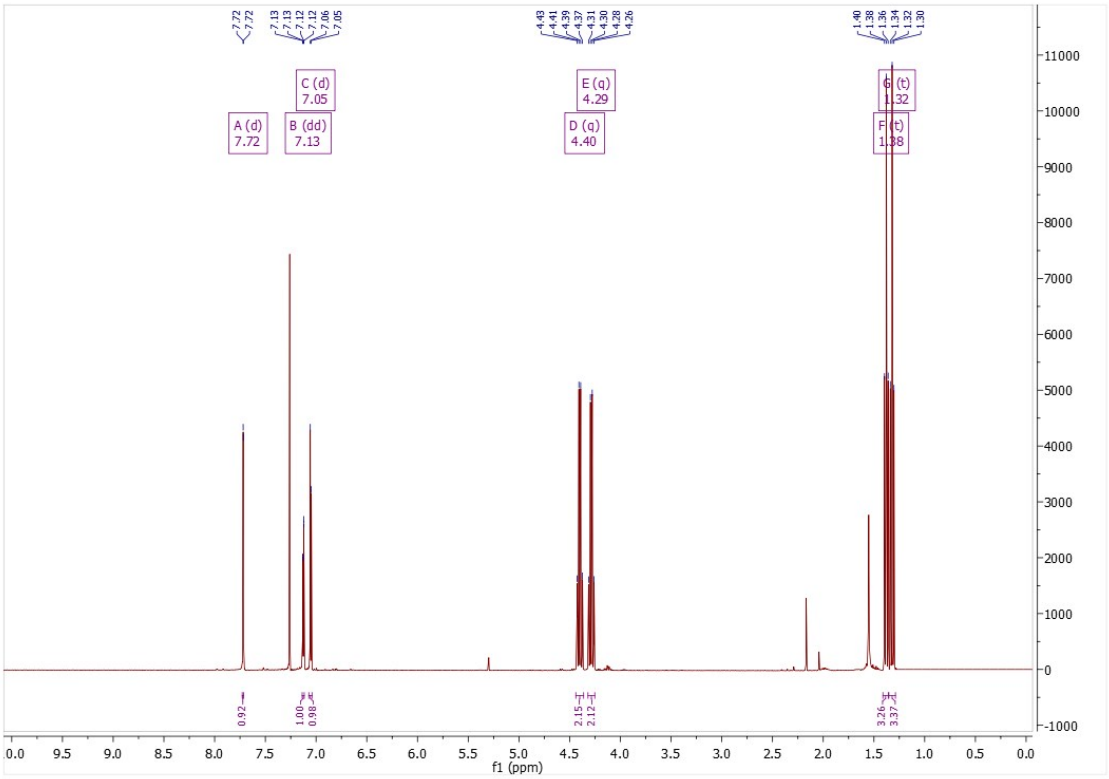

Fig. S5 ^{1}H NMR spectrum of **BrThDEM**.

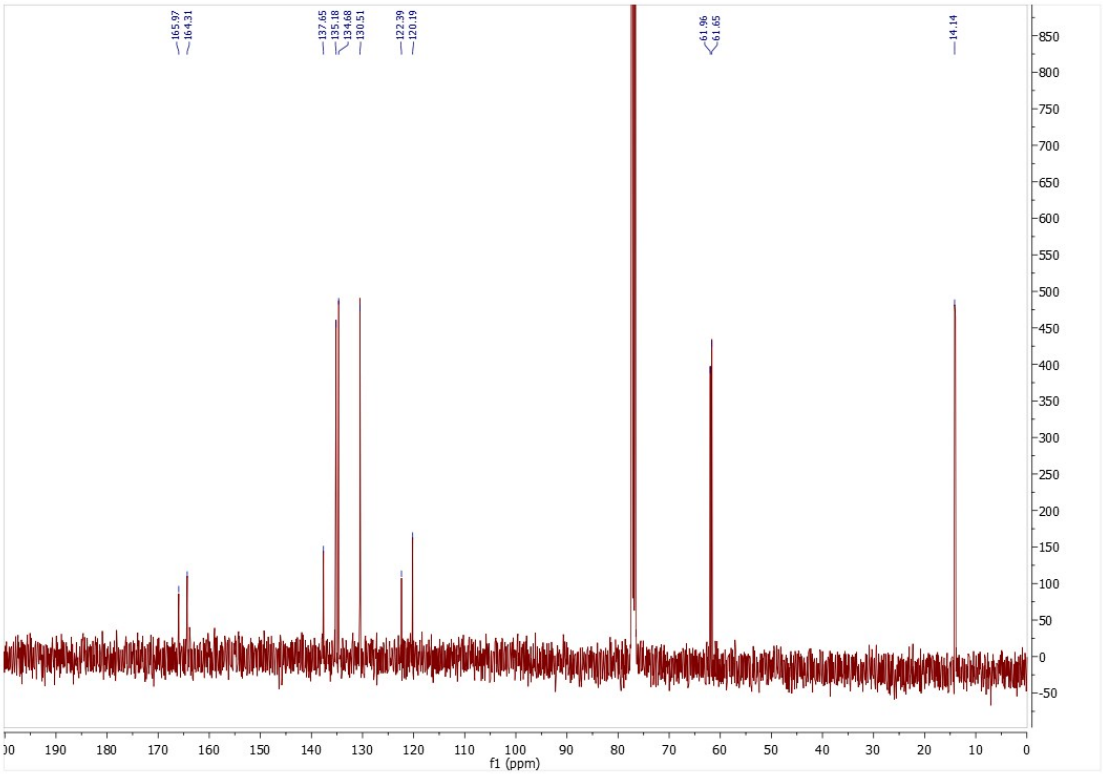

Fig. S6 ^{13}C NMR spectrum of **BrThDEM**.

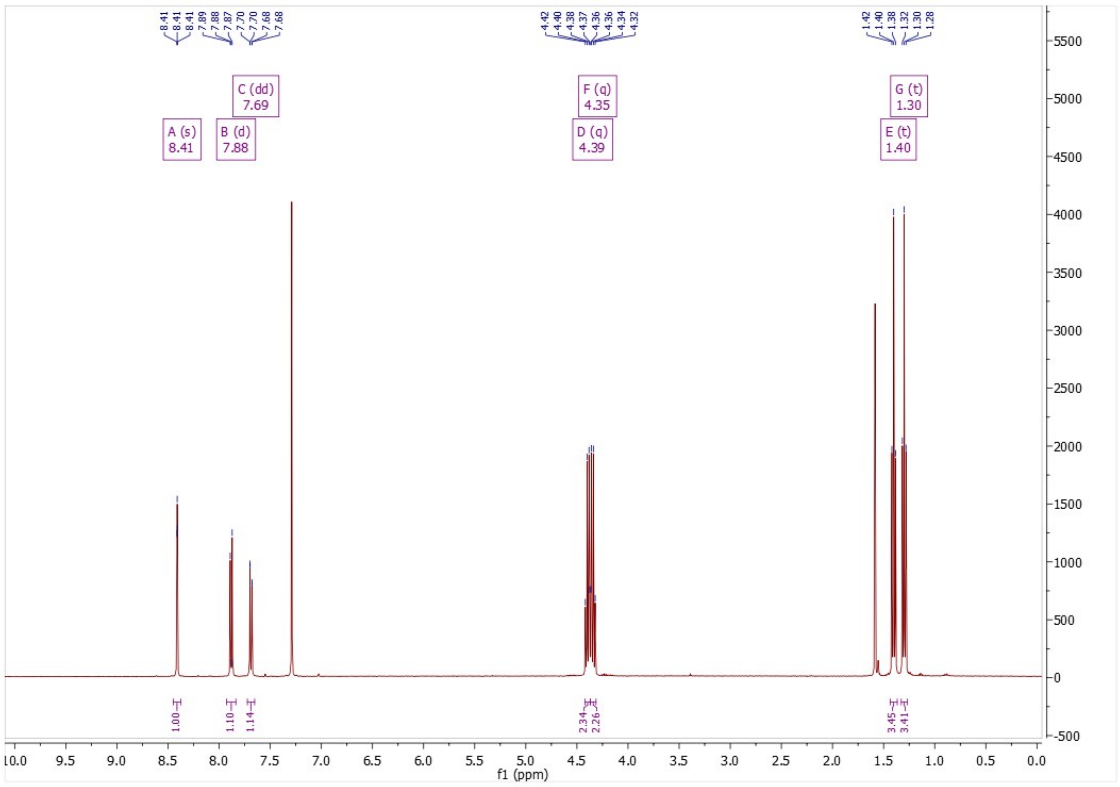

Fig. S7 ^{1}H NMR spectrum of **BrBTDEM**.

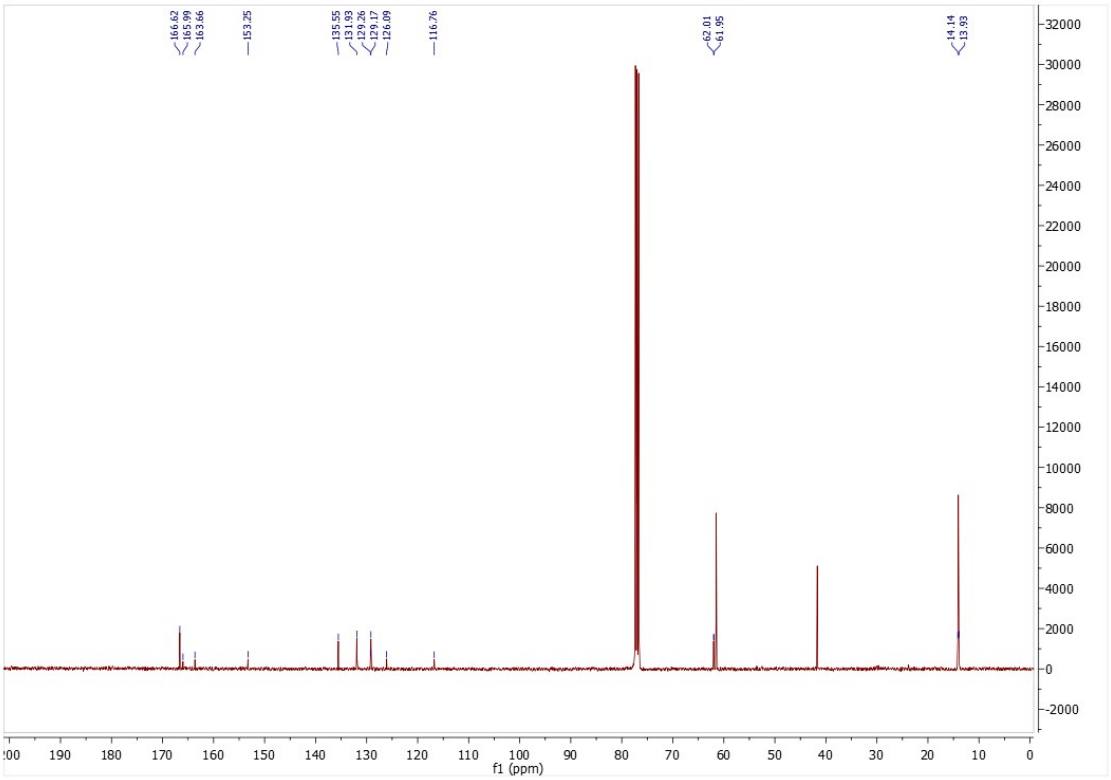

Fig. S8 ^{13}C NMR spectrum of **BrBTDEM**.

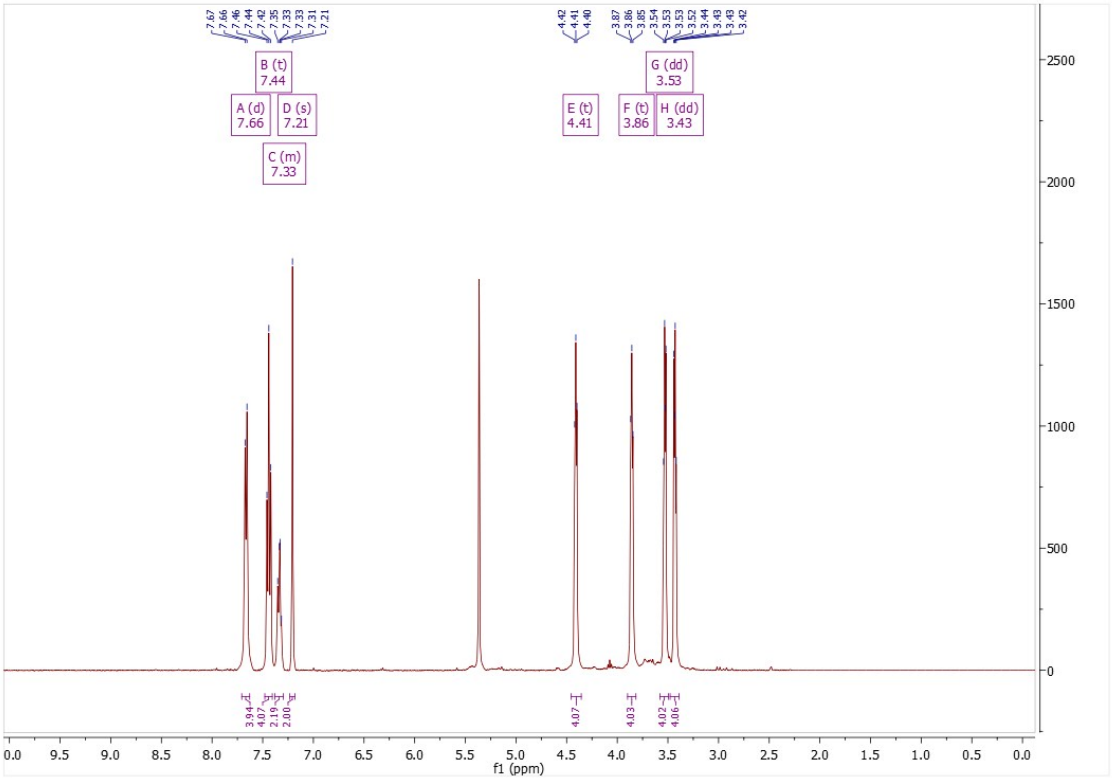

Fig. S9 ^{1}H NMR spectrum of **S1**.

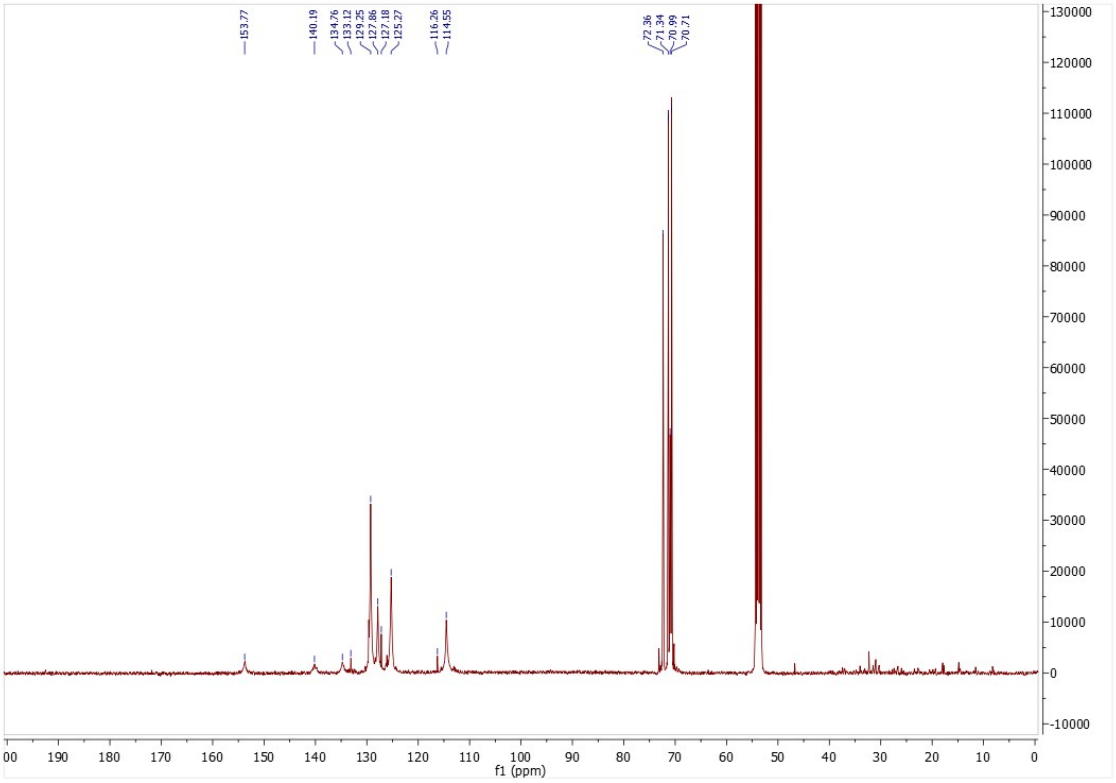

Fig. S10 ^{13}C NMR spectrum of **S1**.

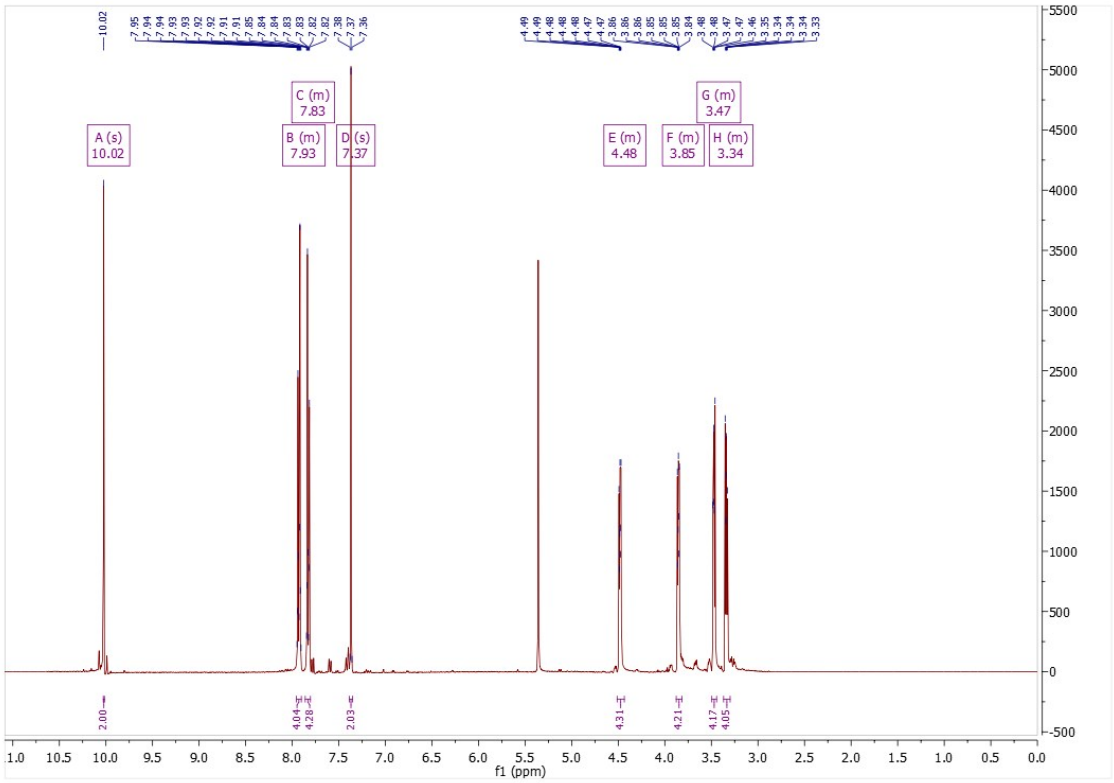

Fig. S11 ^{1}H NMR spectrum of **S2**.

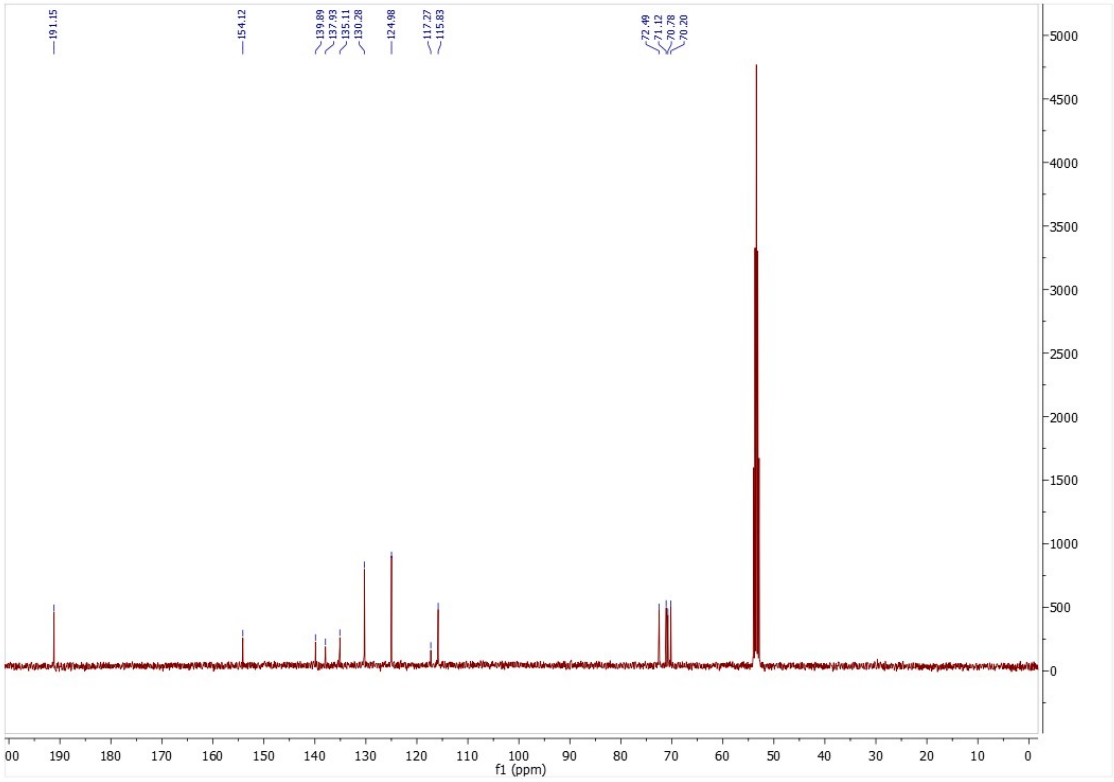

Fig. S12 ^{13}C NMR spectrum of **S2**.

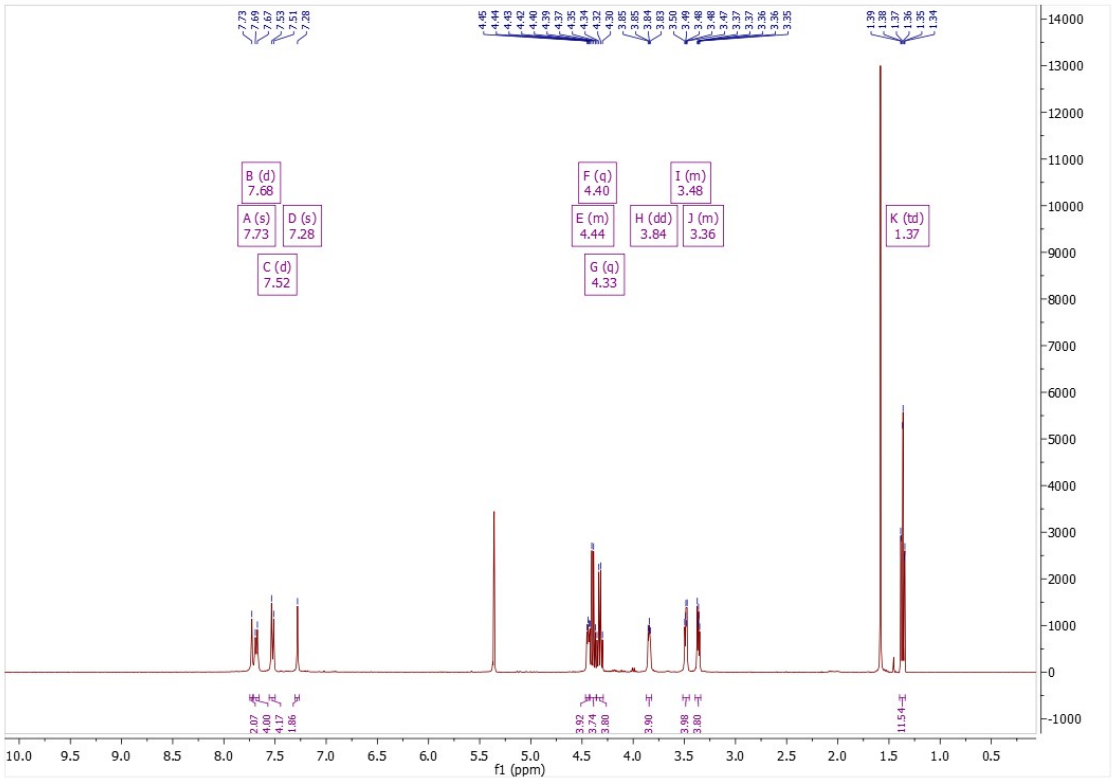

Fig. S13 ^{1}H NMR spectrum of **S3**.

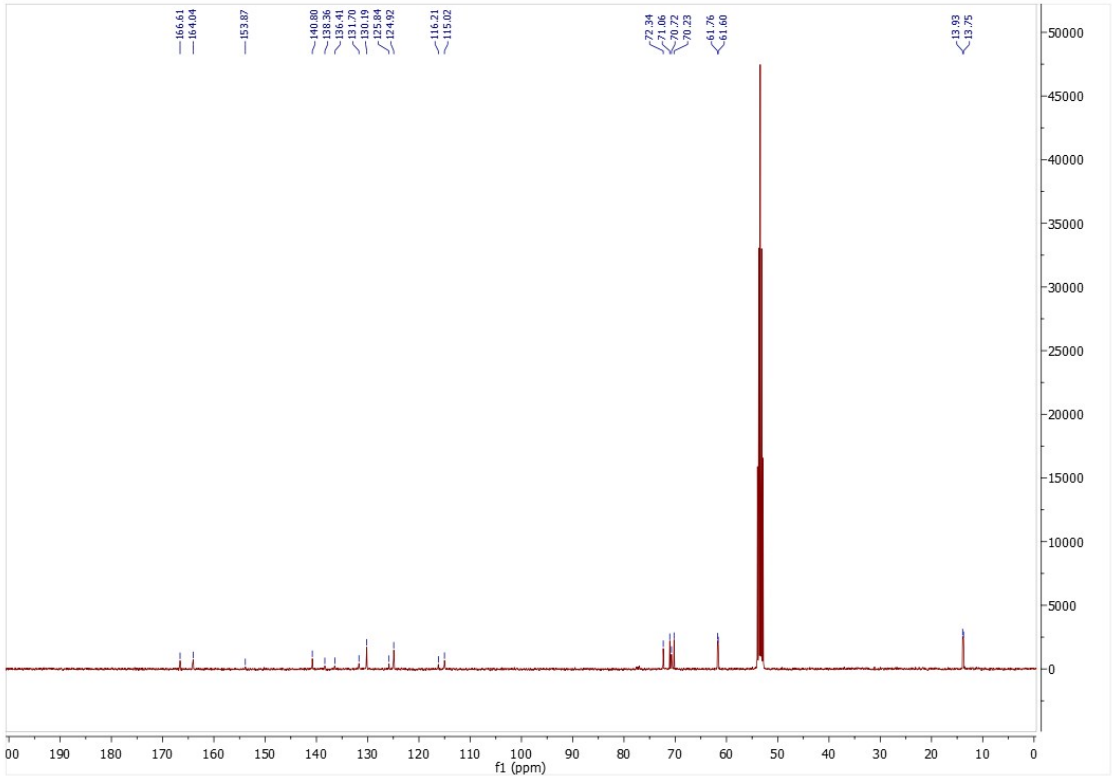

Fig. S14 ^{13}C NMR spectrum of **S3**.

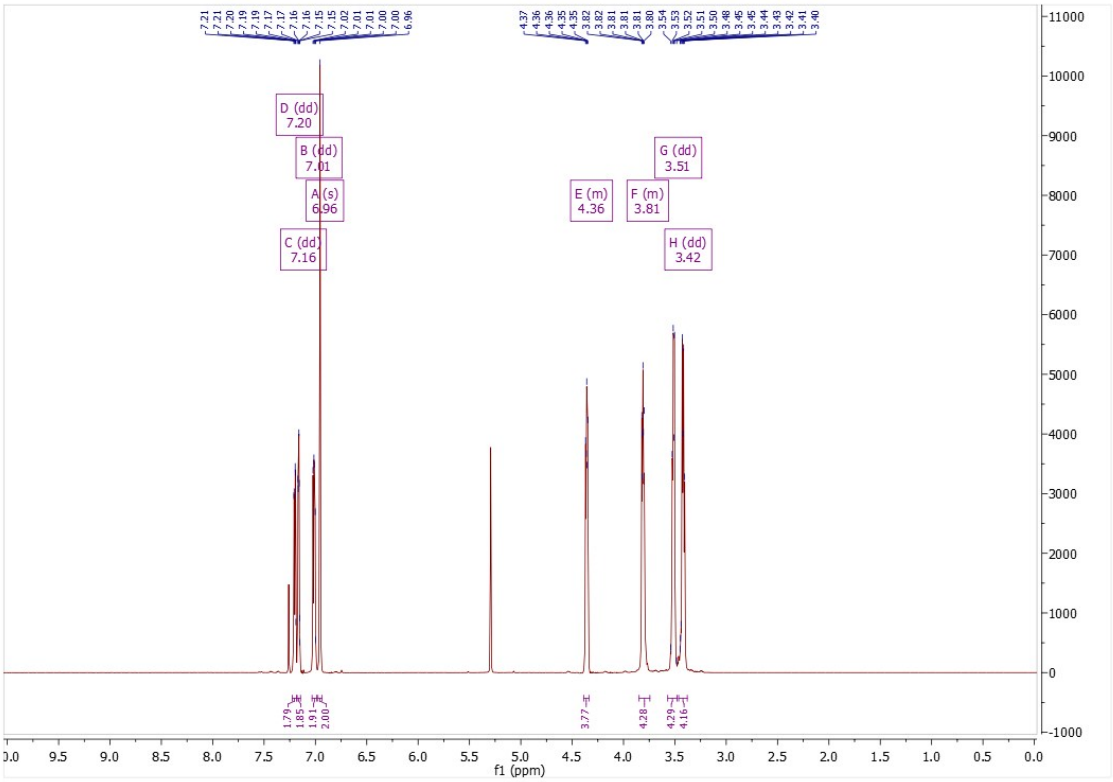

Fig. S15 ^{1}H NMR spectrum of **S4**.

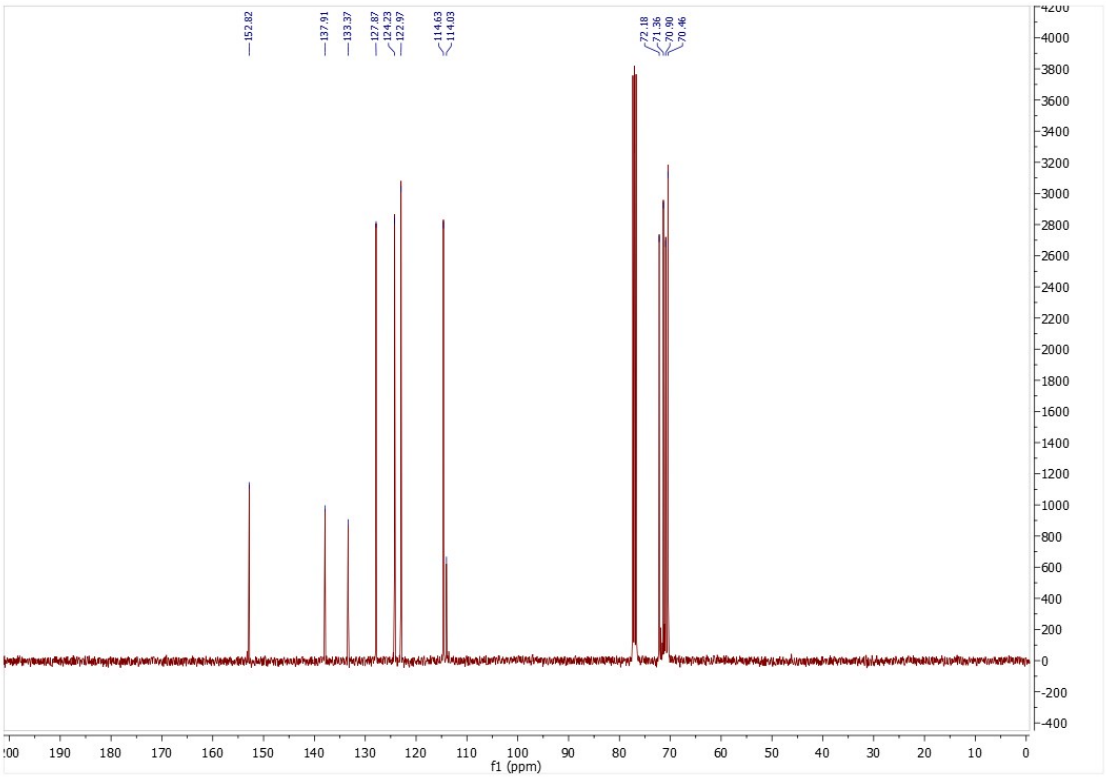

Fig. S16 ^{13}C NMR spectrum of **S4**.

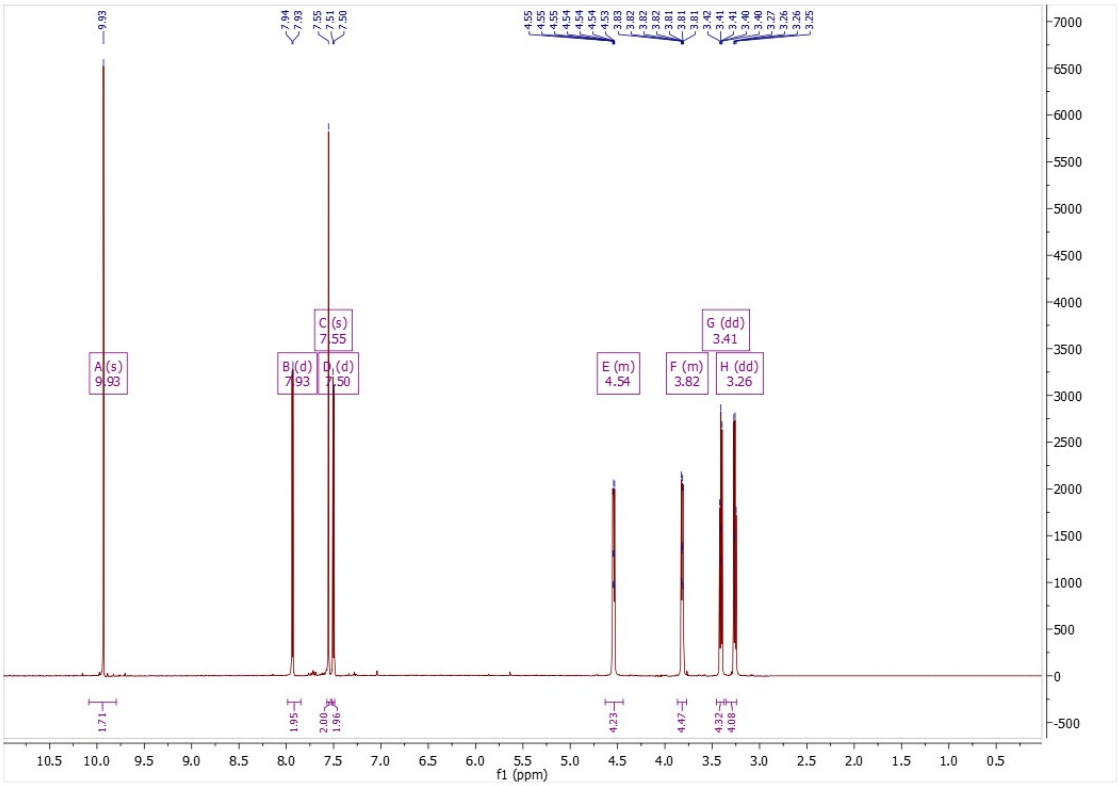

Fig. S17 ^{1}H NMR spectrum of **S5**.

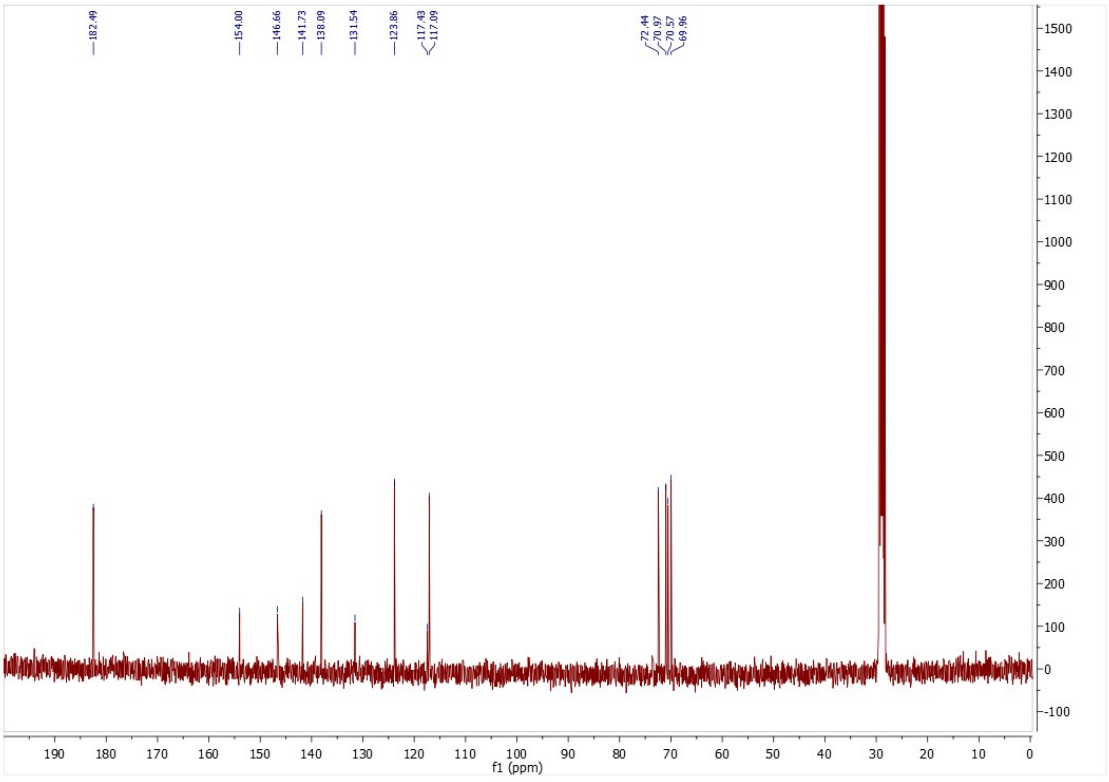

Fig. S18 ^{13}C NMR spectrum of **S5**.

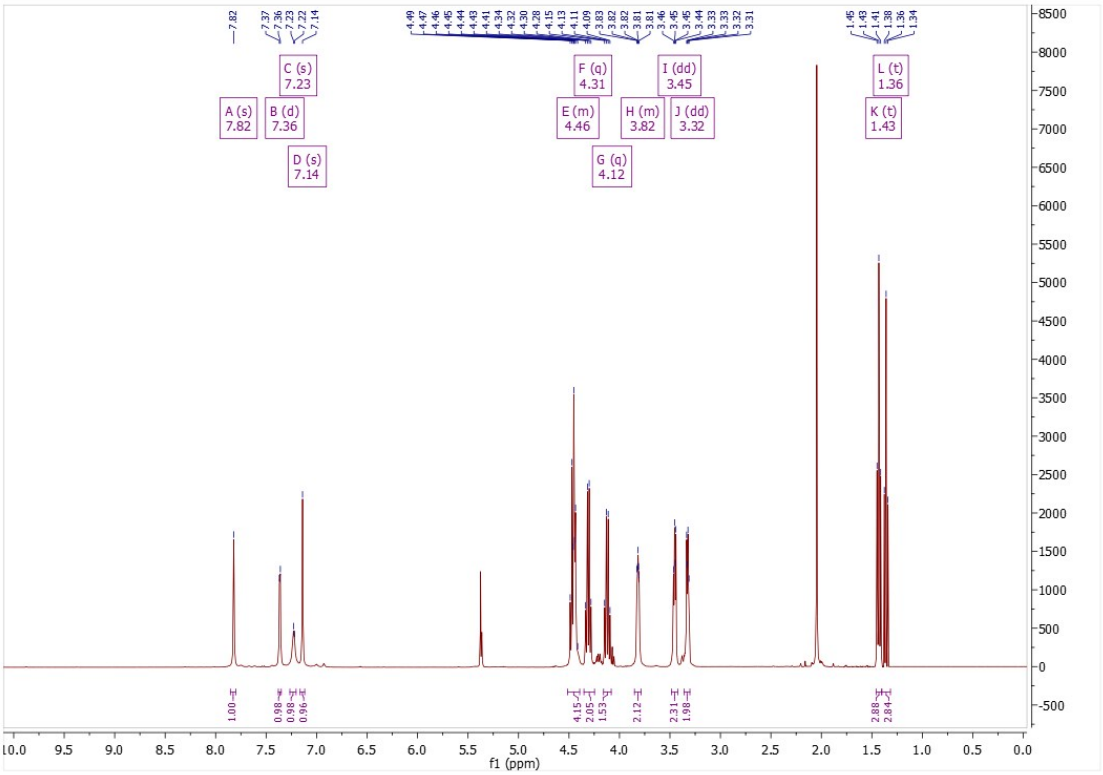

Fig. S19 ^{1}H NMR spectrum of **S6**.

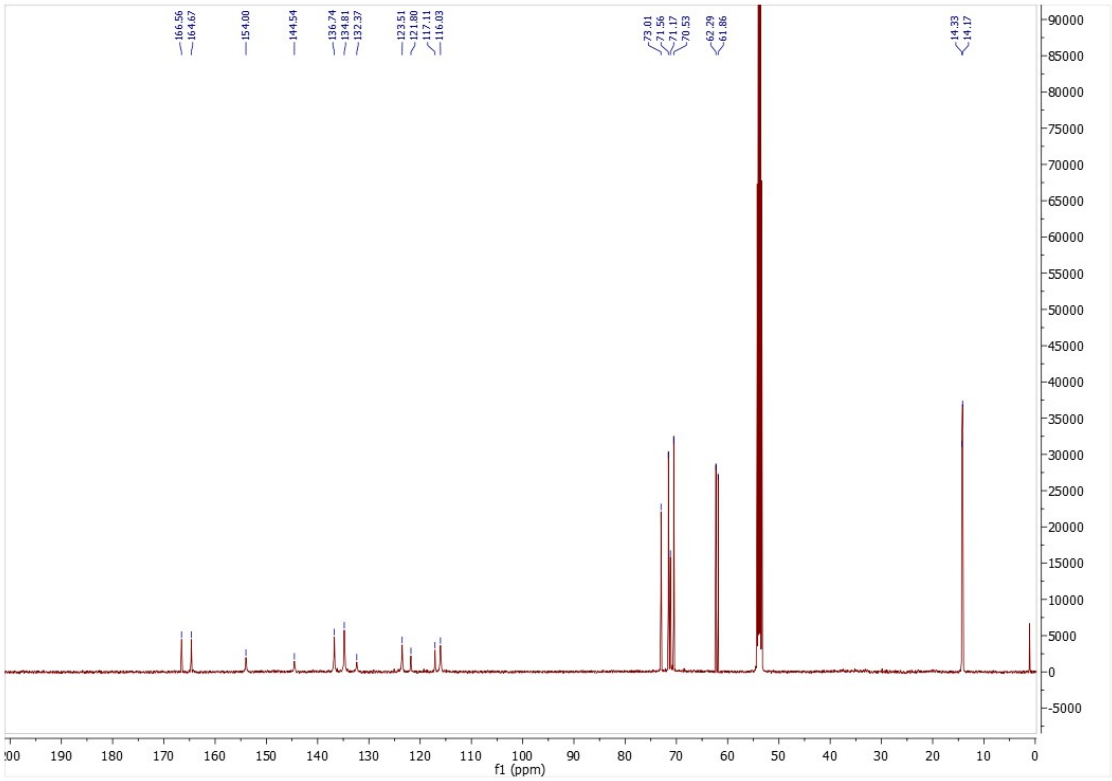

Fig. S20 ^{13}C NMR spectrum of **S6**.

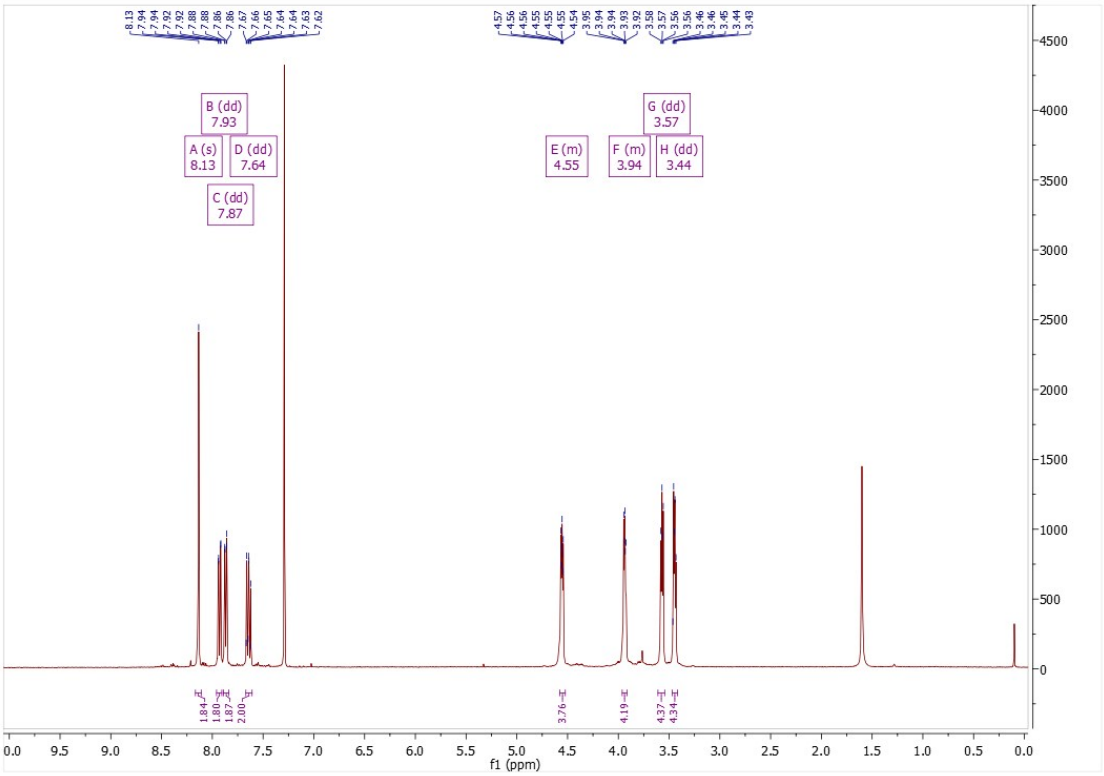

Fig. S21 ^{1}H NMR spectrum of **S7**.

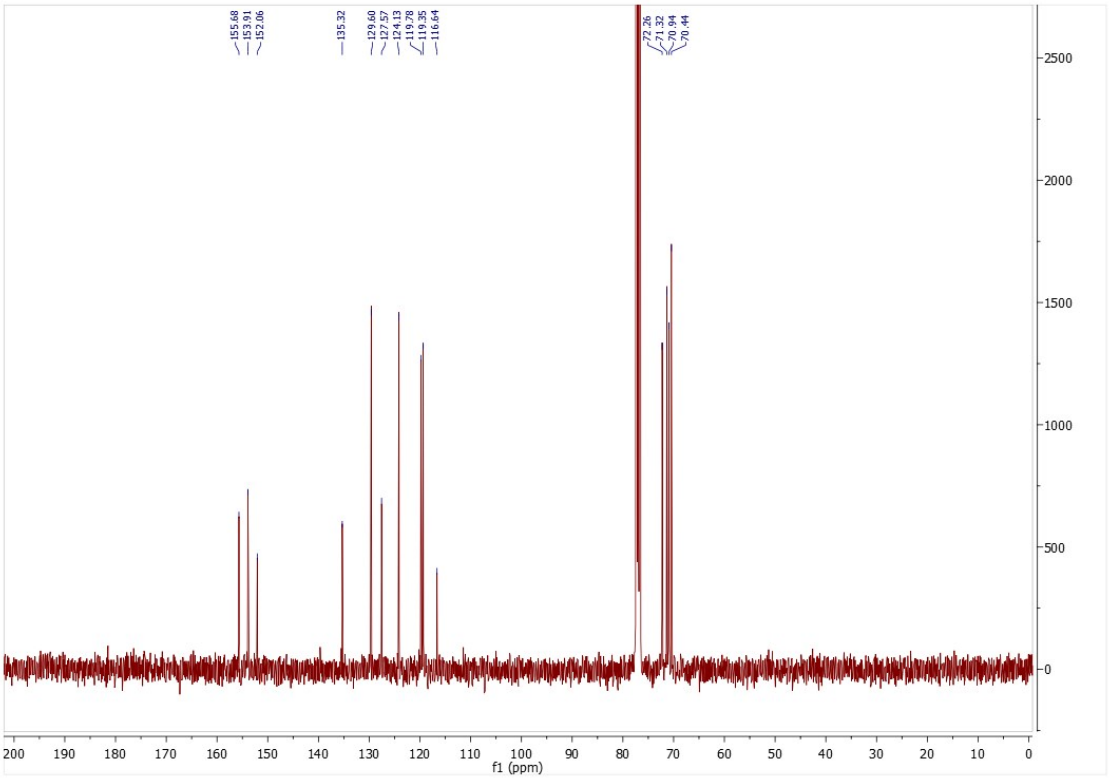

Fig. S22 ^{13}C NMR spectrum of **S7**.

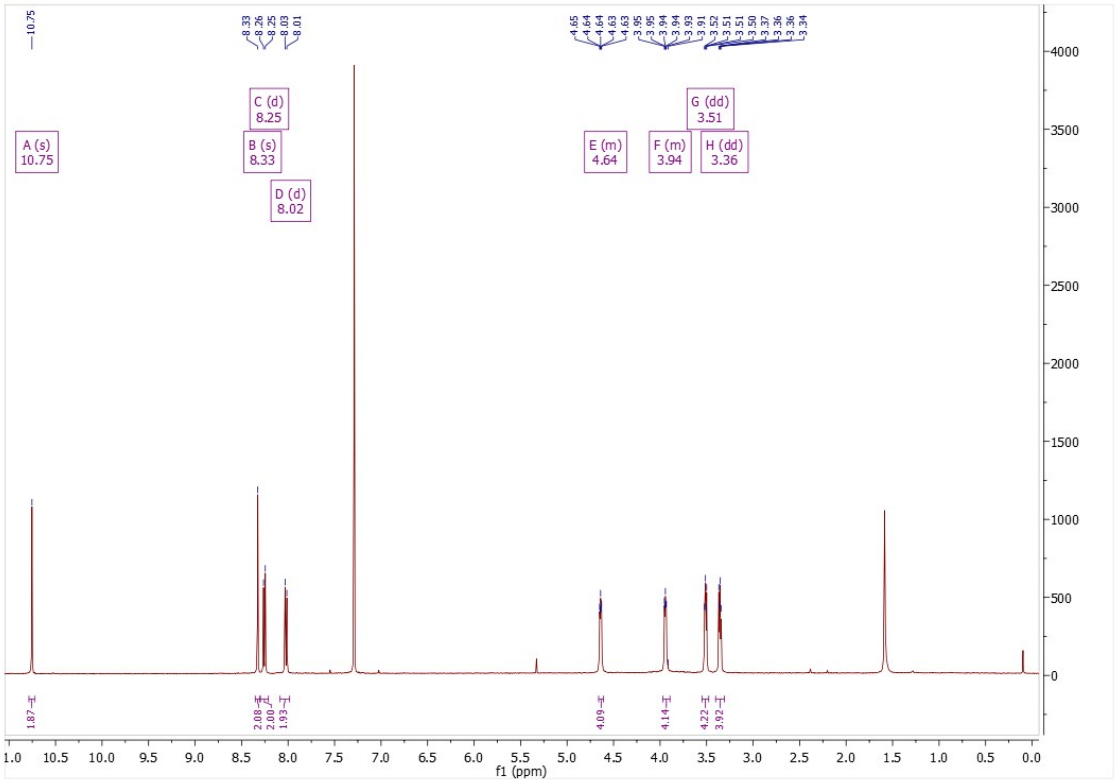

Fig. S23 ^{1}H NMR spectrum of **S8**.

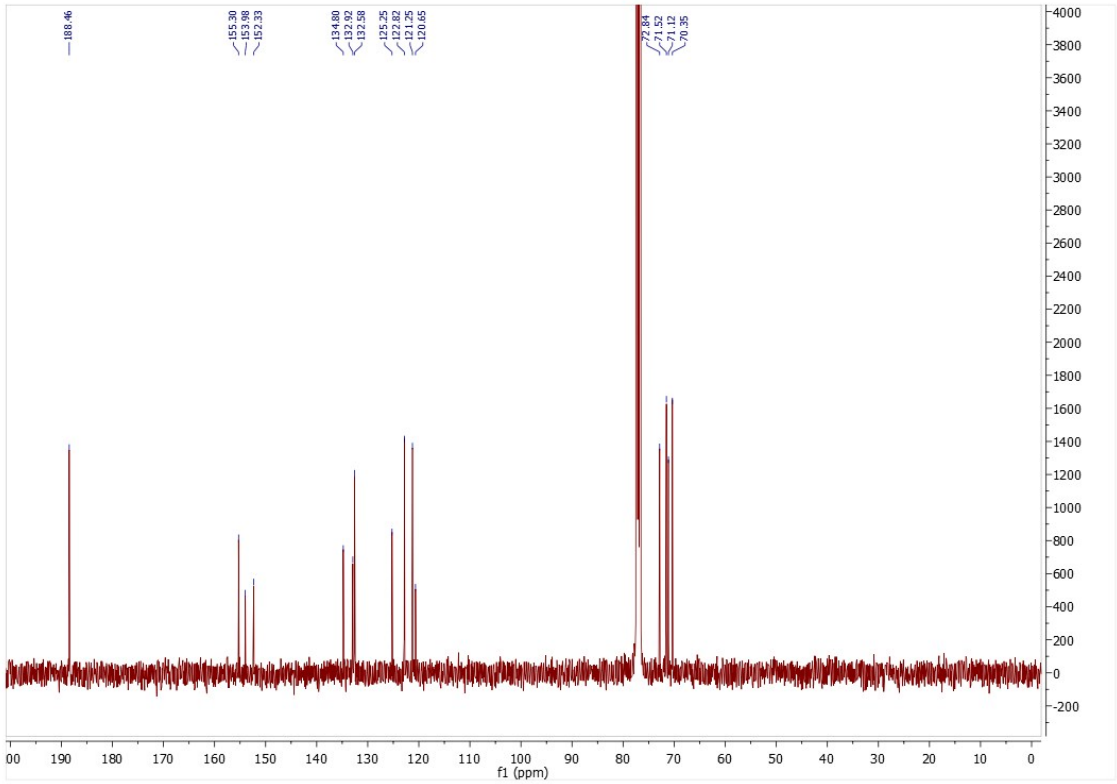

Fig. S24 ^{13}C NMR spectrum of **S8**.

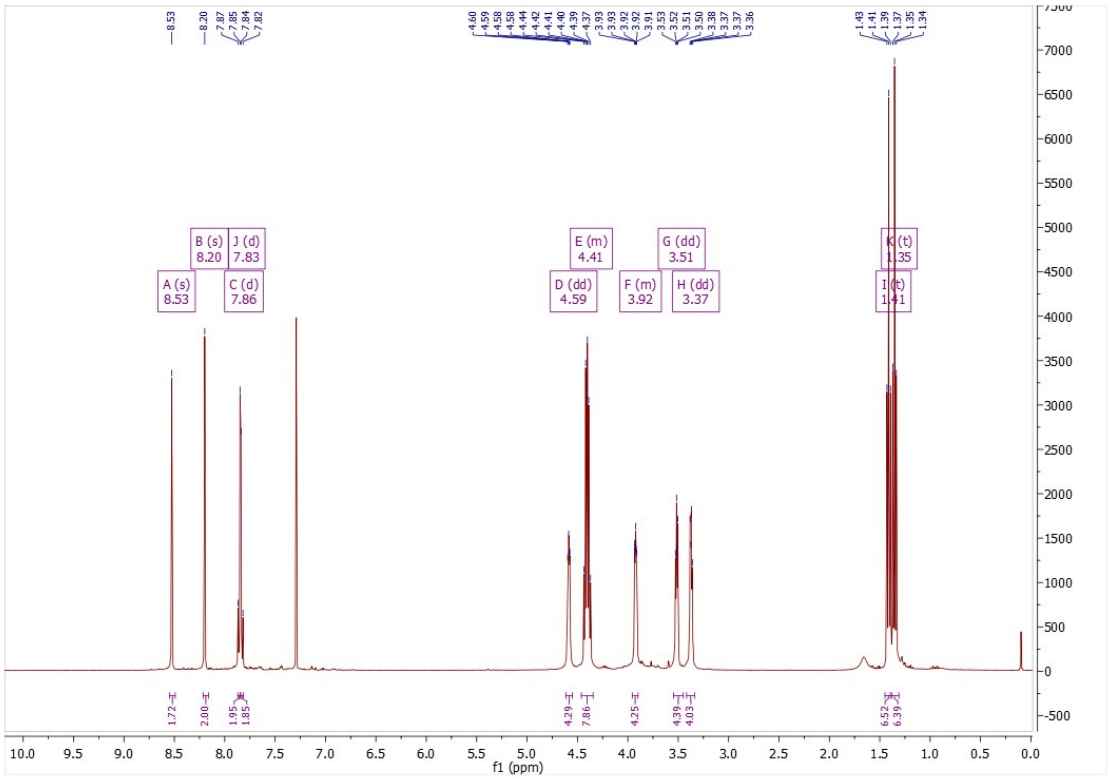

Fig. S25 ^{1}H NMR spectrum of **S9**.

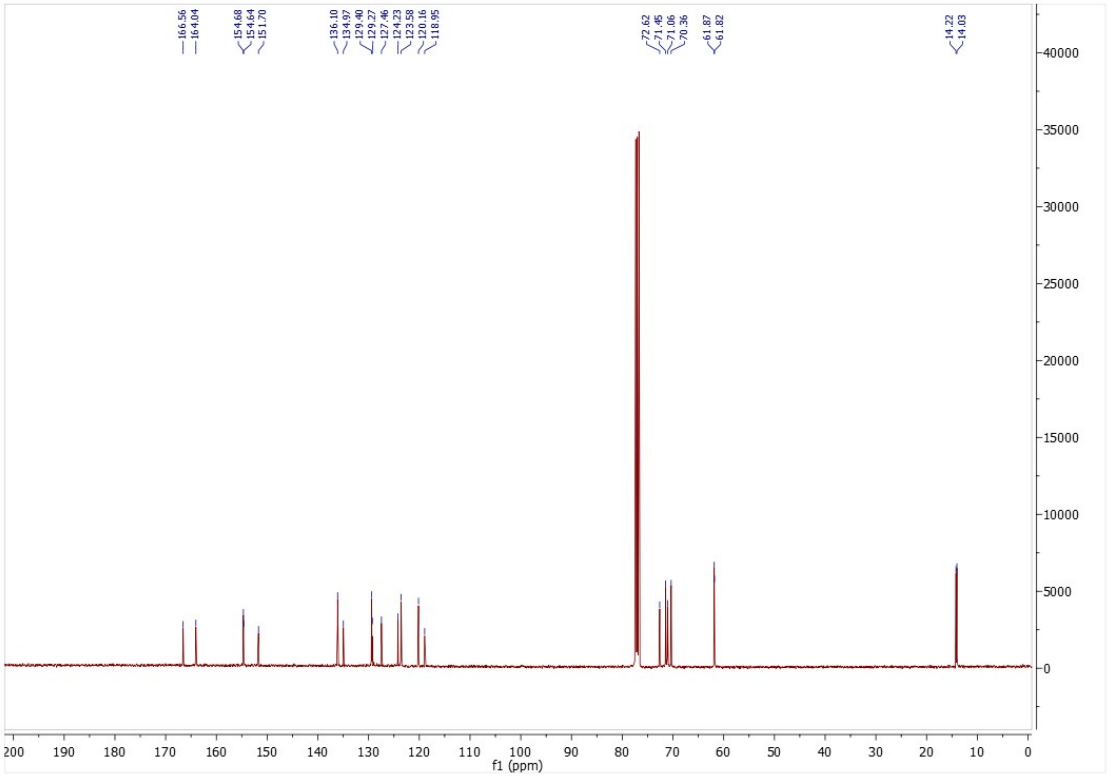

Fig. S26 ^{13}C NMR spectrum of **S9**.

4. Computational details

The geometry of the **(17-crown-5)T2** ionophore core was optimised, starting from the previously reported crystal structures.[3] Optimisations were performed using the ωB97XD functional and 6-31G* basis set, with a polarisable continuum modelling acetonitrile solvent. The central dihedral angles were measured as 180° and 68° for the unbound and Na-bound species.

Geometries of sensor molecules **S1-S9** were performed using the same conditions, except that the crown ether chain was replaced by -OMe groups. To model the twisted geometry of the Na-bound sensor, the central dihedral was fixed to 68°.

Optimised geometries were used to find the ideal range separation parameter, ω, such that Koopmans' theorem was best satisfied.[7] This states that the negative of the highest occupied molecular orbital (HOMO) energy (ε_H) should equal the vertical ionisation potential (*IP*) given by the difference in energy between the neutral and radical cation states. Thus, an optimal functional would satisfy the following equation:

$$J = \varepsilon_H + IP = 0 \qquad \textbf{(S1)}$$

To account for excited states, the same approach can be applied to the N+1 electron system; the energy of the HOMO of the radical anion should equal the *IP* of the radical anion (i.e. difference in energy between radical anion and neutral forms). Thus, a series of calculations of the neutral, radical anion, and radical cation at a range of ω values can be used to obtain the optimal value of ω where the following expression is a minimum:

$$J^2 = \sum_{i=0}^{i} [\varepsilon_H(N+i) + IP(N+i)]^2 \qquad \textbf{(S2)}$$

This tuning procedure was performed in the gas phase for each geometry, meaning the bound and unbound species possess different optimised ω values.

In contrast to previous "golden proportion approach" the number of computations was reduced following a different progression of ω values. This was initially set to 0.1 and increased by 0.1 until both the N and N+1 *J* values were negative, meaning ω is set too large. The value of ω was then decreased in 0.02 increments to achieve more data points close to optimal values. The two data sets (N and N+1 electrons) were then fit to separate exponential decay curves. These could be used to find the ω value where J = 0 if only the ionisation potential or only the electron affinity were of interest. Data points for the J^2 term were calculated numerically using the exponential fit equations at ω

intervals of 0.0001 over the range investigated, and the minimum J^2 point found. Given that all optimal ω values lay between 0.1 and 0.2, this gave tuned ω values to 4 decimal places from testing only 6 values (golden proportion method is typically 10 values). In addition to being easily scripted, plots of J and J^2 can be easily generated to check the fit of the data and identify potential outlier points:

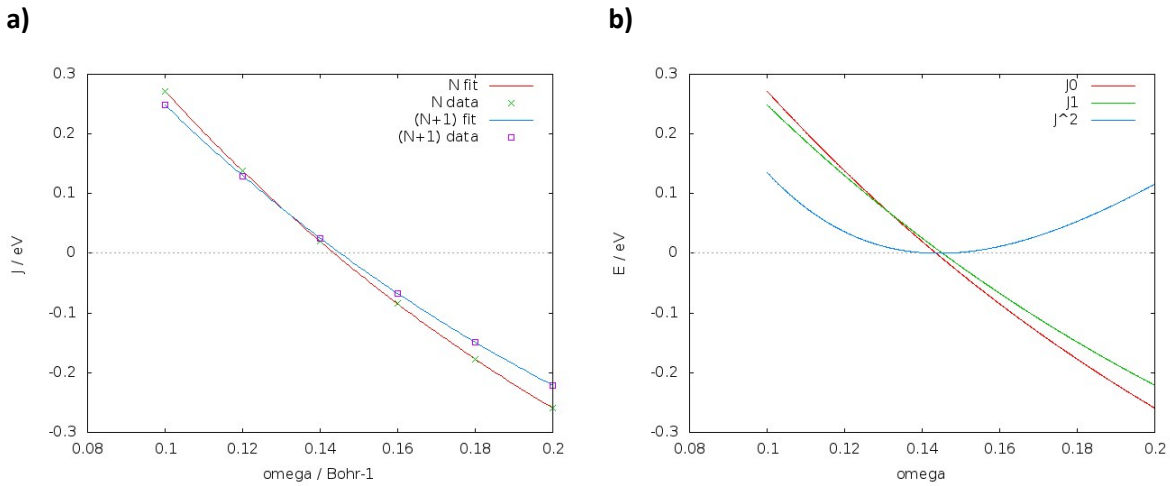

Fig. S27 a) Data points and exponential fit of two J functions (N and N+1 electron); b) numerically generated J and J^2 curves, from which the minimum value of J^2 can be found.

With the optimal ω value, time dependent DFT was used to calculate excitation energies and oscillator strengths for all sensor molecules, using a polarisable continuum to model acetonitrile solvent.

4. Atom economy determinations

The atom economy (*AE*) of the direct C-H heteroarylations between **(17-crown-5)T2** and of the hypothetical Stille cross-coupling of the bistrimethyltin analogue of **(17-crown-5)T2** (employed in previous literature)[2] with the various auxophores were calculated through the following equation:

$$AE(\%) = \frac{mass\ of\ atoms\ in\ desired\ product}{mass\ of\ atoms\ in\ reactants} \cdot 100 \qquad \textbf{(S3)}$$

Table S1. Comparison of the atom economies achieved by employing hypothetical Stille cross-coupling and the experimental direct C-H heteroarylation conditions.

Sensor	*AE* by hypothetical Stille cross-coupling (%)	*AE* by direct C-H heteroarylation (%)
S1	**51%**	**76%**
S2	**54%**	**78%**
S3	**63%**	**84%**
S4	**52%**	**76%**
S5	**54%**	**78%**
S6	**64%**	**84%**
S7	**56%**	**80%**
S8	**58%**	**81%**
S9	**66%**	**86%**

5. UV-Vis spectroscopy titration sample preparation and procedure in organic media

All of the UV-Vis spectroscopy measurements were conducted at 20 °C. $LiClO_4$, $NaClO_4$, $KClO_4$ and $Ca(ClO_4)_2.4H_2O$ salts were dissolved in 100 mL acetonitrile to afford stock solutions with concentrations of 0.02 M. 1 µmol of the various sensors (**S1-S9**) were dissolved in 25 mL of tetrahydrofuran to give stock solutions with concentrations of $4 \cdot 10^{-5}$ M. The various samples were then prepared by mixing different volumes from the above two solutions and an acetonitrile diluent as described in **table S2**. The concentration of each sensor in each sample was 0.02 mM. For the samples labelled as 15-crown-5, the samples were prepared in the same way as the 20 µmol ones, followed by addition of 50 µL of 15-crown-5.

Table S2. Sample preparation guidelines

Sample name	Volume of THF stock sensor solution (mL)	Volume of stock salt solution (mL)	Volume of acetonitrile diluent added (mL)	v/v ratio of THF/acetonitrile in samples
0.00 mM	1.500	0.000	1.500	1:1
0.66 mM	1.500	0.100	1.400	1:1
1.33 mM	1.500	0.200	1.300	1:1
2.00 mM	1.500	0.300	1.200	1:1
2.66 mM	1.500	0.400	1.100	1:1
3.33 mM	1.500	0.500	1.000	1:1
4.00 mM	1.500	0.600	0.900	1:1
4.66 mM	1.500	0.700	0.800	1:1
5.33 mM	1.500	0.800	0.700	1:1
6.00 mM	1.500	0.900	0.600	1:1
6.66 mM	1.500	1.000	0.500	1:1
15-crown-5	1.500	1.000	0.500	1:1

6. UV-Vis spectroscopy titration sample preparation and procedure in mixed aqueous/organic media

All of the UV-Vis spectroscopy measurements were conducted at 20 °C. 1 µmol of the various sensors (**S1-S9**) were dissolved in 5 mL of tetrahydrofuran to give stock solutions with concentrations of $2 \cdot 10^{-4}$ M. 0.3 mL of the sensor stock solution were then taken and diluted with 1.95 mL THF and 0.75 mL H_2O to afford a sensor solution in 3:1 THF/H_2O with a sensor concentration of 0.02 mM. $LiClO_4$, $NaClO_4$, $KClO_4$ and $Ca(ClO_4)_2.4H_2O$ salts were then added progressively in 0.15 mmol increments for 10 times.

For the samples labelled as 15-crown-5, the samples were prepared in the same way as the ones with the highest salt concentration, followed by addition of 50 μL of 15-crown-5.

7. UV-Vis spectroscopy titrations of S1-S9 against Na^+ in organic media

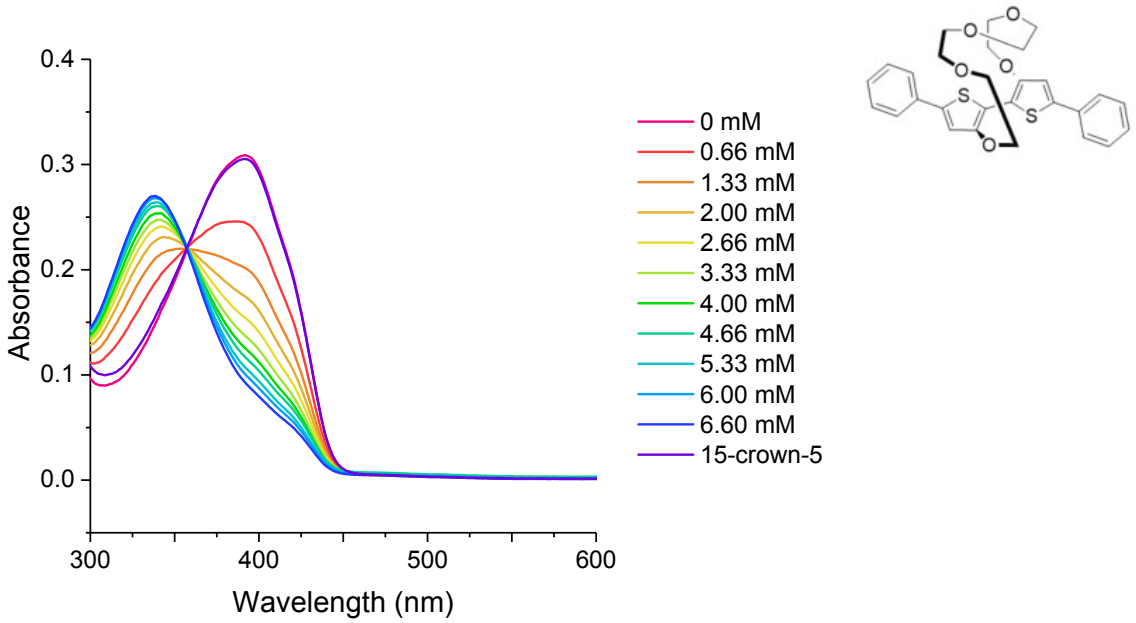

Fig. S28 UV-Vis absorption spectrum of **S1** in a 1:1 mixture of tetrahydrofuran:acetonitrile (**S1** concentration $4 \cdot 10^{-5}$ M) upon incrementing Na^+ concentrations (0-6.66 mM).

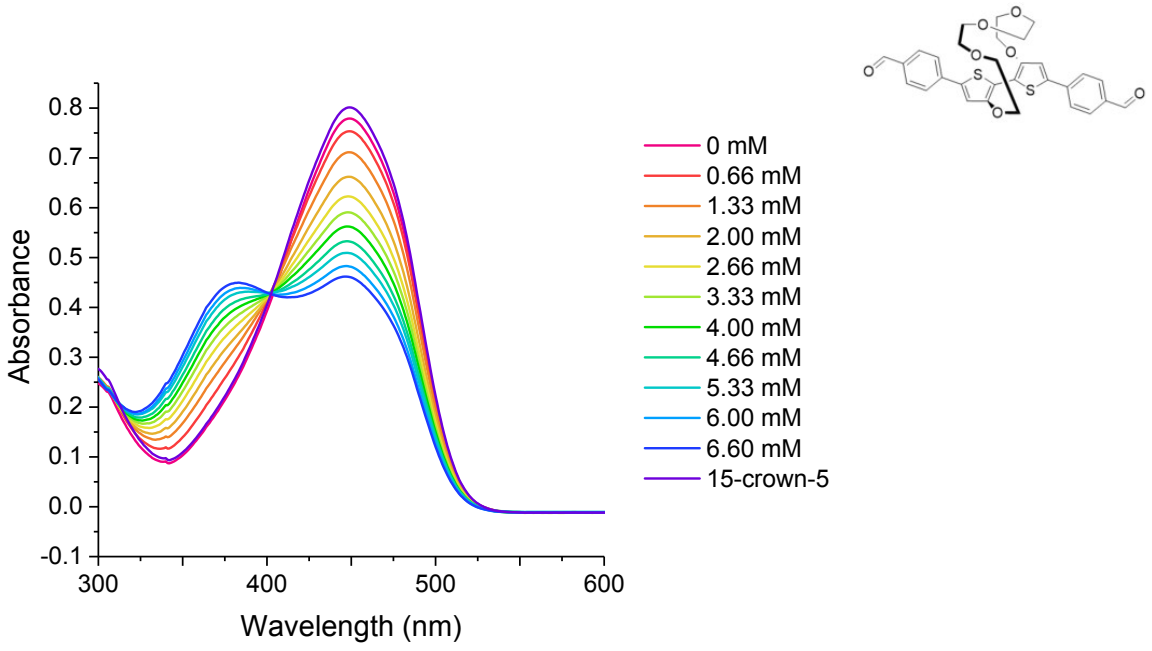

Fig. S29 UV-Vis absorption spectrum of **S2** in a 1:1 mixture of tetrahydrofuran:acetonitrile (**S2** concentration $4 \cdot 10^{-5}$ M) upon incrementing Na^+ concentrations (0-6.66 mM).

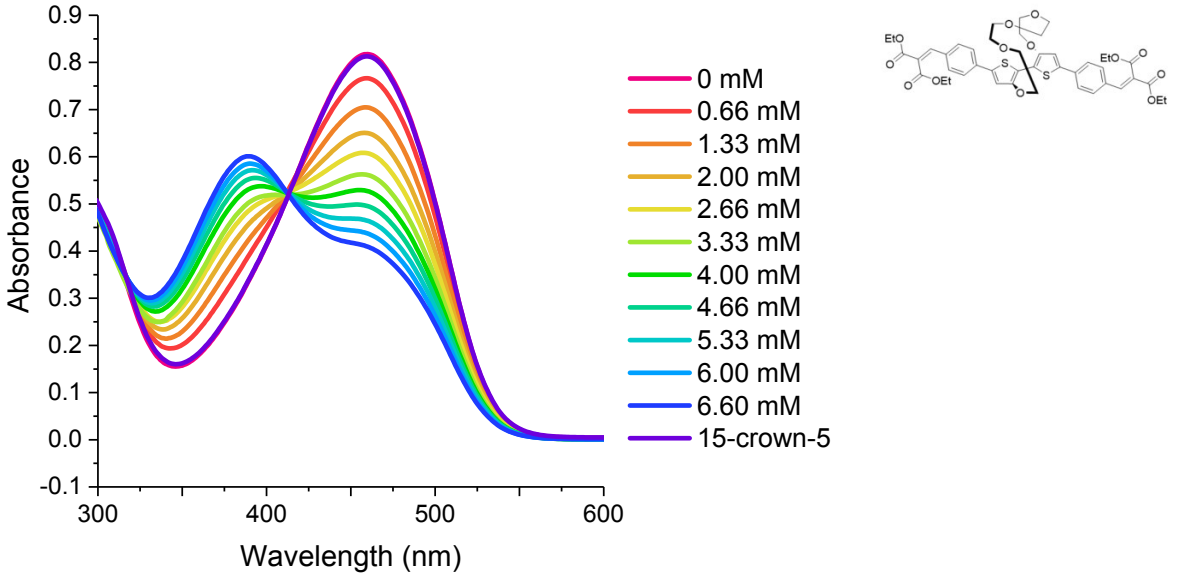

Fig. S30 UV-Vis absorption spectrum of **S3** in a 1:1 mixture of tetrahydrofuran:acetonitrile (**S3** concentration $4 \cdot 10^{-5}$ M) upon incrementing Na^+ concentrations (0-6.66 mM).

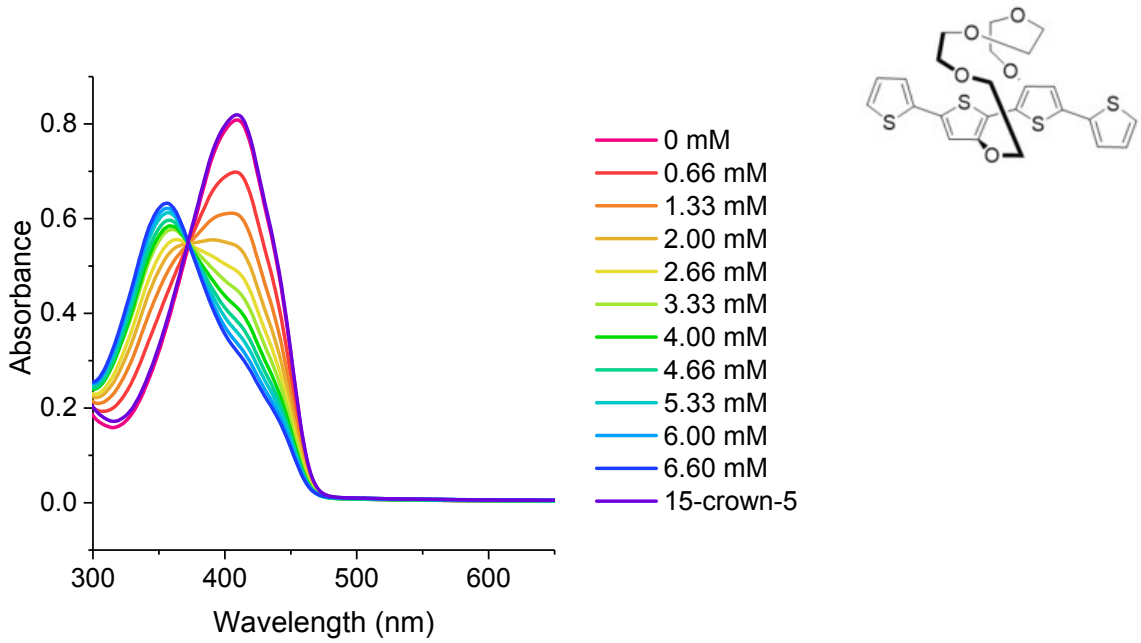

Fig. S31 UV-Vis absorption spectrum of **S4** in a 1:1 mixture of tetrahydrofuran:acetonitrile (**S4** concentration $4 \cdot 10^{-5}$ M) upon incrementing Na^+ concentrations (0-6.66 mM).

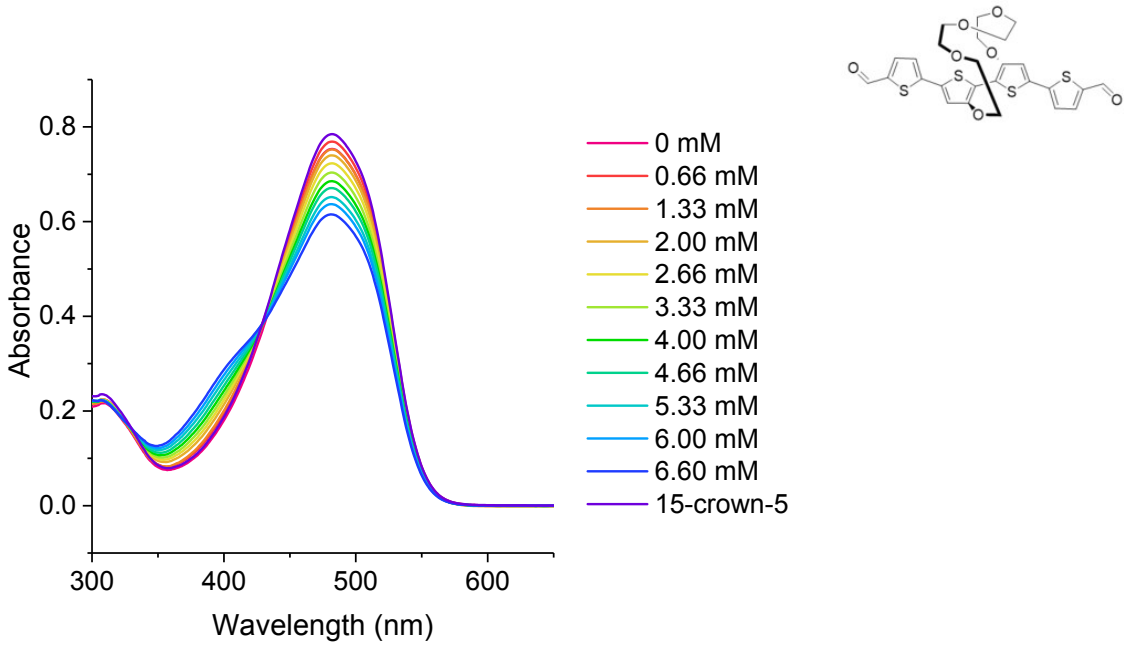

Fig. S32 UV-Vis absorption spectrum of **S5** in a 1:1 mixture of tetrahydrofuran:acetonitrile (**S5** concentration $4 \cdot 10^{-5}$ M) upon incrementing Na^+ concentrations (0-6.66 mM).

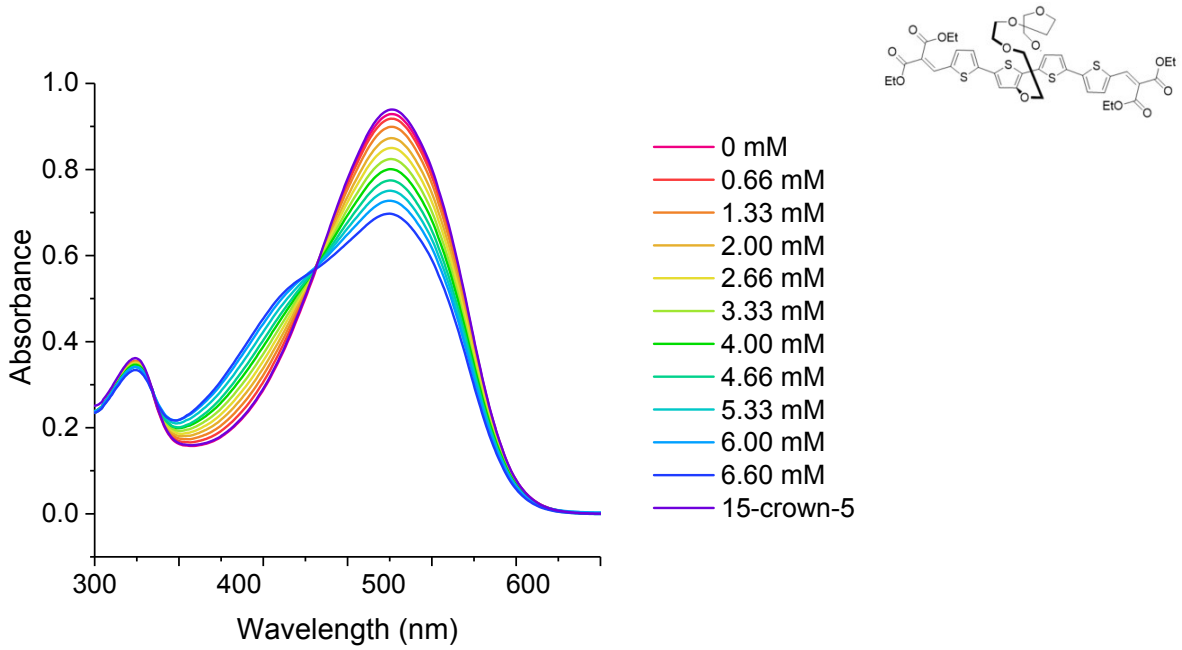

Fig. S33 UV-Vis absorption spectrum of **S6** in a 1:1 mixture of tetrahydrofuran:acetonitrile (**S6** concentration $4 \cdot 10^{-5}$ M) upon incrementing Na^+ concentrations (0-6.66 mM).

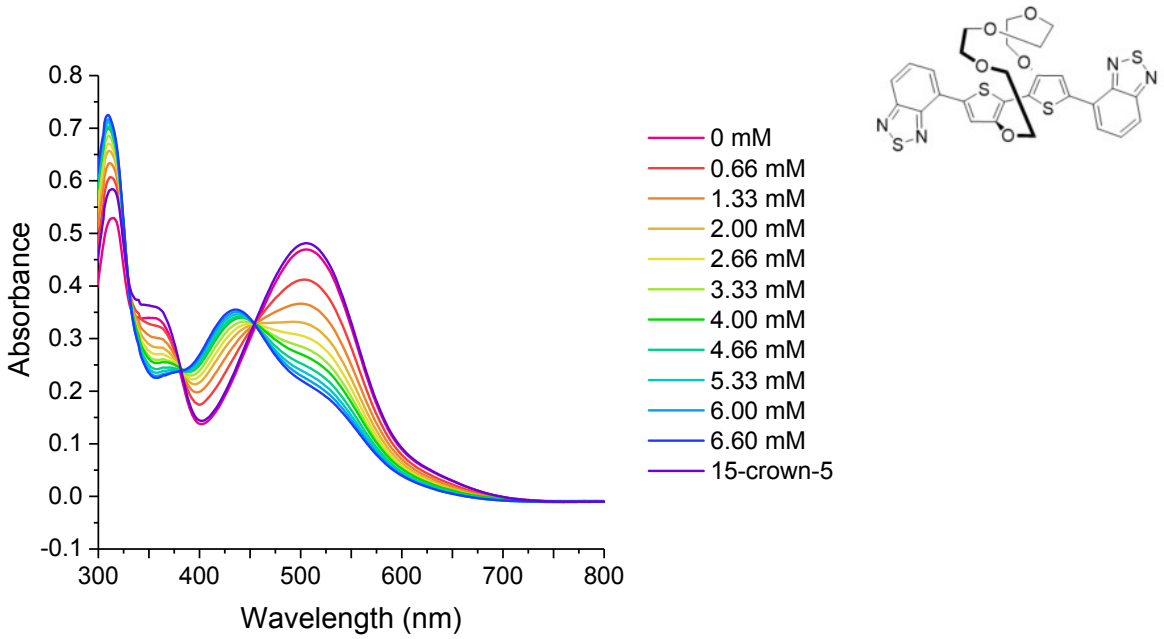

Fig. S34 UV-Vis absorption spectrum of **S7** in a 1:1 mixture of tetrahydrofuran:acetonitrile (**S7** concentration $4 \cdot 10^{-5}$ M) upon incrementing Na^+ concentrations (0-6.66 mM).

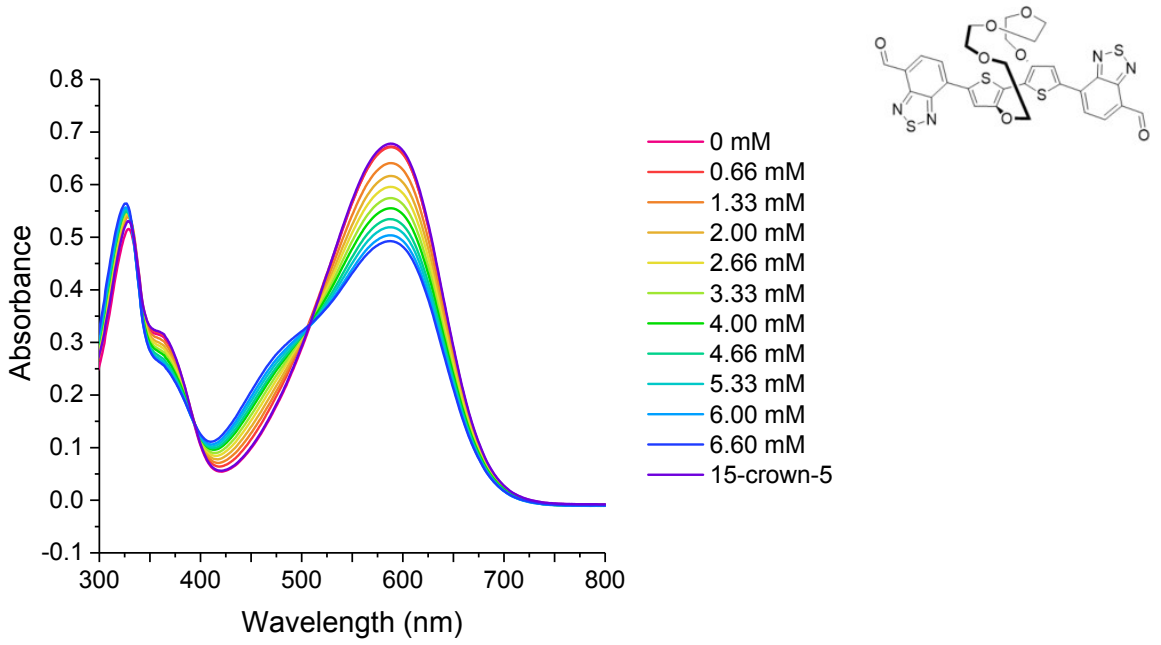

Fig. S35 UV-Vis absorption spectrum of **S8** in a 1:1 mixture of tetrahydrofuran:acetonitrile (**S8** concentration $4 \cdot 10^{-5}$ M) upon incrementing Na^+ concentrations (0-6.66 mM).

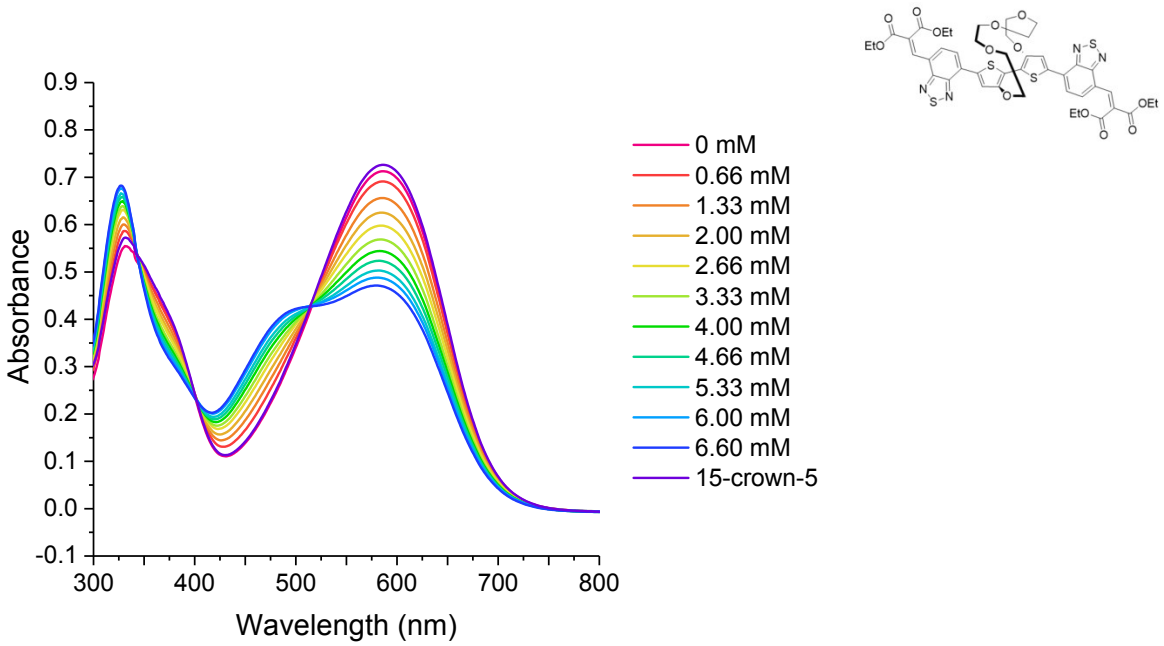

Fig. S36 UV-Vis absorption spectrum of **S9** in a 1:1 mixture of tetrahydrofuran:acetonitrile (**S9** concentration $4 \cdot 10^{-5}$ M) upon incrementing Na^+ concentrations (0-6.66 mM).

8. UV-Vis spectroscopy titrations of S1-S9 against Li^+, K^+ and Ca^{2+} in organic media

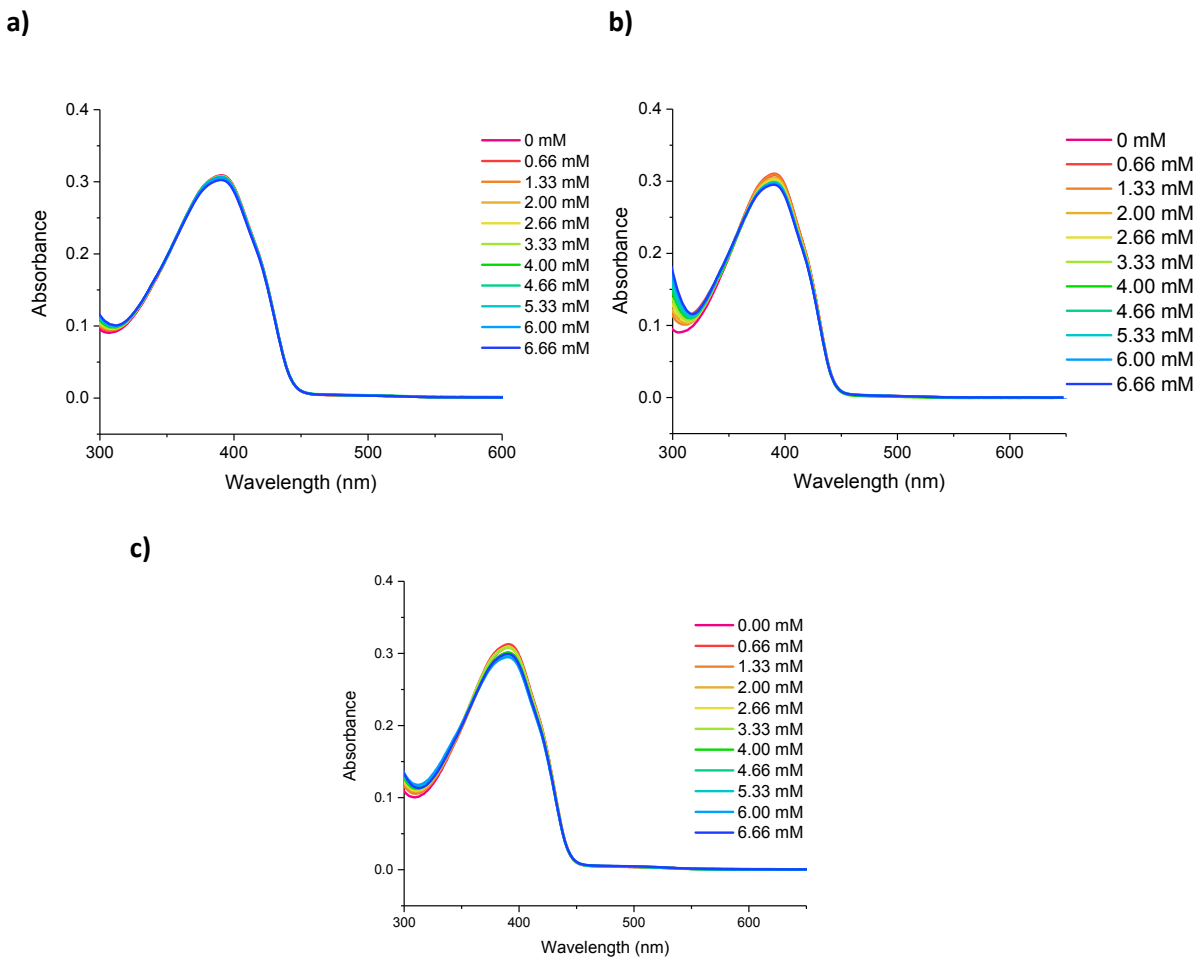

Fig. S37 UV-Vis absorption spectra of **S1** in a 1:1 mixture of tetrahydrofuran:acetonitrile (**S1** concentration $4 \cdot 10^{-5}$ M) upon incrementing a) Li^+, b) K^+ and c) Ca^{2+} concentrations (0-6.66 mM).

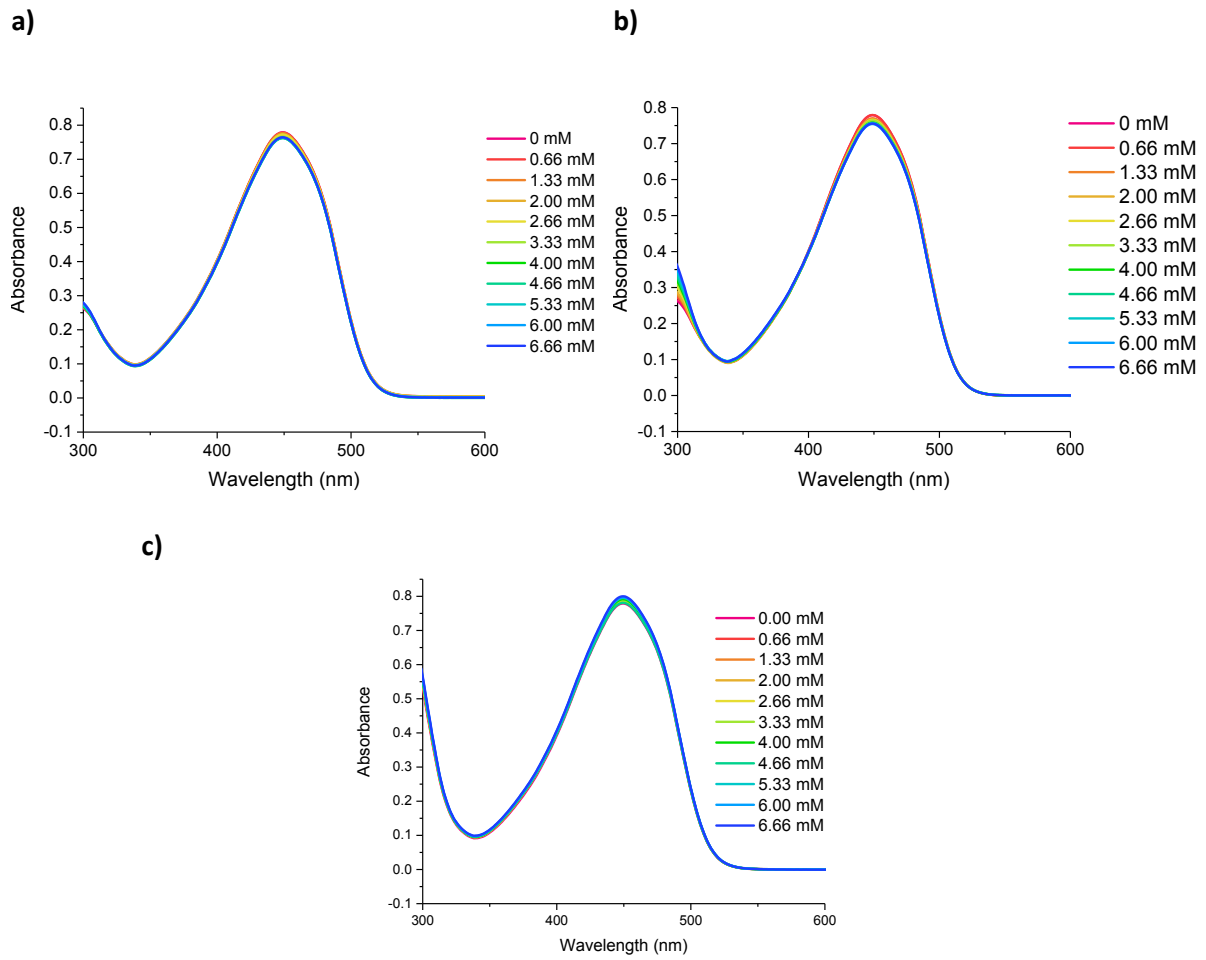

Fig. S38 UV-Vis absorption spectra of **S2** in a 1:1 mixture of tetrahydrofuran:acetonitrile (**S2** concentration $4 \cdot 10^{-5}$ M) upon incrementing a) Li^+, b) K^+ and c) Ca^{2+} concentrations (0-6.66 mM).

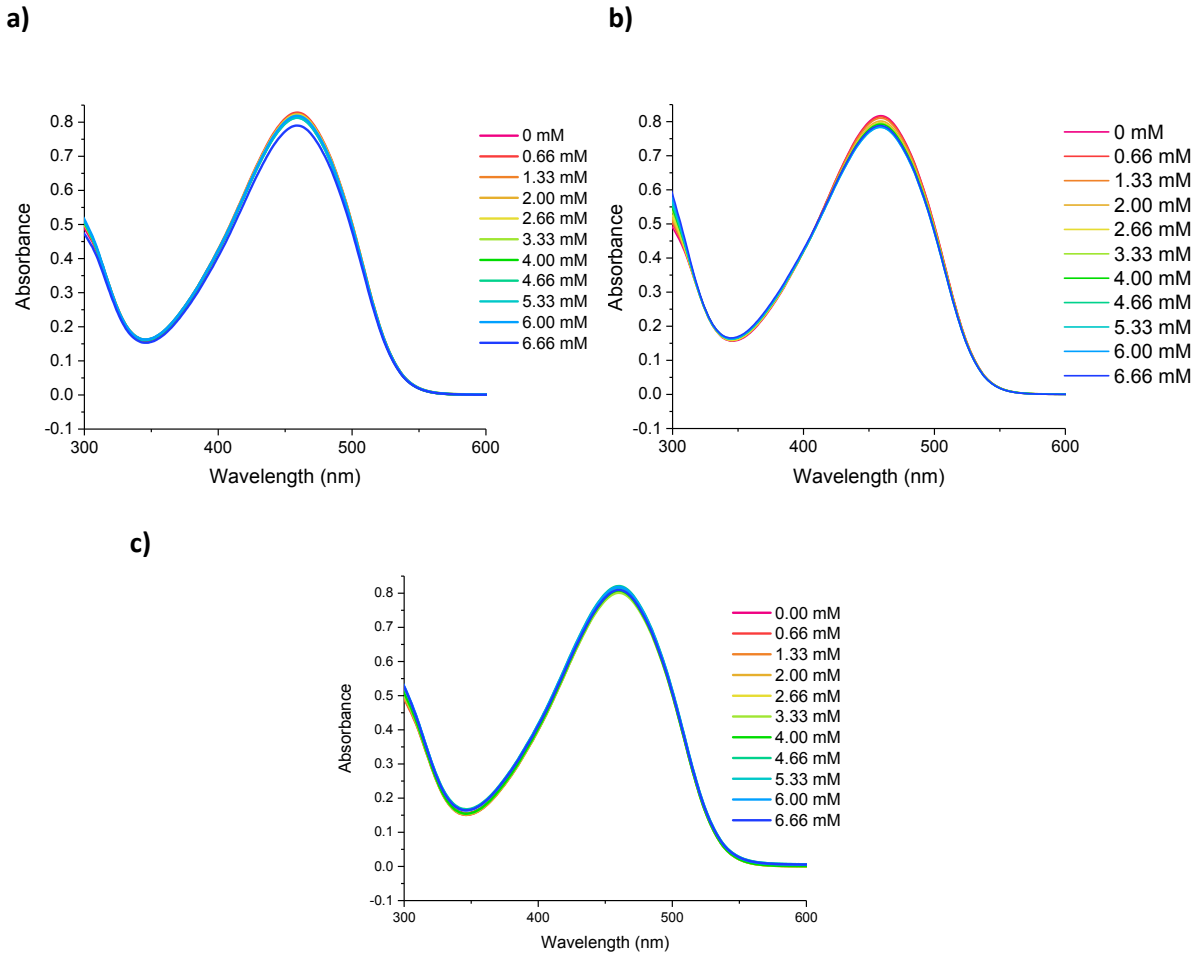

Fig. S39 UV-Vis absorption spectra of **S3** in a 1:1 mixture of tetrahydrofuran:acetonitrile (**S3** concentration $4 \cdot 10^{-5}$ M) upon incrementing a) Li^+, b) K^+ and c) Ca^{2+} concentrations (0-6.66 mM).

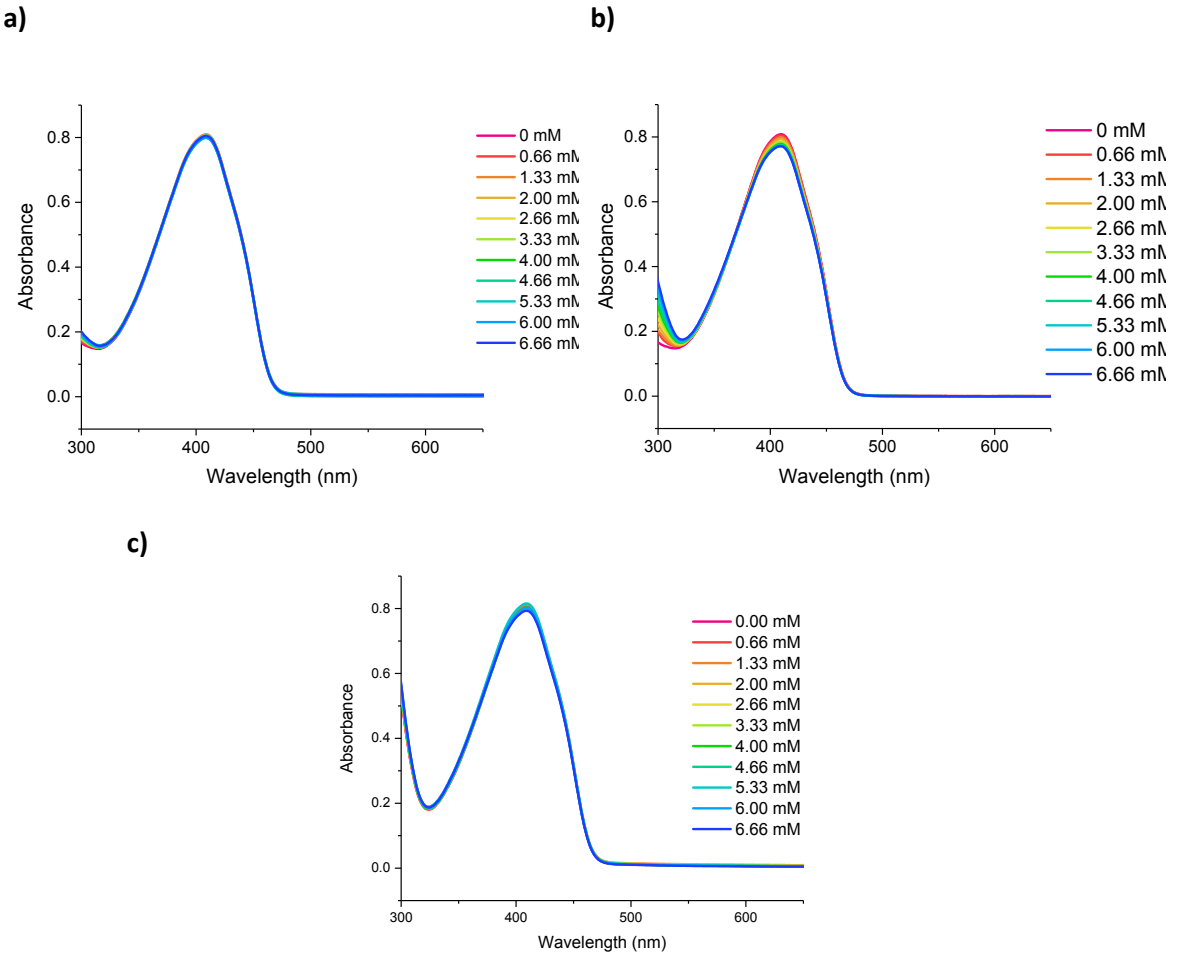

Fig. S40 UV-Vis absorption spectra of **S4** in a 1:1 mixture of tetrahydrofuran:acetonitrile (**S4** concentration $4 \cdot 10^{-5}$ M) upon incrementing a) Li^+, b) K^+ and c) Ca^{2+} concentrations (0-6.66 mM).

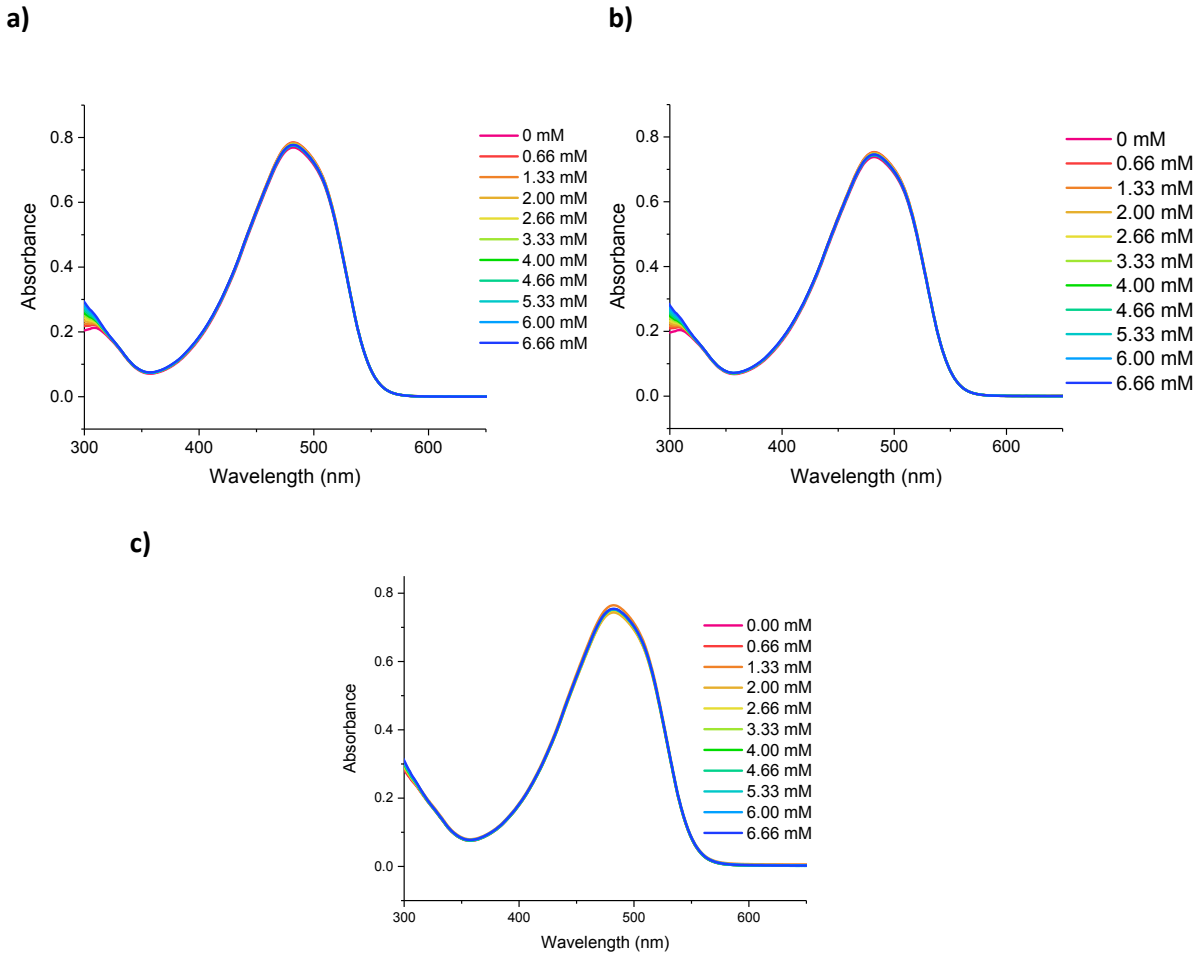

Fig. S41 UV-Vis absorption spectra of **S5** in a 1:1 mixture of tetrahydrofuran:acetonitrile (**S5** concentration $4 \cdot 10^{-5}$ M) upon incrementing a) Li^+, b) K^+ and c) Ca^{2+} concentrations (0-6.66 mM).

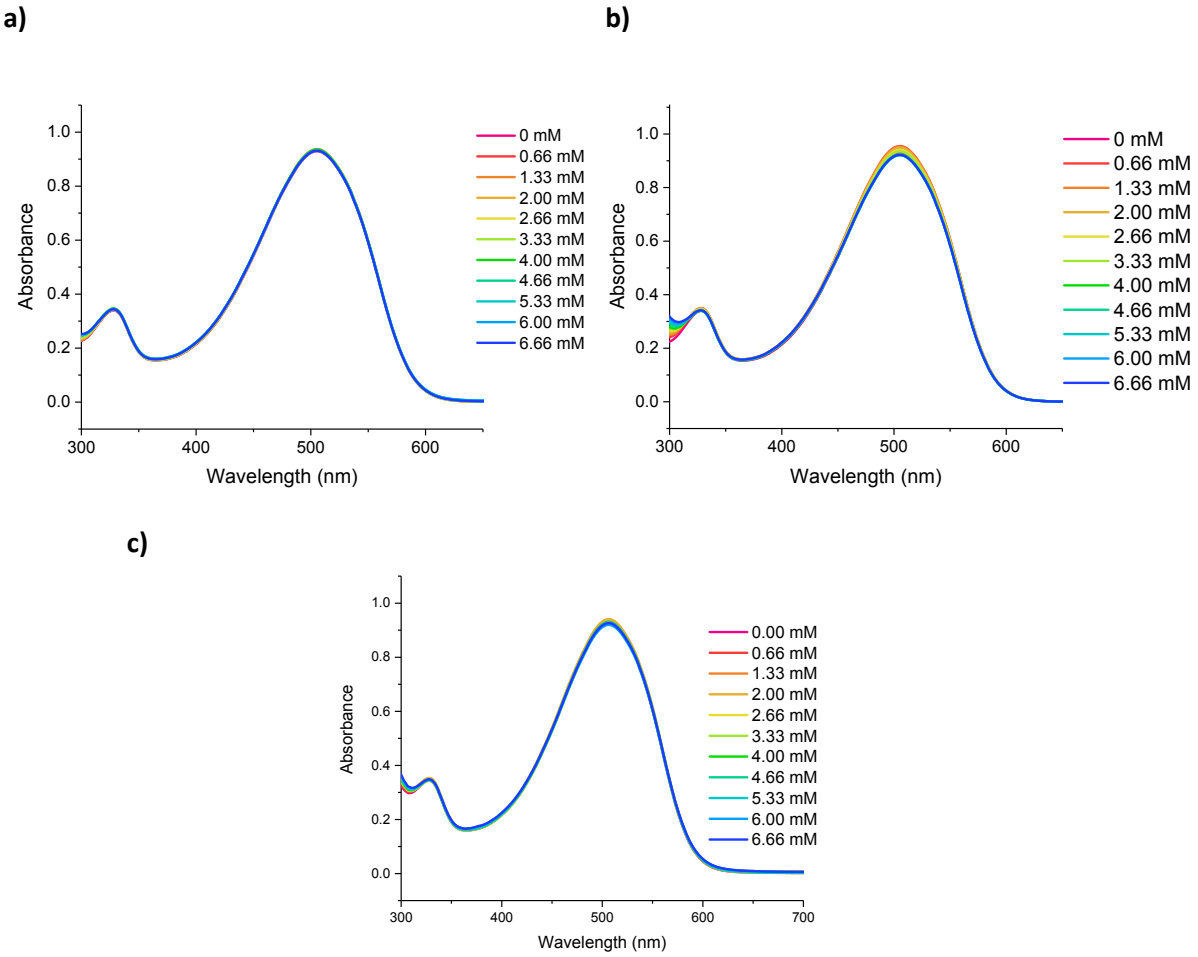

Fig. S42 UV-Vis absorption spectra of **S6** in a 1:1 mixture of tetrahydrofuran:acetonitrile (**S6** concentration $4 \cdot 10^{-5}$ M) upon incrementing a) Li^+, b) K^+ and c) Ca^{2+} concentrations (0-6.66 mM).

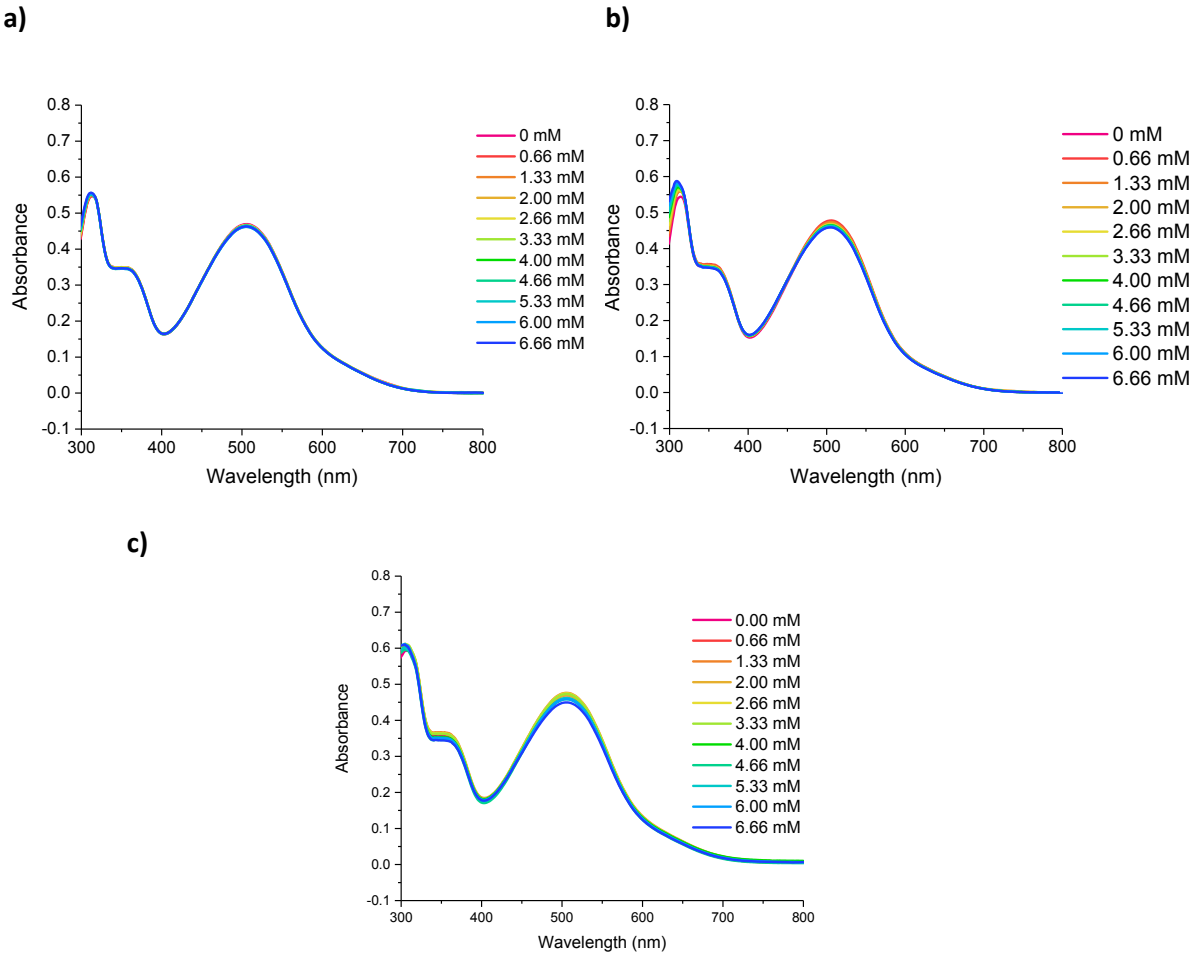

Fig. S43 UV-Vis absorption spectra of **S7** in a 1:1 mixture of tetrahydrofuran:acetonitrile (**S7** concentration $4 \cdot 10^{-5}$ M) upon incrementing a) Li^+, b) K^+ and c) Ca^{2+} concentrations (0-6.66 mM).

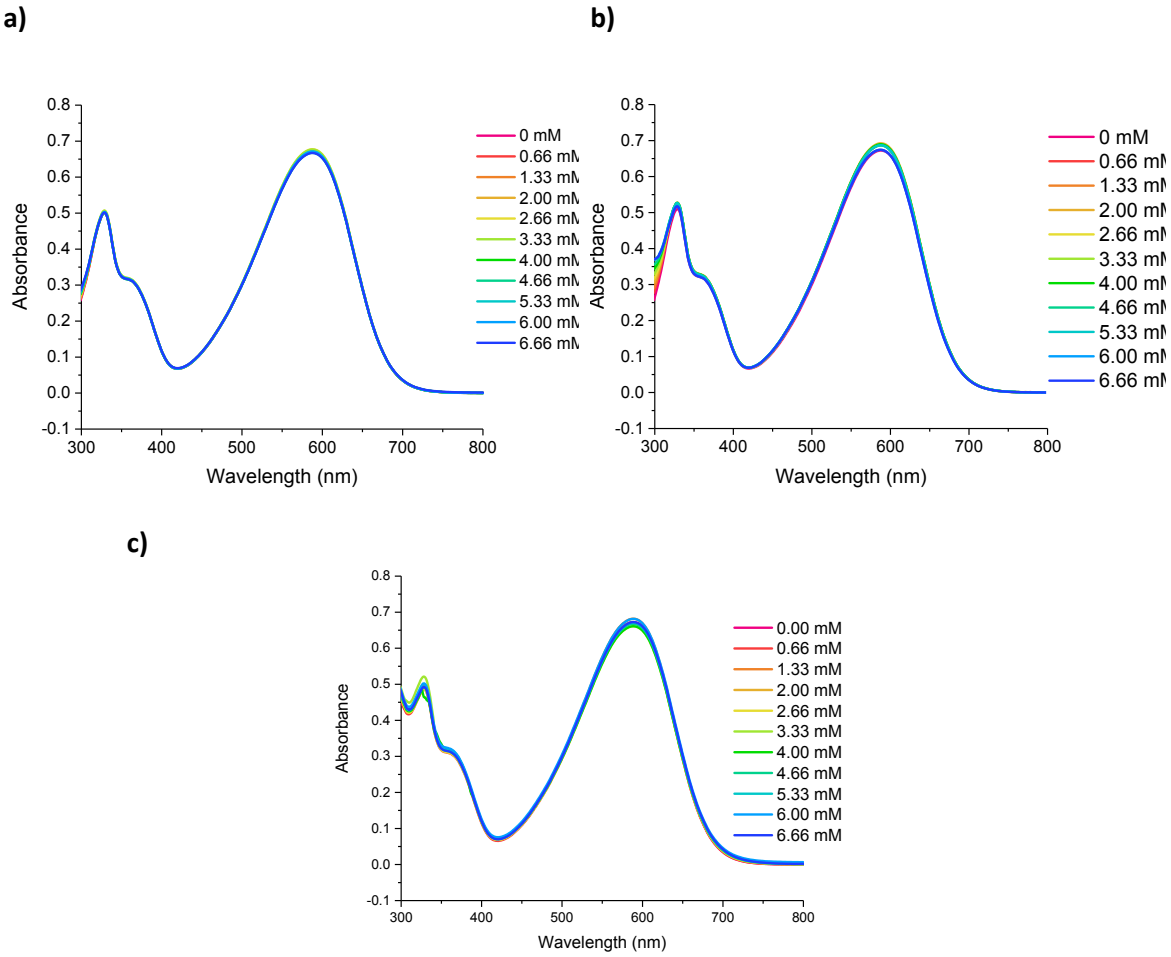

Fig. S44 UV-Vis absorption spectra of **S8** in a 1:1 mixture of tetrahydrofuran:acetonitrile (**S8** concentration $4 \cdot 10^{-5}$ M) upon incrementing a) Li^+, b) K^+ and c) Ca^{2+} concentrations (0-6.66 mM).

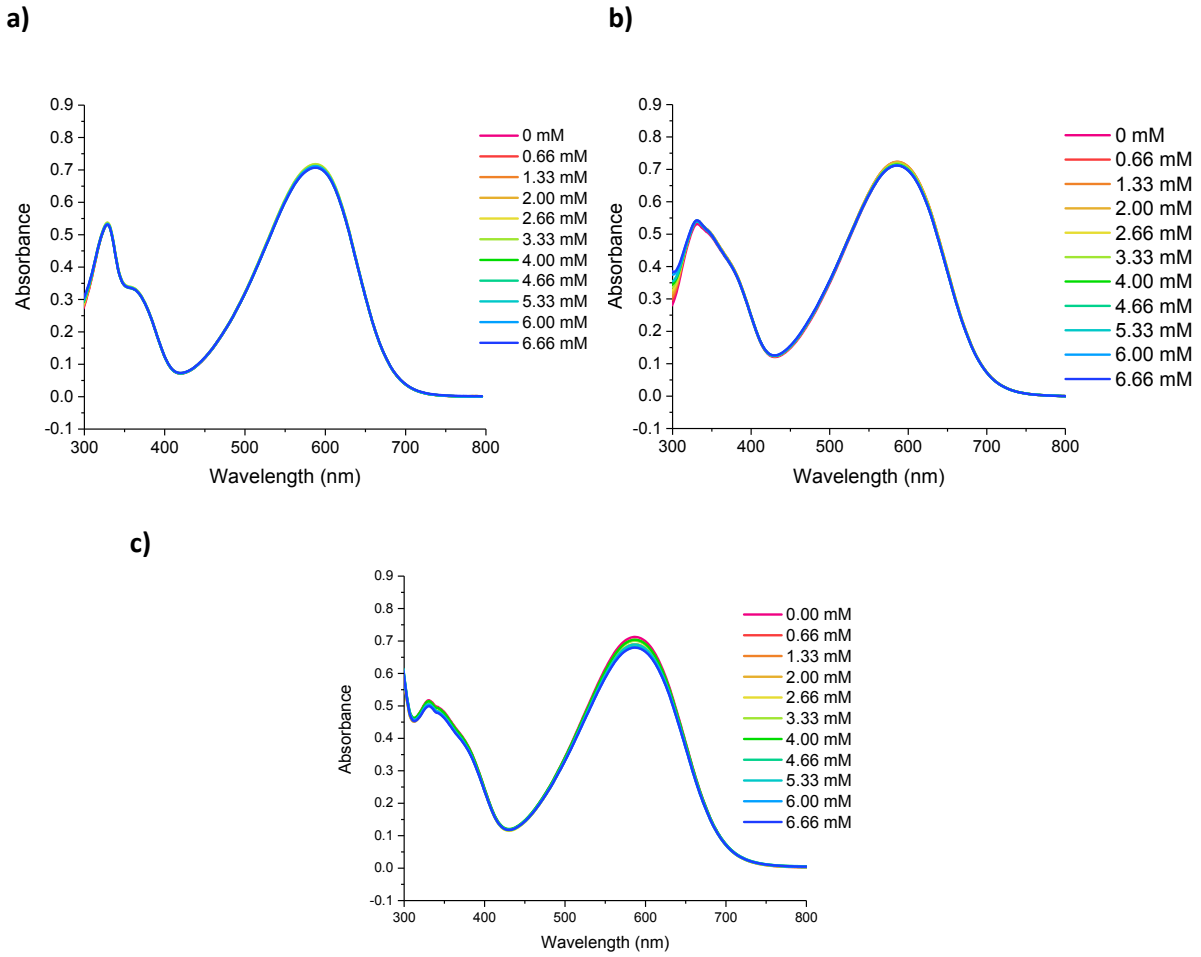

Fig. S45 UV-Vis absorption spectra of **S9** in a 1:1 mixture of tetrahydrofuran:acetonitrile (**S9** concentration $4 \cdot 10^{-5}$ M) upon incrementing a) Li^+, b) K^+ and c) Ca^{2+} concentrations (0-6.66 mM).

9. UV-Vis spectroscopy titrations of S1-S9 against Na^+, Li^+, K^+ and Ca^{2+} in mixed aqueous/organic media

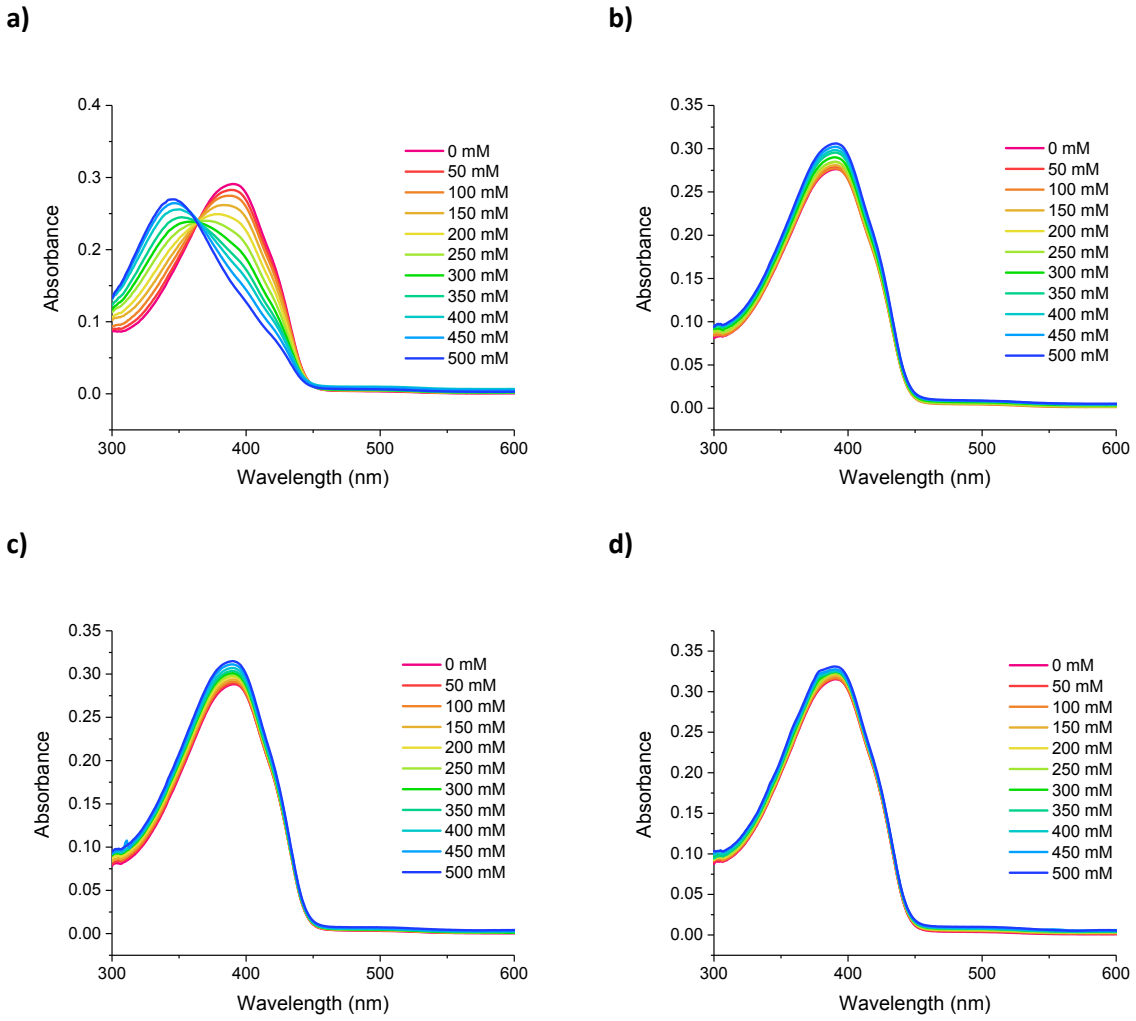

Fig. S46 UV-Vis absorption spectra of **S1** in a 1:3 mixture of water:tetrahydrofuran (**S1** concentration $4 \cdot 10^{-5}$ M) upon incrementing a) Na^+, b) Li^+, c) K^+ and d) Ca^{2+} concentrations (0-500 mM).

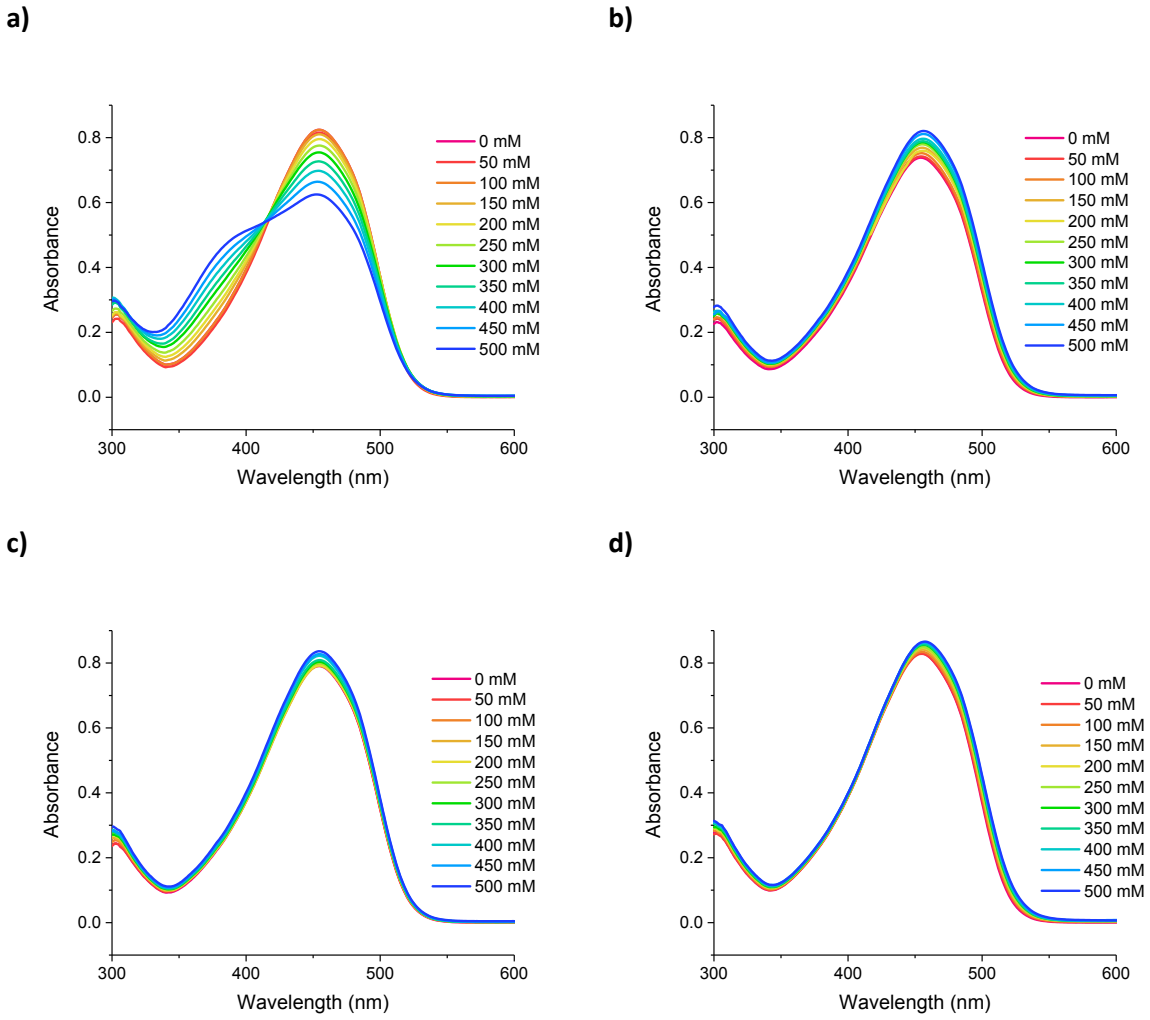

Fig. S47 UV-Vis absorption spectra of **S2** in a 1:3 mixture of water:tetrahydrofuran (**S2** concentration $4 \cdot 10^{-5}$ M) upon incrementing a) Na^+, b) Li^+, c) K^+ and d) Ca^{2+} concentrations (0-500 mM).

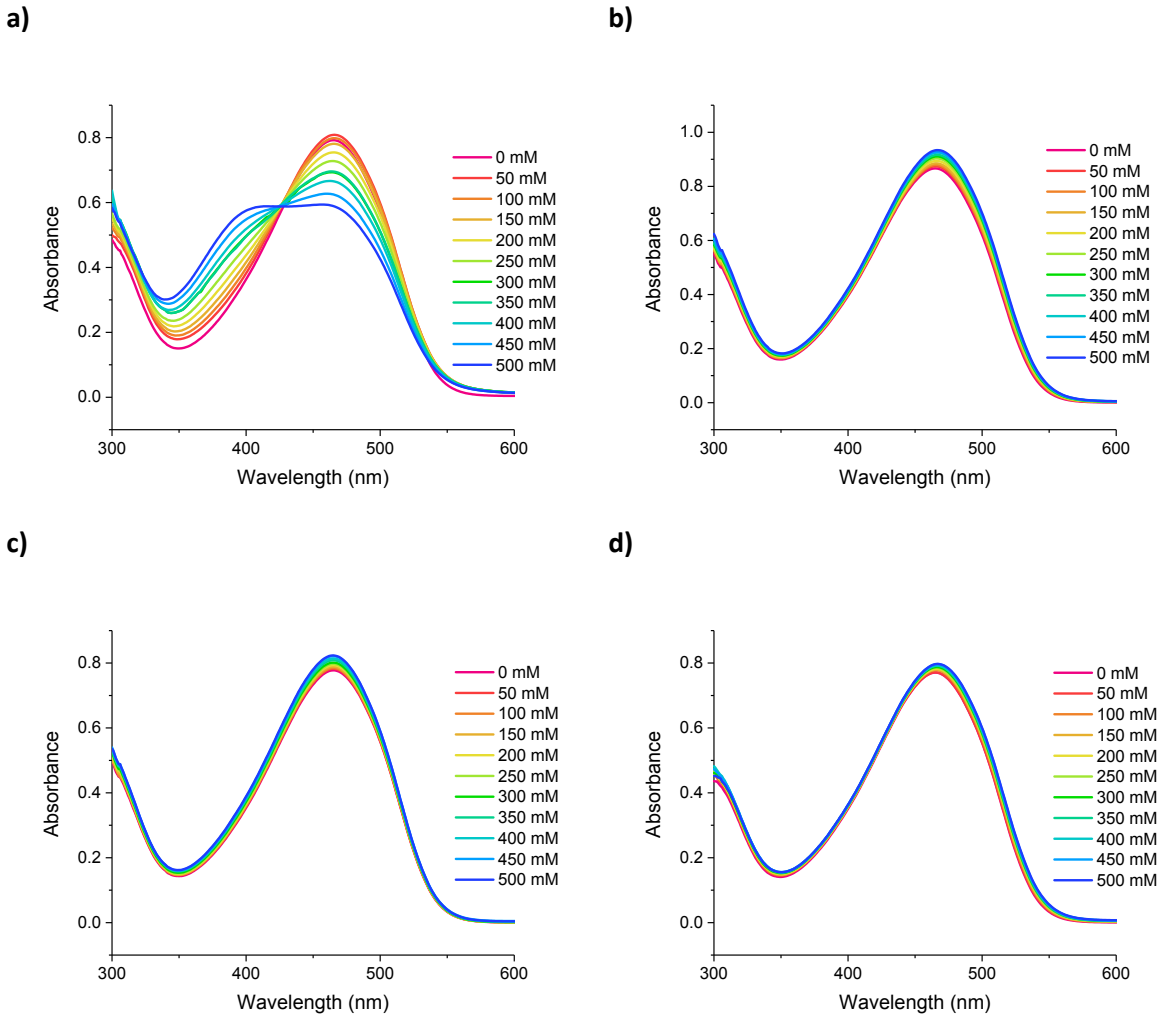

Fig. S48 UV-Vis absorption spectra of **S3** in a 1:3 mixture of water:tetrahydrofuran (**S3** concentration $4 \cdot 10^{-5}$ M) upon incrementing a) Na^+, b) Li^+, c) K^+ and d) Ca^{2+} concentrations (0-500 mM).

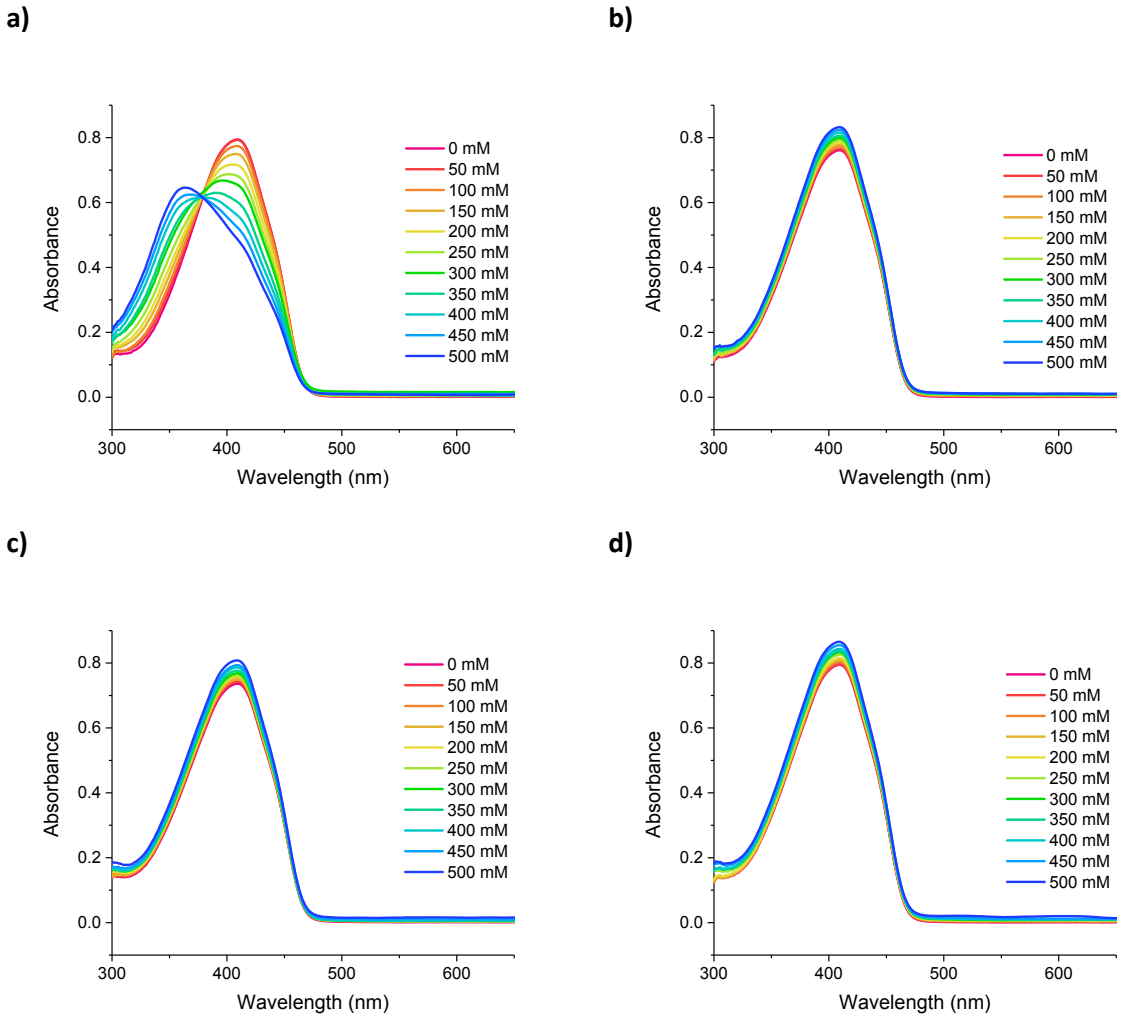

Fig. S49 UV-Vis absorption spectra of **S4** in a 1:3 mixture of water:tetrahydrofuran (**S4** concentration $4 \cdot 10^{-5}$ M) upon incrementing a) Na^+, b) Li^+, c) K^+ and d) Ca^{2+} concentrations (0-500 mM).

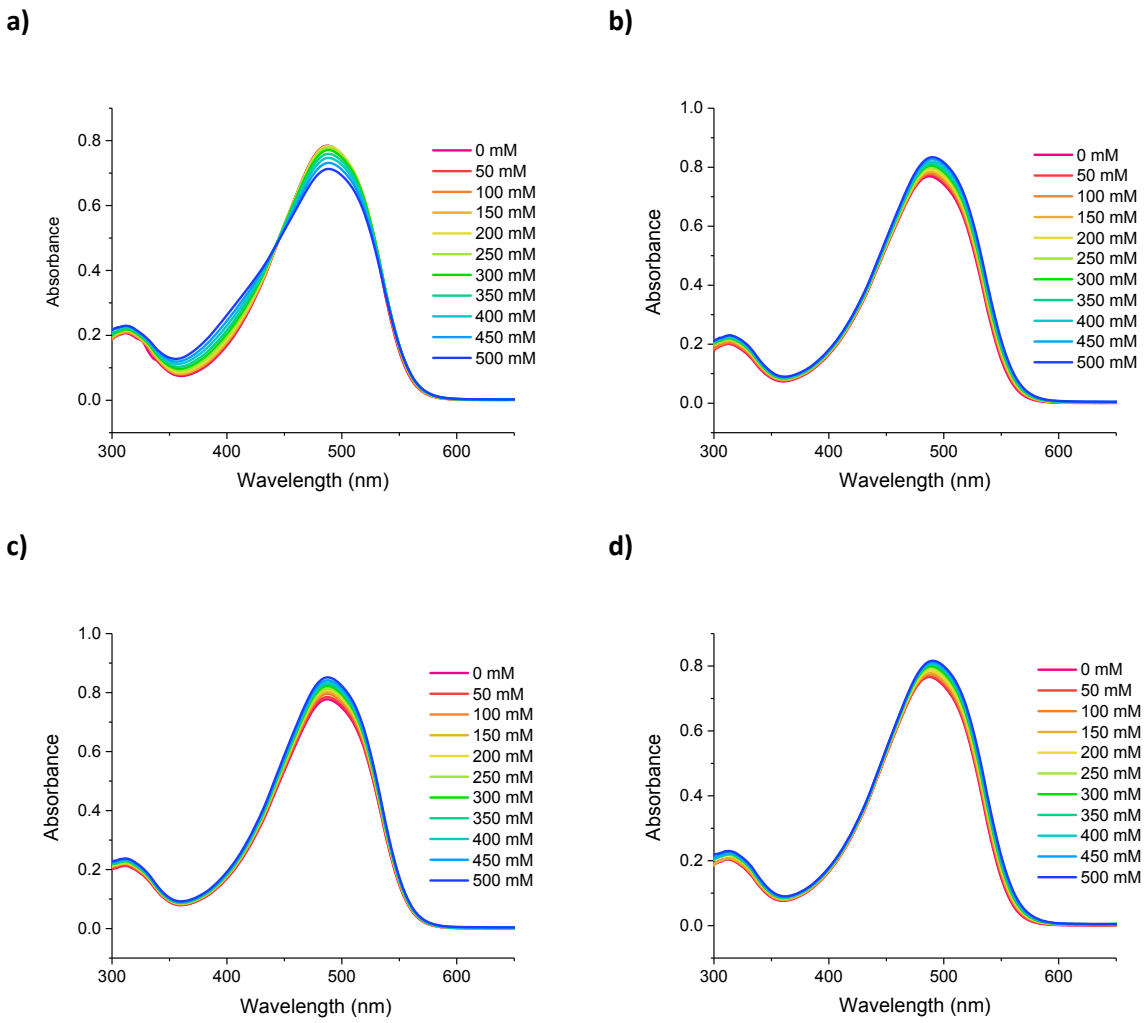

Fig. S50 UV-Vis absorption spectra of **S5** in a 1:3 mixture of water:tetrahydrofuran (**S5** concentration $4 \cdot 10^{-5}$ M) upon incrementing a) Na^+, b) Li^+, c) K^+ and d) Ca^{2+} concentrations (0-500 mM).

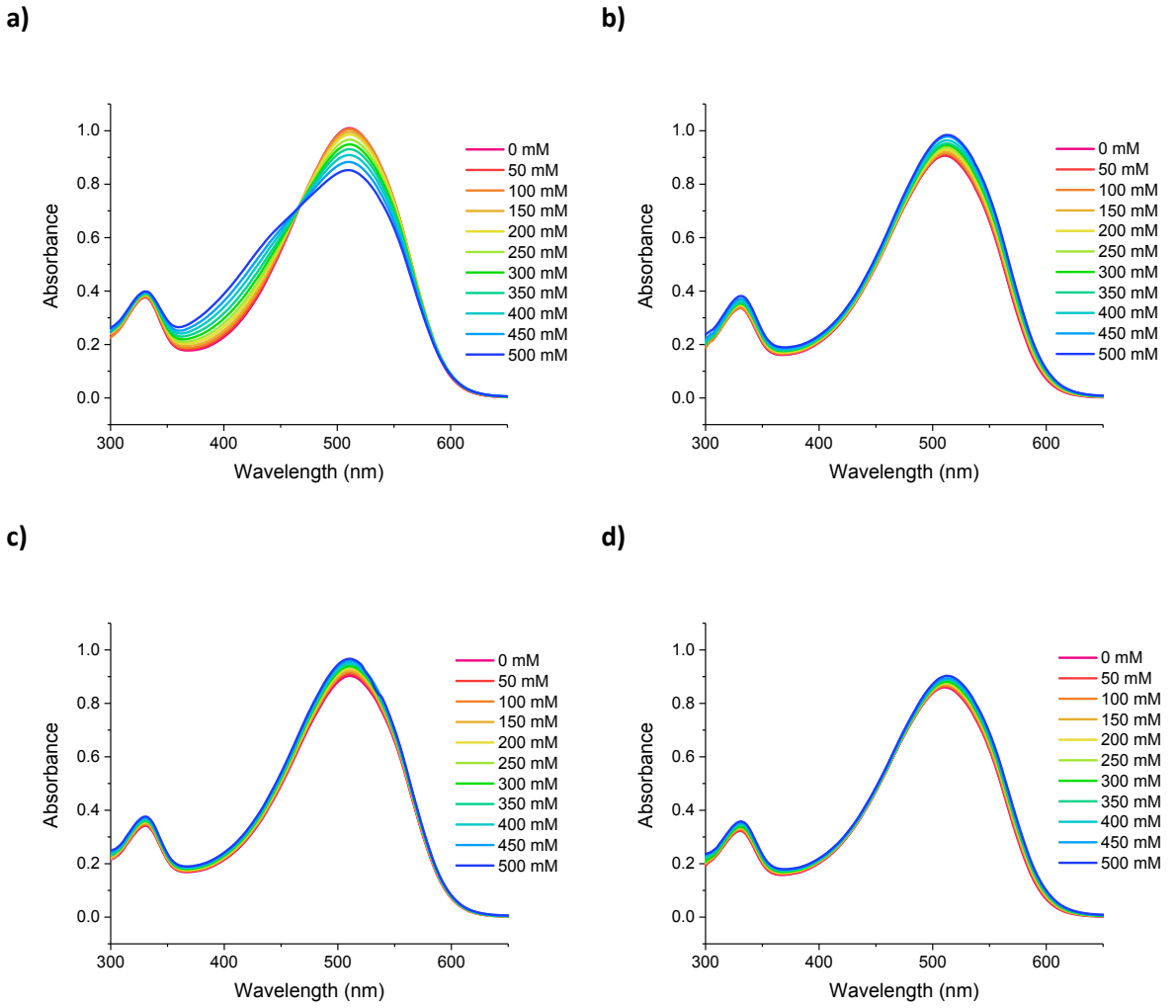

Fig. S51 UV-Vis absorption spectra of **S6** in a 1:3 mixture of water:tetrahydrofuran (**S6** concentration $4 \cdot 10^{-5}$ M) upon incrementing a) Na^+, b) Li^+, c) K^+ and d) Ca^{2+} concentrations (0-500 mM).

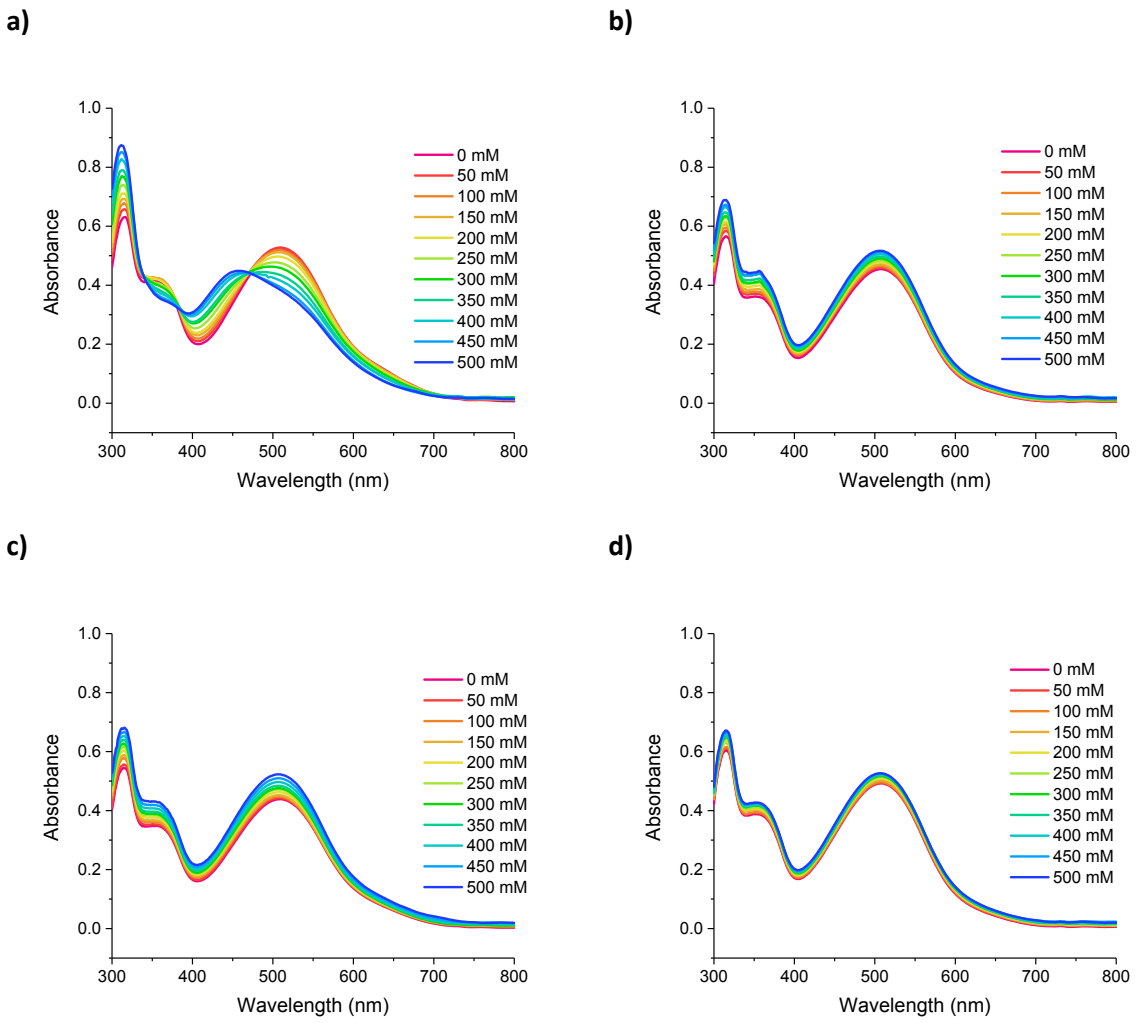

Fig. S52 UV-Vis absorption spectra of **S7** in a 1:3 mixture of water:tetrahydrofuran (**S7** concentration $4 \cdot 10^{-5}$ M) upon incrementing a) Na^+, b) Li^+, c) K^+ and d) Ca^{2+} concentrations (0-500 mM).

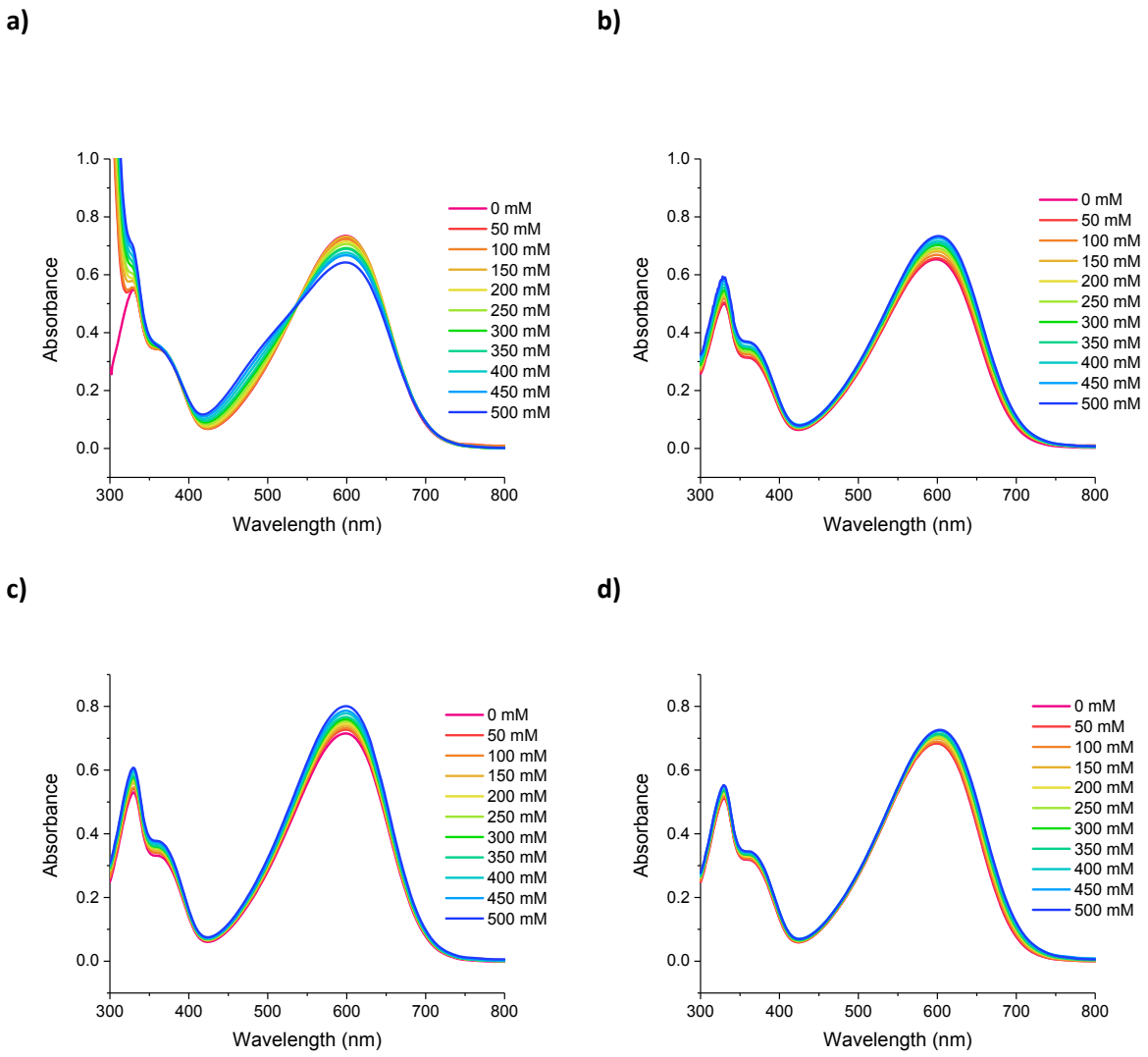

Fig. S53 UV-Vis absorption spectra of **S8** in a 1:3 mixture of water:tetrahydrofuran (**S8** concentration $4 \cdot 10^{-5}$ M) upon incrementing a) Na^+, b) Li^+, c) K^+ and d) Ca^{2+} concentrations (0-500 mM).

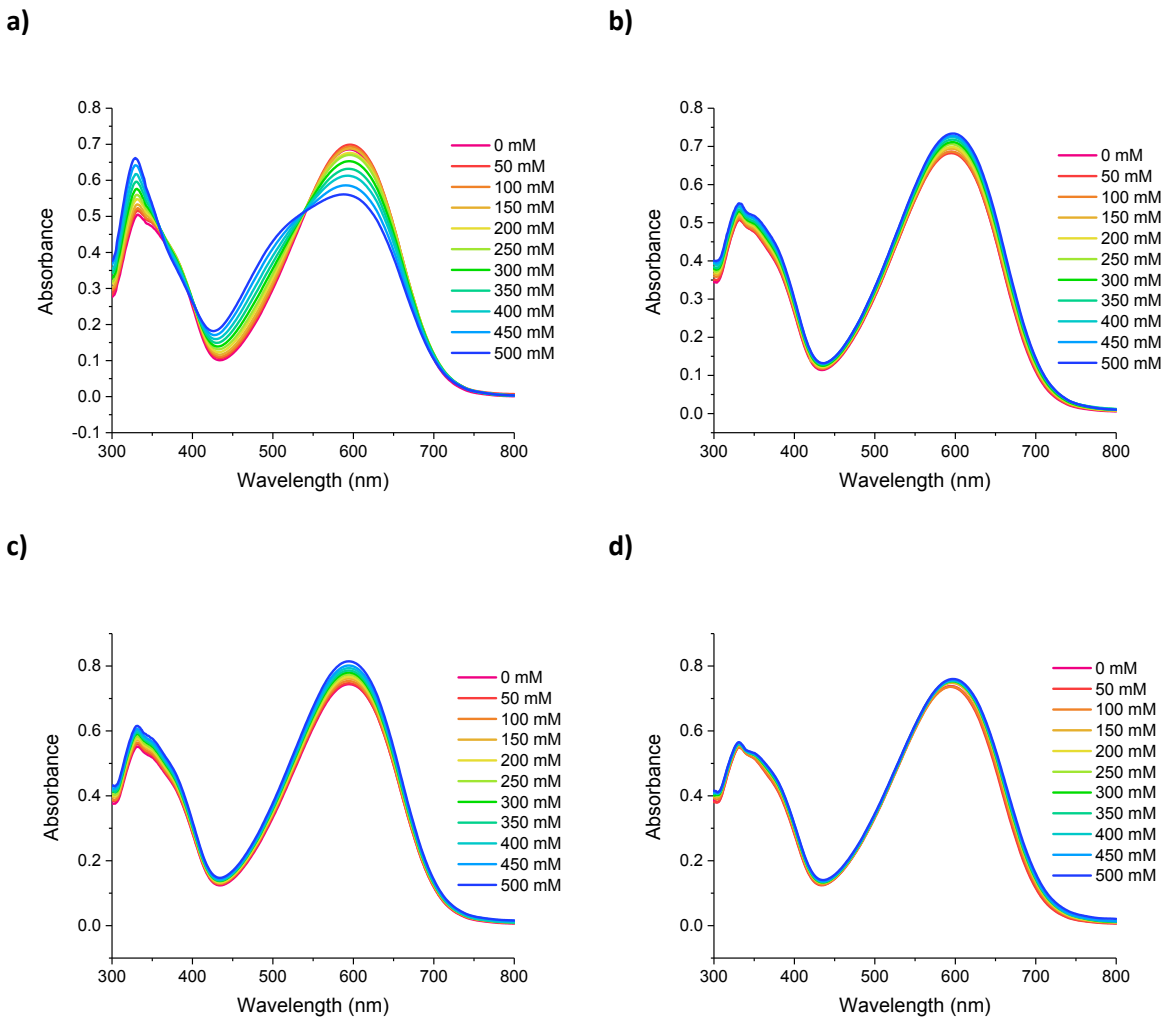

Fig. S54 UV-Vis absorption spectra of **S9** in a 1:3 mixture of water:tetrahydrofuran (**S9** concentration $4 \cdot 10^{-5}$ M) upon incrementing a) Na^+, b) Li^+, c) K^+ and d) Ca^{2+} concentrations (0-500 mM).

10. Calculation of the dissociation constants of sensors S1-S9

The association constant (K_a) for the various sensors was then calculated by the Benesi-Hildebrand method according to the following equation:[8,9]

$$\frac{1}{(A - A_0)} = \frac{1}{K_a(A_{max} - A_0)[G]} + \frac{1}{(A_{max} - A_0)} \quad \textbf{(S4)}$$

Where A = absorbance of the host recorded in the presence of the guest, A_0 = absorbance of the host recorded in the absence of the guest, A_{max} = absorbance of the host recorded in the presence of the maximum guest concentration and $[G]$ = concentration of the guest.

Solving equation S2 graphically by plotting $\frac{1}{(A - A_0)}$ against $\frac{1}{[G]}$ afforded a straight line plot with a slope (m) given by:

$$m = \frac{1}{K_a(A_{max} - A_0)} \quad \textbf{(S5)}$$

Rearranging for K_a:

$$K_a = \frac{1}{m(A_{max} - A_0)} \quad \textbf{(S6)}$$

Finally, K_d was obtained by the following relationship:

$$K_d = \frac{1}{K_a} \quad \textbf{(S7)}$$

11. Benesi-Hildebrand plots of sensors S1-S9 in organic media

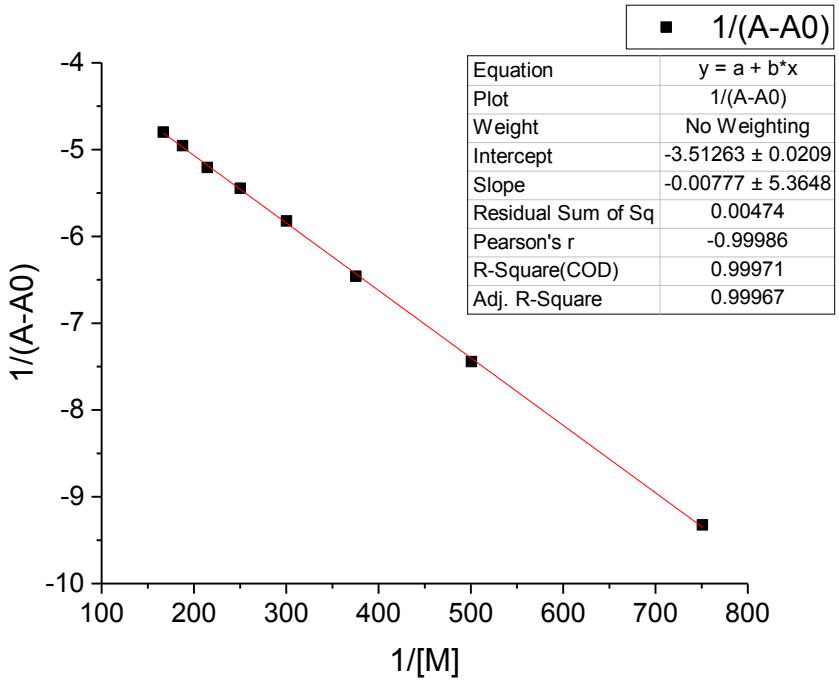

Fig. S55 Benesi-Hildebrand plot of **S1** in a 1:1 mixture of tetrahydrofuran:acetonitrile.

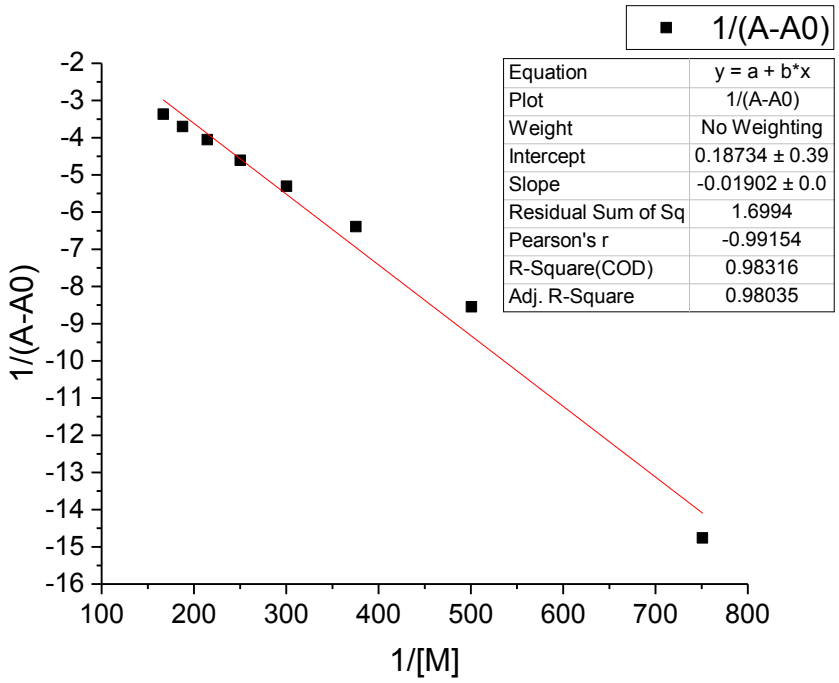

Fig. S56 Benesi-Hildebrand plot of **S2** in a 1:1 mixture of tetrahydrofuran:acetonitrile.

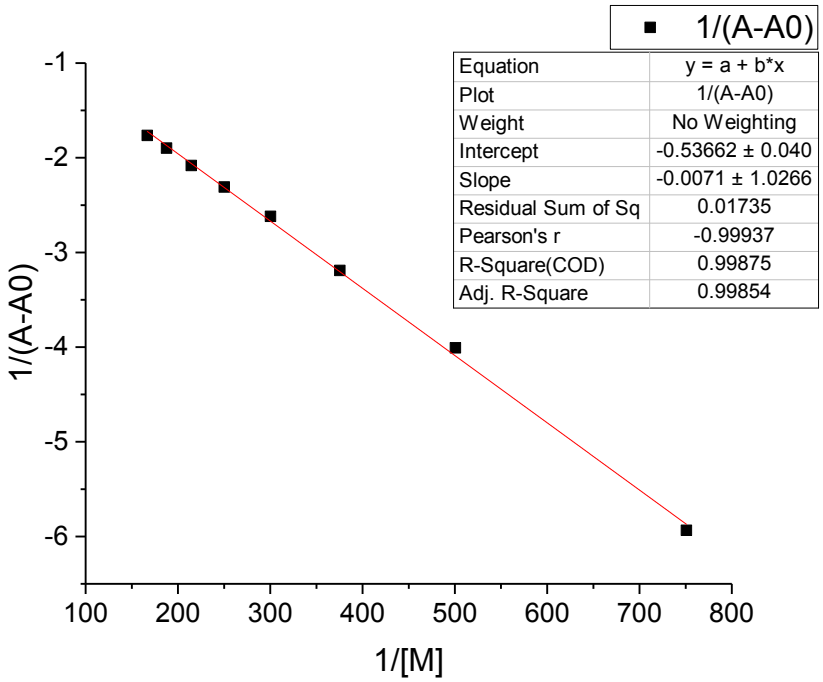

Fig. S57 Benesi-Hildebrand plot of **S3** in a 1:1 mixture of tetrahydrofuran:acetonitrile.

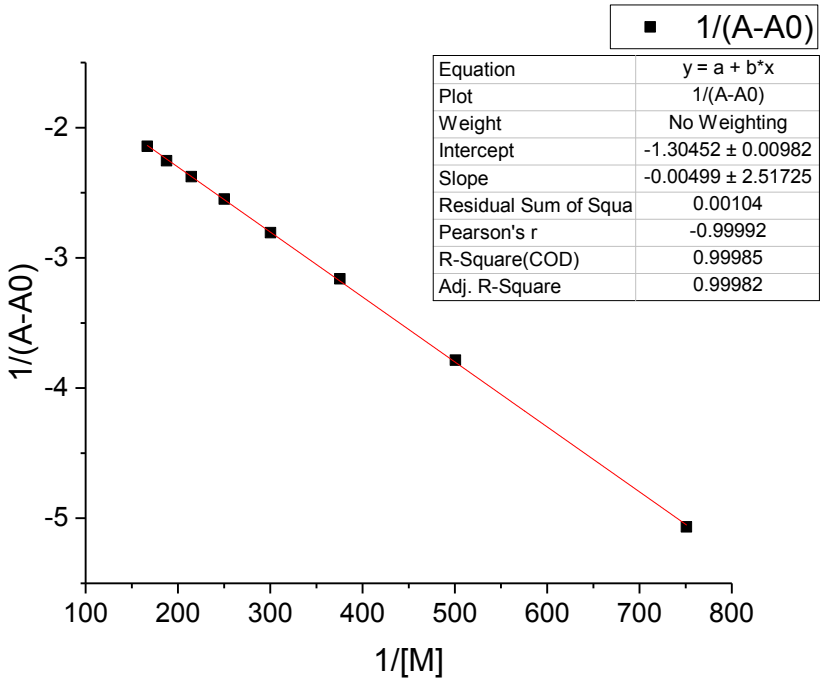

Fig. S58 Benesi-Hildebrand plot of **S4** in a 1:1 mixture of tetrahydrofuran:acetonitrile.

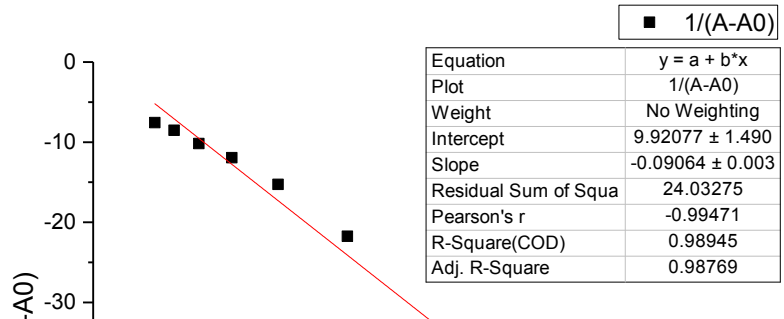

Fig. S59 Benesi-Hildebrand plot of **S5** in a 1:1 mixture of tetrahydrofuran:acetonitrile.

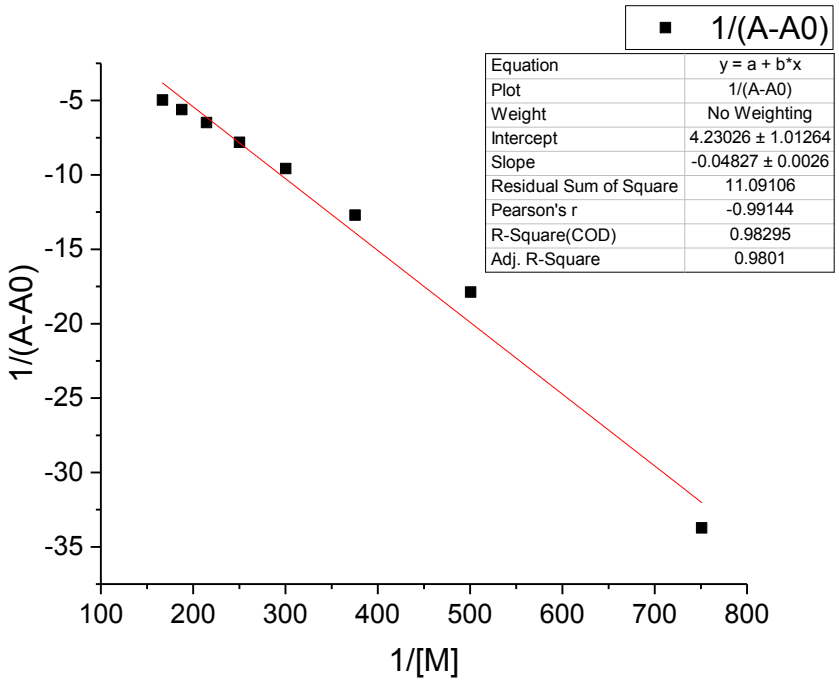

Fig. S60 Benesi-Hildebrand plot of **S6** in a 1:1 mixture of tetrahydrofuran:acetonitrile.

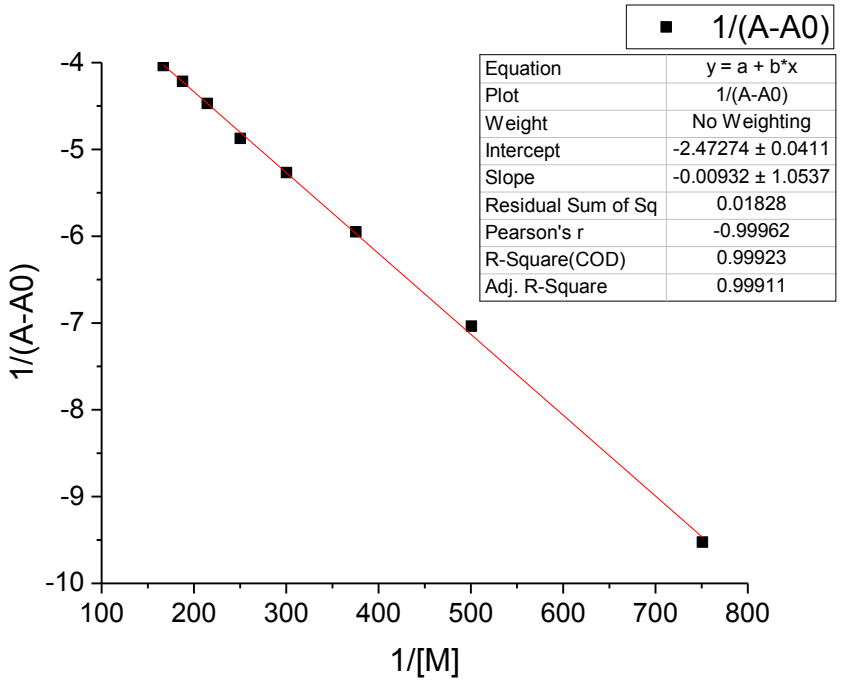

Fig. S61 Benesi-Hildebrand plot of **S7** in a 1:1 mixture of tetrahydrofuran:acetonitrile.

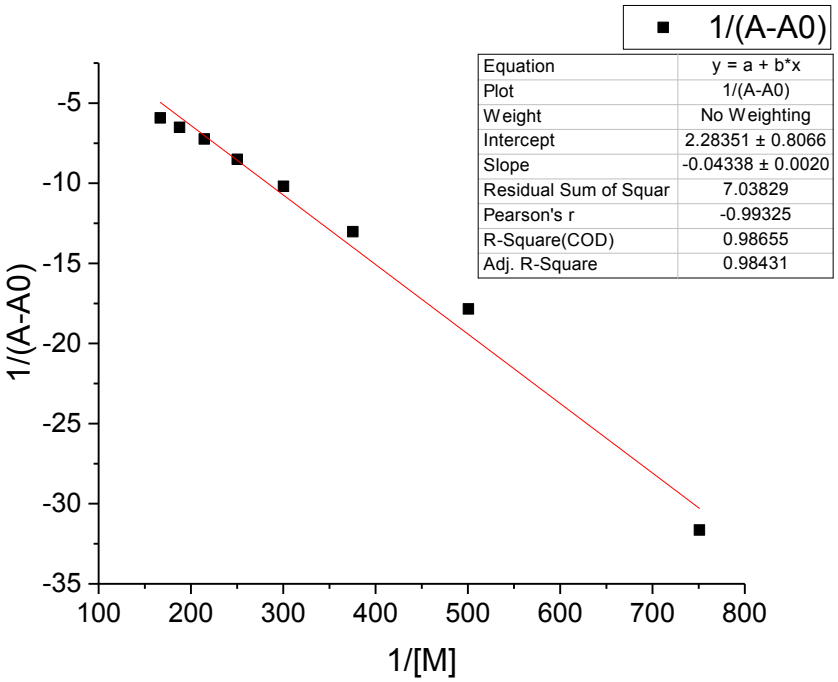

Fig. S62 Benesi-Hildebrand plot of **S8** in a 1:1 mixture of tetrahydrofuran:acetonitrile.

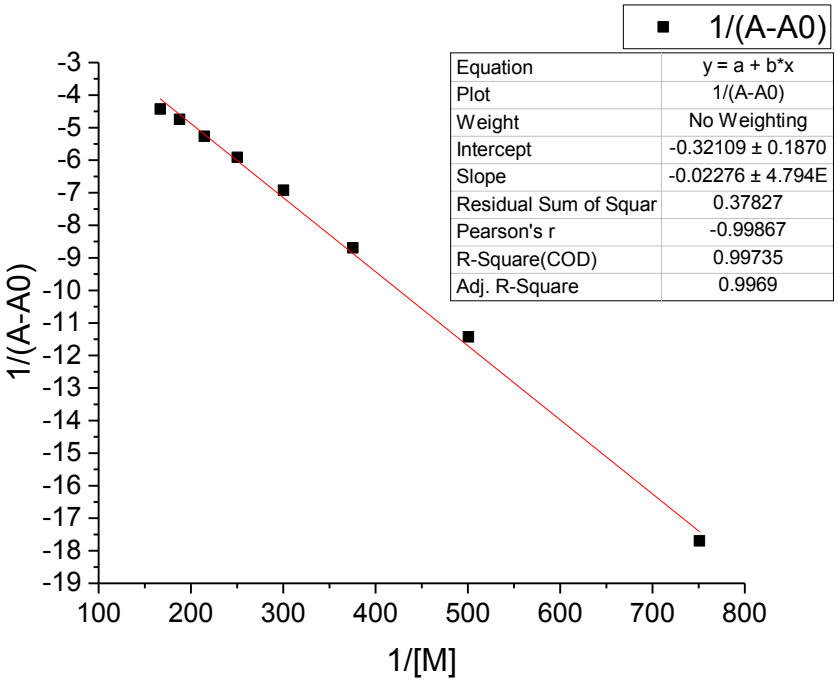

Fig. S63 Benesi-Hildebrand plot of **S9** in a 1:1 mixture of tetrahydrofuran:acetonitrile.

12. Limit of Detection (LOD) and Limit of Quantification (LOQ) Determinations

The LOD and LOQ for sensors **S1-S9** were determined by the same approach as has been employed in previous literature.[10-13]

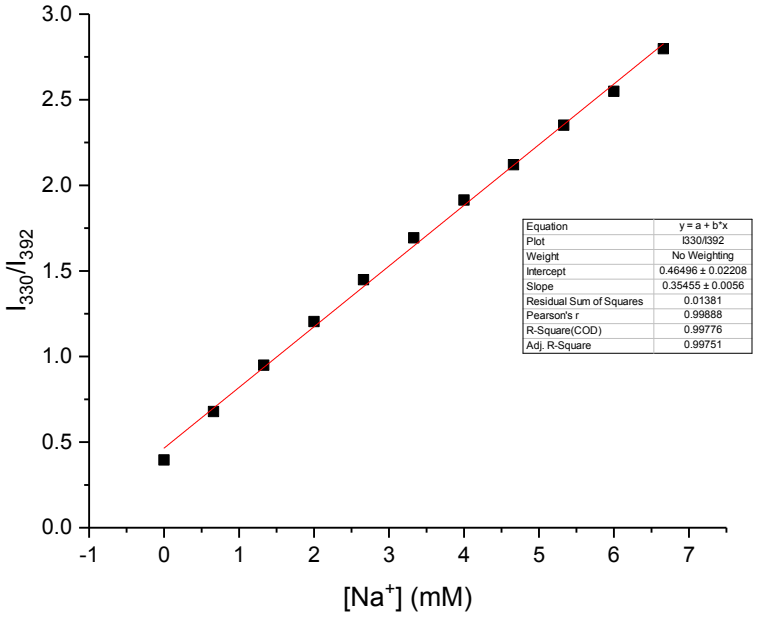

Fig. S64 Ratiometric UV-vis response of sensor **S1** at the absorption maxima of the bound (330 nm) and unbound (392 nm) sensor as a function of added Na^+ concentration.

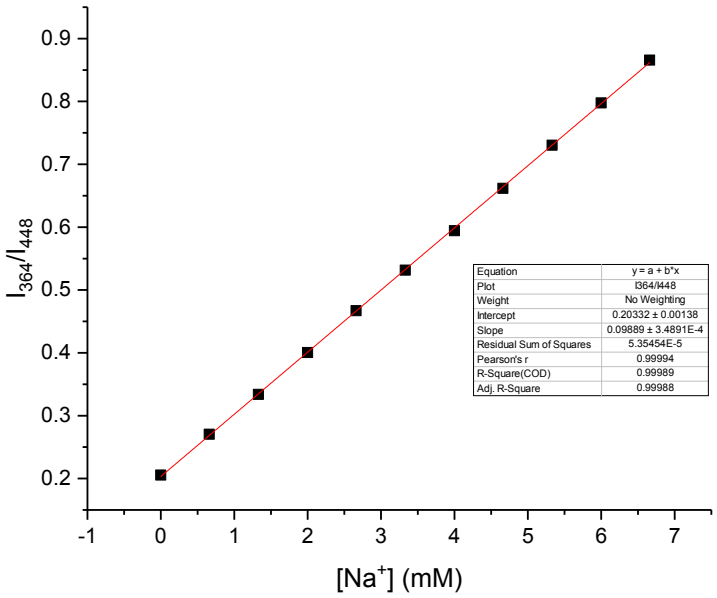

Fig. S65 Ratiometric UV-vis response of sensor **S2** at the absorption maxima of the bound (364 nm) and unbound (392 nm) sensor as a function of added Na^+ concentration.

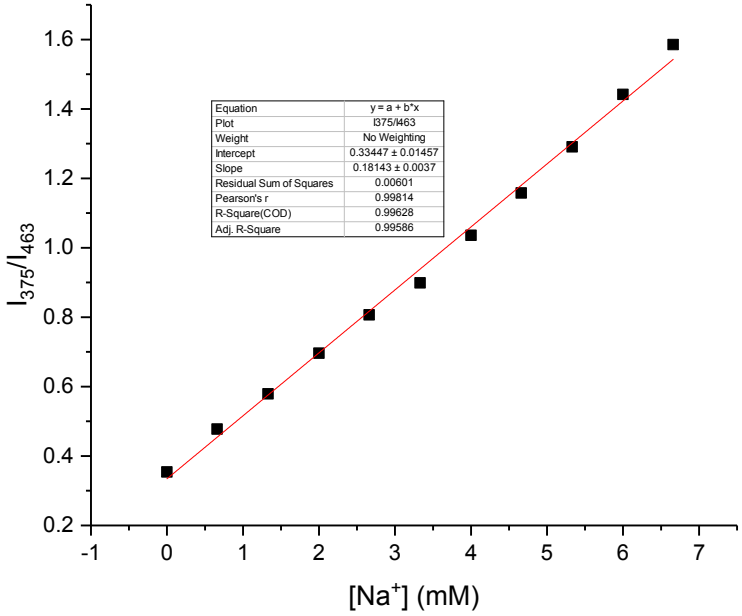

Fig. S66 Ratiometric UV-vis response of sensor **S3** at the absorption maxima of the bound (375 nm) and unbound (463 nm) sensor as a function of added Na^+ concentration.

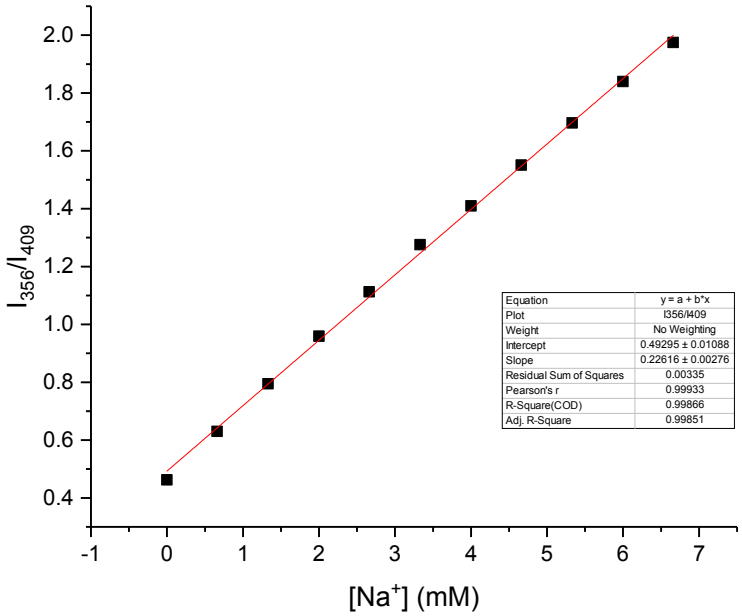

Fig. S67 Ratiometric UV-vis response of sensor **S4** at the absorption maxima of the bound (356 nm) and unbound (409 nm) sensor as a function of added Na^+ concentration.

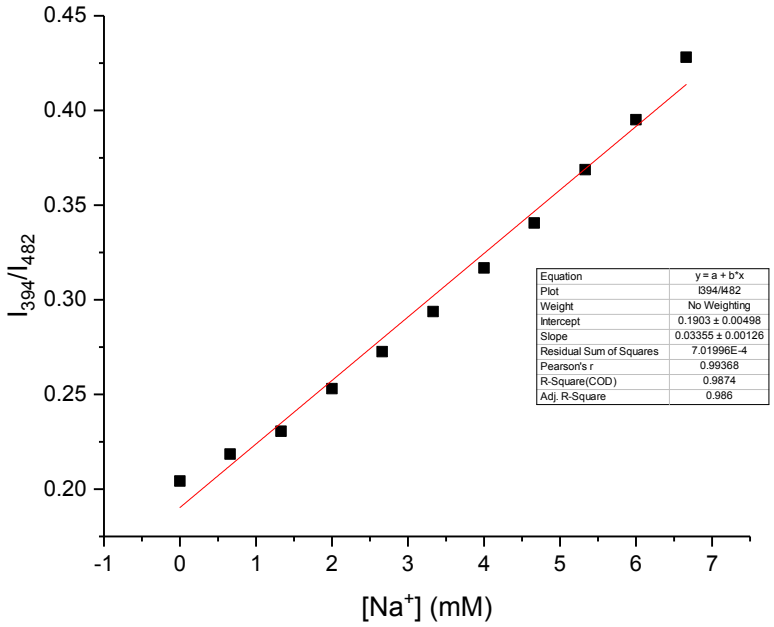

Fig. S68 Ratiometric UV-vis response of sensor **S5** at the absorption maxima of the bound (394 nm) and unbound (482 nm) sensor as a function of added Na^+ concentration.

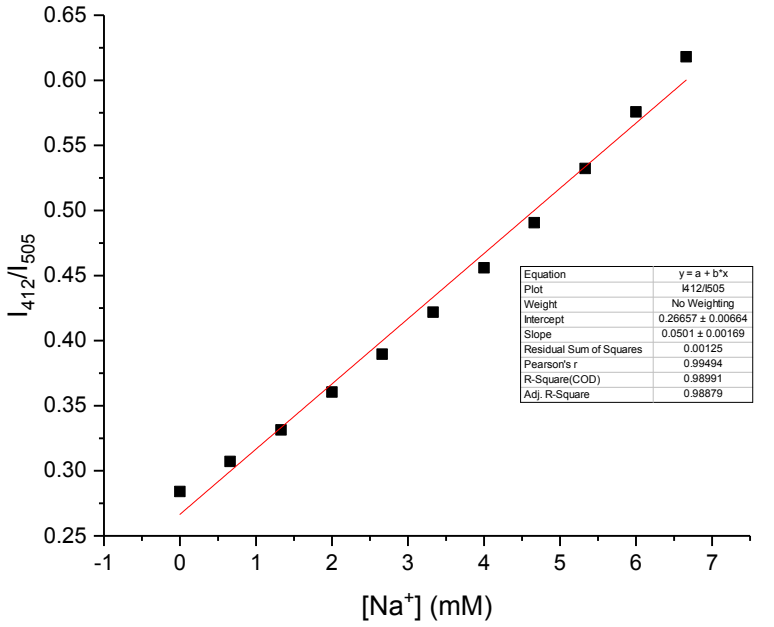

Fig. S69 Ratiometric UV-vis response of sensor **S6** at the absorption maxima of the bound (412 nm) and unbound (505 nm) sensor as a function of added Na^+ concentration.

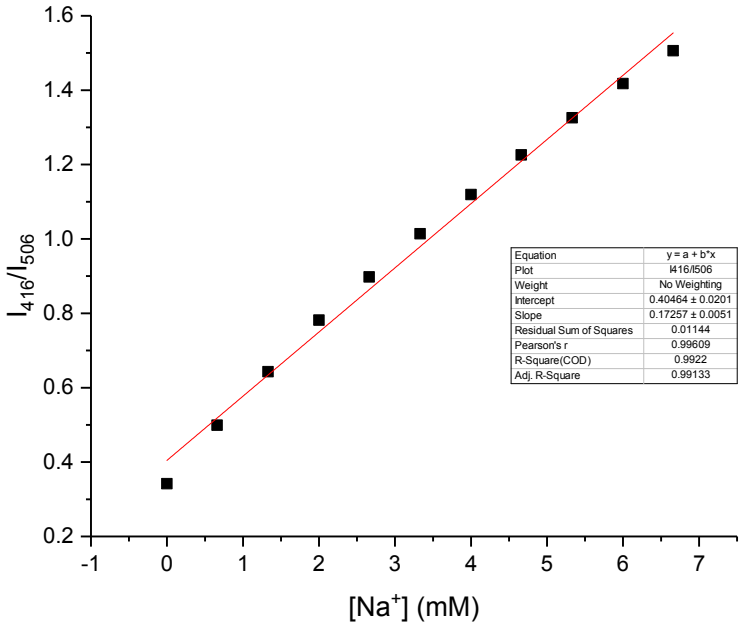

Fig. S70 Ratiometric UV-vis response of sensor **S7** at the absorption maxima of the bound (416 nm) and unbound (506 nm) sensor as a function of added Na^+ concentration.

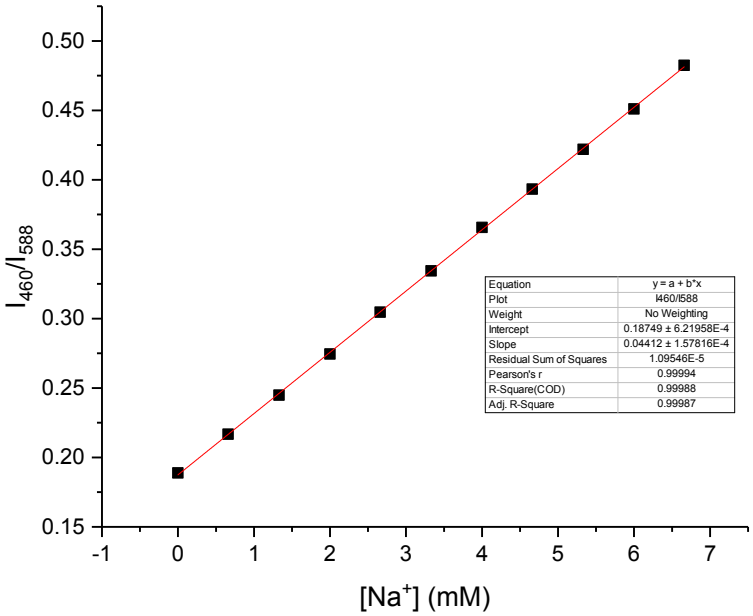

Fig. S71 Ratiometric UV-vis response of sensor **S8** at the absorption maxima of the bound (460 nm) and unbound (588 nm) sensor as a function of added Na^+ concentration.

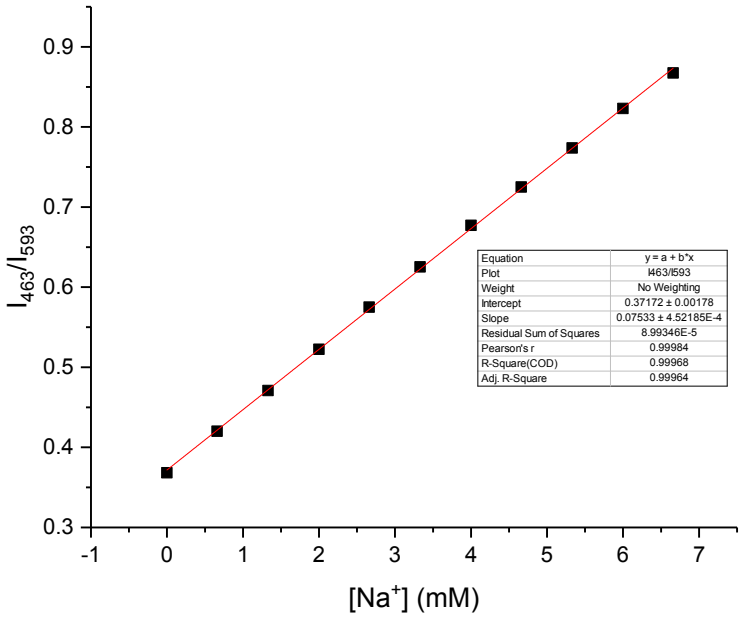

Fig. S72 Ratiometric UV-vis response of sensor **S9** at the absorption maxima of the bound (463 nm) and unbound (593 nm) sensor as a function of added Na^+ concentration.

13. Stability measurements

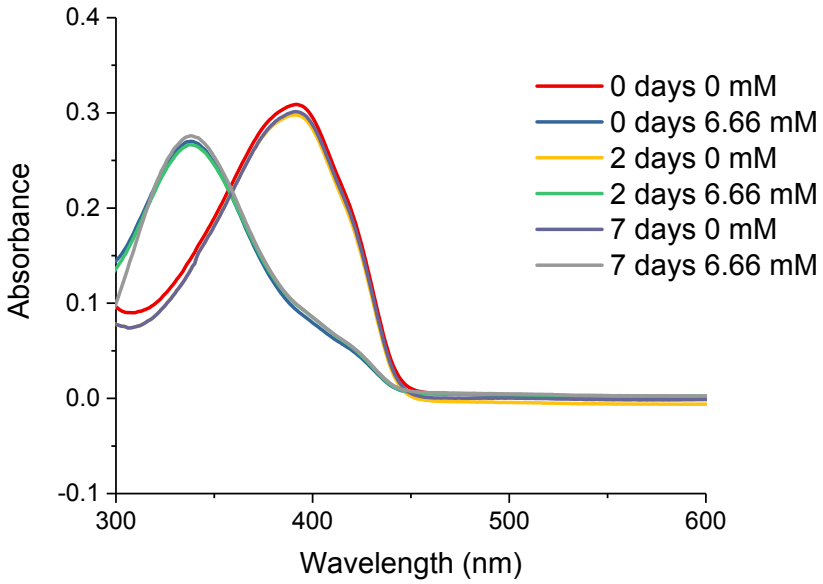

Fig. S73 UV-Vis absorption spectra of **S1** in a 1:1 mixture of tetrahydrofuran:acetonitrile (**S1** concentration $4 \cdot 10^{-5}$ M) with 0 mM and 6.66 mM added Na^+ at 0 days, 2 days and 7 days after sample preparation.

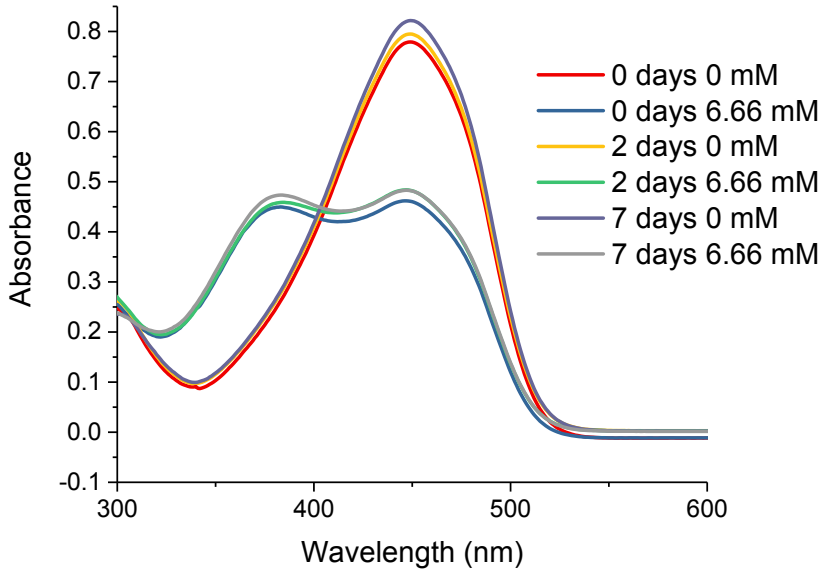

Fig. S74 UV-Vis absorption spectra of **S2** in a 1:1 mixture of tetrahydrofuran:acetonitrile (**S2** concentration $4 \cdot 10^{-5}$ M) with 0 mM and 6.66 mM added Na^+ at 0 days, 2 days and 7 days after sample preparation.

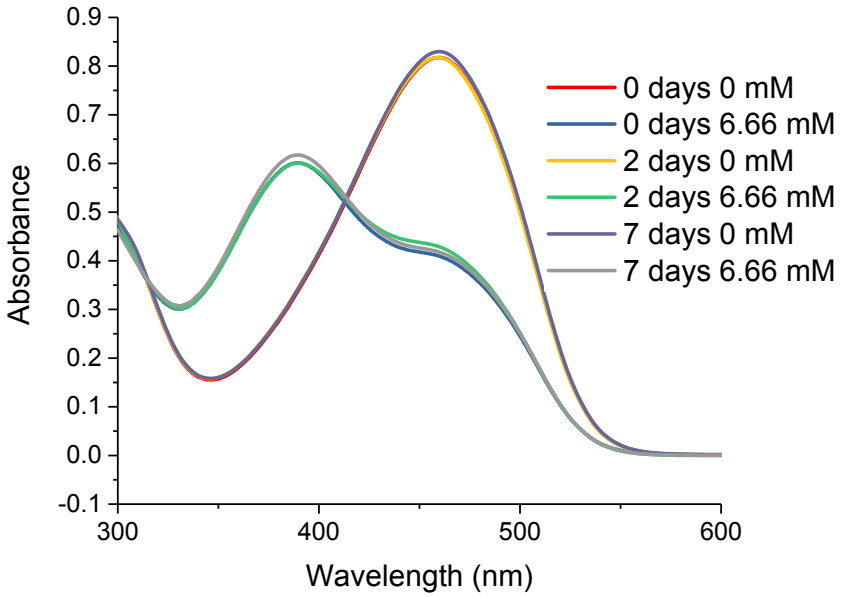

Fig. S75 UV-Vis absorption spectra of **S3** in a 1:1 mixture of tetrahydrofuran:acetonitrile (**S3** concentration $4 \cdot 10^{-5}$ M) with 0 mM and 6.66 mM added Na^+ at 0 days, 2 days and 7 days after sample preparation.

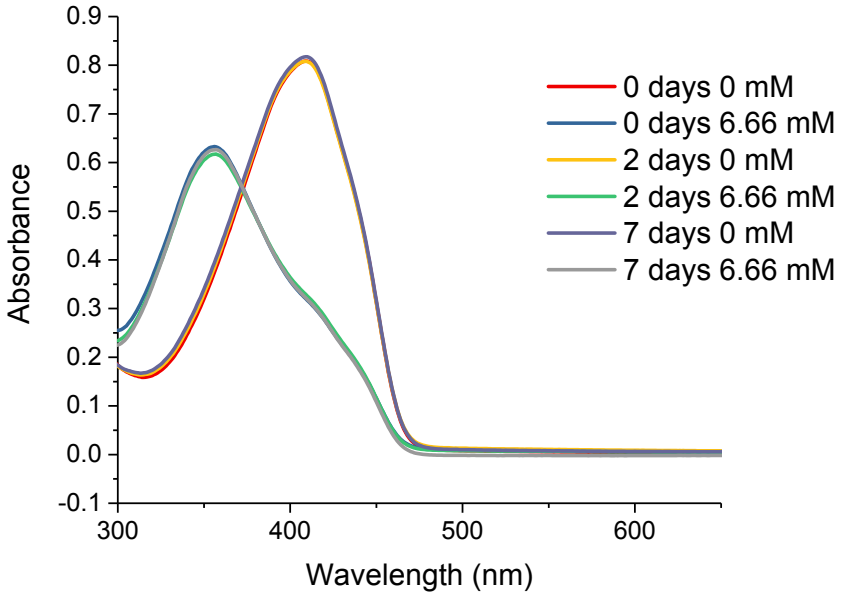

Fig. S76 UV-Vis absorption spectra of **S4** in a 1:1 mixture of tetrahydrofuran:acetonitrile (**S4** concentration $4 \cdot 10^{-5}$ M) with 0 mM and 6.66 mM added Na^+ at 0 days, 2 days and 7 days after sample preparation.

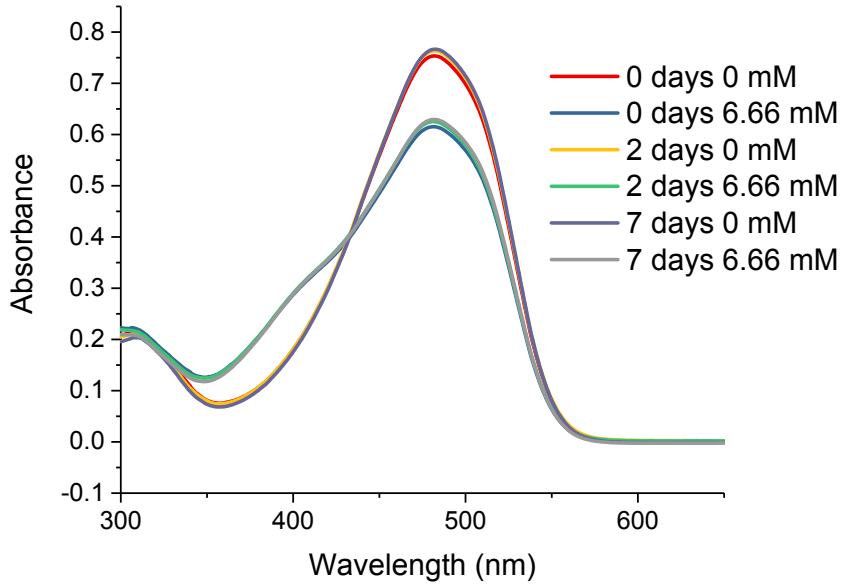

Fig. S77 UV-Vis absorption spectra of **S5** in a 1:1 mixture of tetrahydrofuran:acetonitrile (**S5** concentration $4 \cdot 10^{-5}$ M) with 0 mM and 6.66 mM added Na^+ at 0 days, 2 days and 7 days after sample preparation.

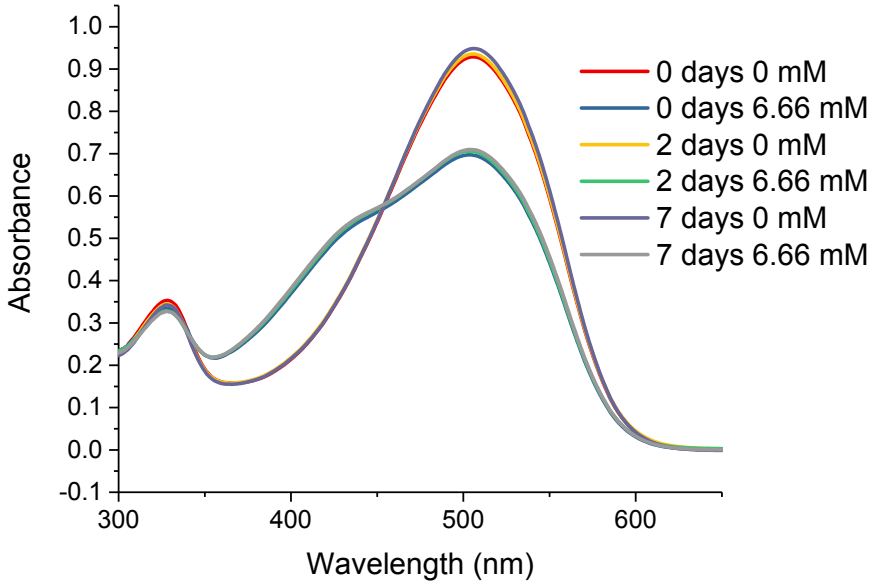

Fig. S78 UV-Vis absorption spectra of **S6** in a 1:1 mixture of tetrahydrofuran:acetonitrile (**S6** concentration $4 \cdot 10^{-5}$ M) with 0 mM and 6.66 mM added Na^+ at 0 days, 2 days and 7 days after sample preparation.

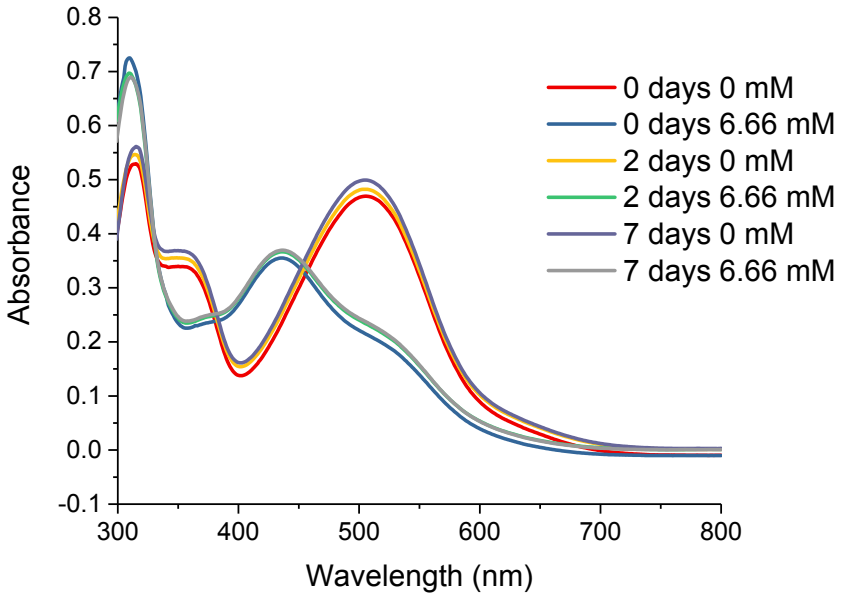

Fig. S79 UV-Vis absorption spectra of **S7** in a 1:1 mixture of tetrahydrofuran:acetonitrile (**S7** concentration $4 \cdot 10^{-5}$ M) with 0 mM and 6.66 mM added Na^+ at 0 days, 2 days and 7 days after sample preparation.

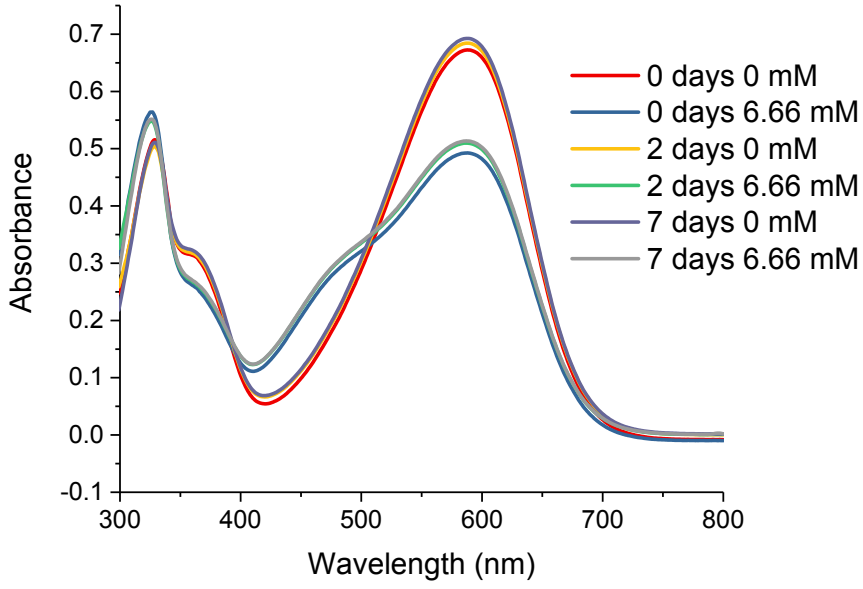

Fig. S80 UV-Vis absorption spectra of **S8** in a 1:1 mixture of tetrahydrofuran:acetonitrile (**S8** concentration $4 \cdot 10^{-5}$ M) with 0 mM and 6.66 mM added Na^+ at 0 days, 2 days and 7 days after sample preparation.

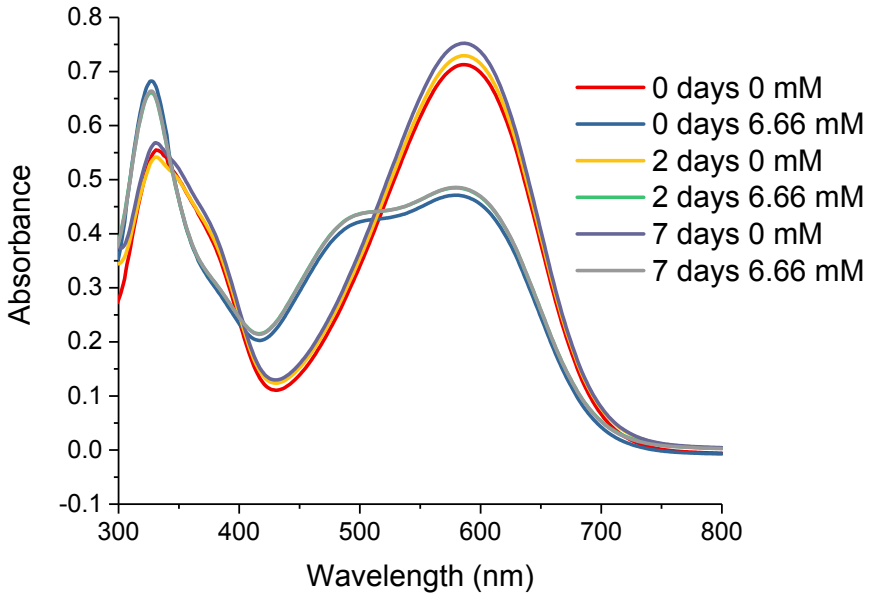

Fig. S81 UV-Vis absorption spectra of **S9** in a 1:1 mixture of tetrahydrofuran:acetonitrile (**S9** concentration $4 \cdot 10^{-5}$ M) with 0 mM and 6.66 mM added Na^+ at 0 days, 2 days and 7 days after sample preparation.

14. Calculation of the saturation S_{ab}

The saturation (S_{ab}) of the various sensors was calculated by employing the following equation:[14,15]

$$S_{ab} = \frac{\sqrt{a^{*2} + b^{*2}}}{\sqrt{a^{*2} + b^{*2} + L^{*2}}} \quad \textbf{(S8)}$$

15. Colour tracks of sensors S1-S9 upon addition of Na^+, Li^+, K^+ and Ca^{2+}

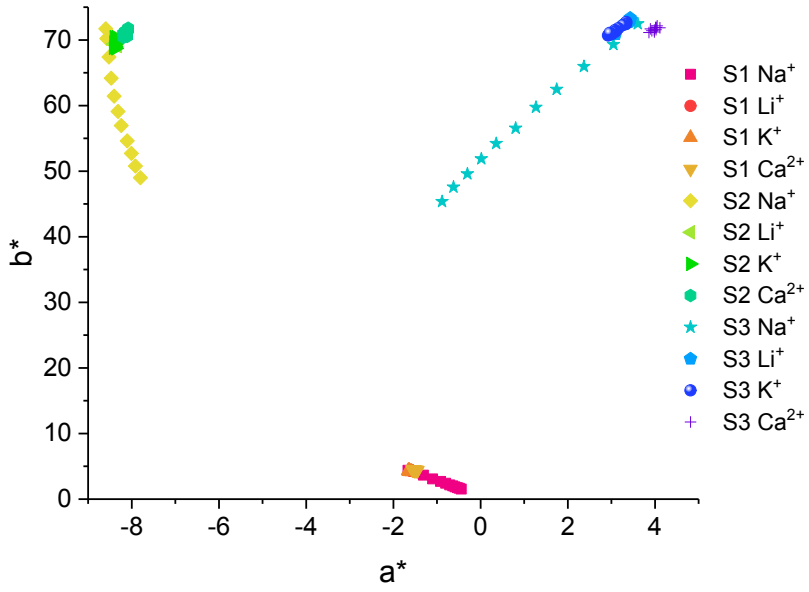

Fig S82 Colour tracks of **S1-S3** when tirating against Na^+, Li^+, K^+ and Ca^{2+}.

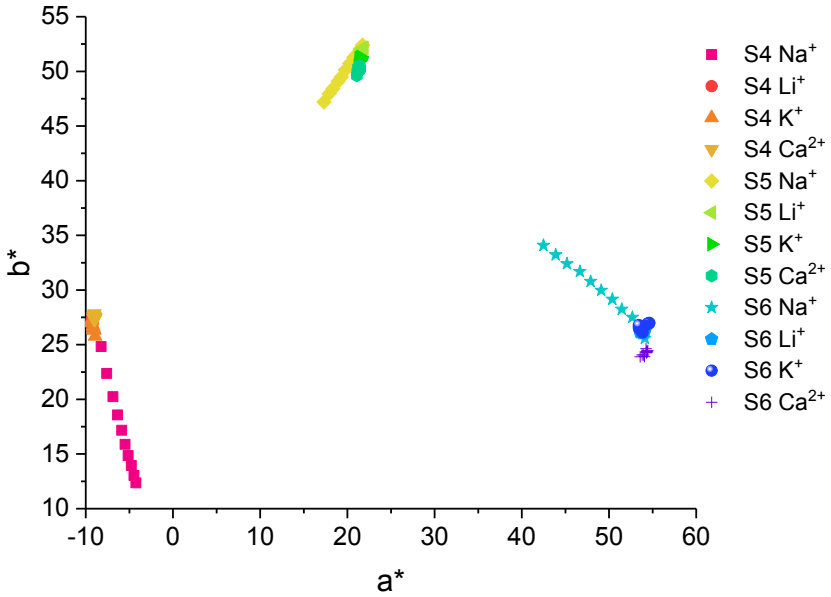

Fig S83. Colour tracks of **S4-S6** when tirating against Na^+, Li^+, K^+ and Ca^{2+}.

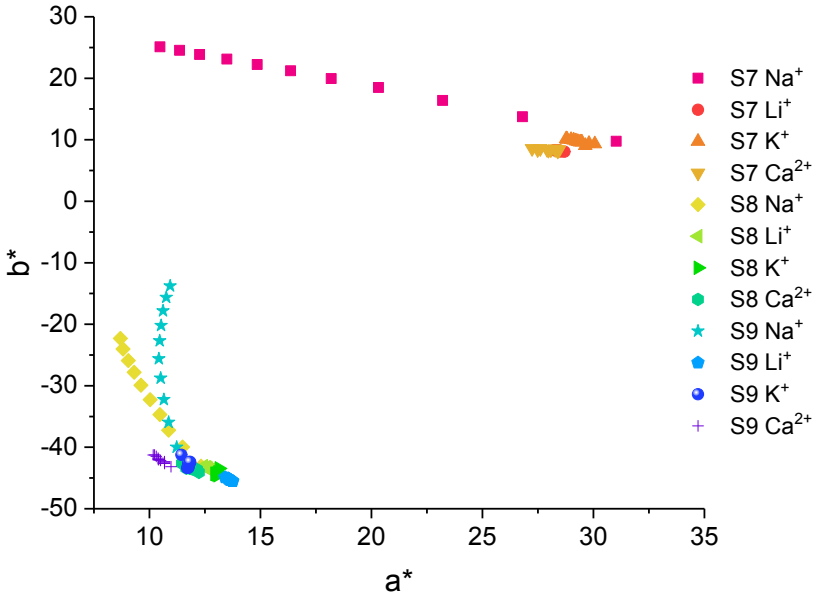

Fig S84. Colour tracks of **S7-S9** when tirating against Na^+, Li^+, K^+ and Ca^{2+}.

16. Na^+ over Li^+ and K^+ selectivity obtained by colorimetry

Table S3. Na^+ over Li^+ and K^+ selectivity measured employing colorimetry.

Sensor	ΔE^*_{ab} (0-6.66 mM) Na^+	ΔE^*_{ab} (0-6.66 mM) Li^+	Na^+/Li^+ selectivity	ΔE^*_{ab} (0-6.66 mM) K^+	Na^+/K^+ selectivity	ΔE^*_{ab} (0-6.66 mM) Ca^{2+}	Na^+/ Ca^{2+} selectivity
S1	3.2	0.7	4.6	0.2	15.3	0.1	29.2
S2	24.2	0.7	35.0	1.6	15.0	1.4	17.4
S3	26.9	0.6	46.3	1.7	15.7	0.4	68.6
S4	16.3	0.2	90.1	1.0	15.7	0.3	59.5
S5	7.1	0.3	22.2	0.7	10.4	0.3	29.0
S6	15.2	0.4	37.2	0.8	18.9	0.9	17.7
S7	27.8	0.5	53.7	1.5	19.2	1.4	19.9
S8	23.8	0.6	37.7	0.6	39.8	0.5	43.7
S9	31.7	0.7	48.1	0.7	43.4	1.8	17.6

17. References

1. Gaussian 09, Revision D.01, M. J. Frisch, G. W. Trucks, H. B. Schlegel, G. E. Scuseria, M. A. Robb, J. R. Cheeseman, G. Scalmani, V. Barone, B. Mennucci, G. A. Petersson, H. Nakatsuji, M. Caricato, X. Li, H. P. Hratchian, A. F. Izmaylov, J. Bloino, G. Zheng, J. L. Sonnenberg, M. Hada, M. Ehara, K. Toyota, R. Fukuda, J. Hasegawa, M. Ishida, T. Nakajima, Y. Honda, O. Kitao, H. Nakai, T. Vreven, J. A. Montgomery, Jr., J. E. Peralta, F. Ogliaro, M. Bearpark, J. J. Heyd, E. Brothers, K. N. Kudin, V. N. Staroverov, T. Keith, R. Kobayashi, J. Normand, K. Raghavachari, A. Rendell, J. C. Burant, S. S. Iyengar, J. Tomasi, M. Cossi, N. Rega, J. M. Millam, M. Klene, J. E. Knox, J. B. Cross, V. Bakken, C. Adamo, J. Jaramillo, R. Gomperts, R. E. Stratmann, O. Yazyev, A. J. Austin, R. Cammi, C. Pomelli, J. W. Ochterski, R. L. Martin, K. Morokuma, V. G. Zakrzewski, G. A. Voth, P. Salvador, J. J. Dannenberg, S. Dapprich, A. D. Daniels, O. Farkas, J. B. Foresman, J. V. Ortiz, J. Cioslowski, and D. J. Fox, Gaussian, Inc., Wallingford CT, 2013.
2. M. J. Marsella and T. M. Swager, *J. Am. Chem. Soc.*, 1993, **115**, 12214;
3. A. Giovannitti, C. B. Nielsen, J. Rivnay, M. Kirkus, D. J. Harkin, A. J. P. White, H. Sirringhaus, G. G. Malliaras and I. McCulloch, *Adv. Funct. Mater.*, 2016, **26**, 514;
4. Y. Ogiwara, K. Takahashi, T. Kitazawa and N. Sakai, *J. Org. Chem.*, 2015, **80**, 3101;
5. J. Wang, Y. Zhou, L. Zhang, Z. Li, X. Chen and H. Liu, *Org. Lett.*, 2013, **15**, 1508;
6. K. Spirkova and M. Dandarova, *Chem. Papers*, 1993, **47**, 48;
7. H. Sun, C. Zhong and J.-L. Brédas, *J. Chem. Theory Comput.*, 2015, **11**, 3851;
8. Y. Shiraishi, S. Sumiya, Y. Kohno and T. Hirai, *J. Org. Chem.*, 2008, **73**, 8571;
9. S. Goswami, K. Aich, S. Das, A. K. Das, A. Manna and S. Halder, *Analyst*, 2013, **138**, 1903;
10. K. Du, S. Niu, L. Qiao, Y. Dou, Q. Zhu, X. Chen and P. Zhang, *RSC Adv.*, 2017, **7**, 40615;
11. Q. Mei, Y. Shi, Q. Hua and B. Tong, *RSC Adv.*, 2015, **5**, 74924;
12. A. Shrivastava and V. B. Gupta, *Chron. Young Sci.*, 2011, **2**, 21;
13. A. R. Sarkar, C. H. Heo, M. Y. Park, H. W. Lee and H. M. Kim, *Chem. Commun.*, 2014, **50**, 1309;
14. J. F. Ponder, Jr., A. M. Österholm and J. R. Reynolds, *Macromolecules*, 2016, **49**, 2106;
15. G. Wyszecki and W. S. Stiles, *Color Science: Concepts and Methods, Quantitative Data and Formulae*, Wiley, Hoboken (NJ), 2000.